

**UNIVERSITA' DEGLI STUDI DI MILANO**  
*Facoltà di Medicina e Chirurgia*  
**Scuola di dottorato di Medicina Clinica e Sperimentale**  
**XXIX ciclo**



**A multidisciplinary approach to characterize the role  
of prokineticin receptor 2 (*PROKR2*) in Congenital  
Hypogonadotropic Hypogonadism (CHH)**

**Relatore: Chiar.ma Prof.ssa Laura FUGAZZOLA**  
**Correlatore: Dott. Marco BONOMI**

**BASSI IVAN**  
**Matricola N. R10493**  
**Anno Accademico 2016-2017**



## Table of contents

List of acronyms .....	6
Abstract.....	8
Introduction.....	11
Congenital Hypogonadotropic Hypogonadism.....	12
The hypothalamic-pituitary-gonadal (HPG) axis.....	12
Genetic of CHH .....	14
a. Causal genes .....	14
b. Critical aspect in CHH phenomics and genomics .....	26
c. Open issues .....	26
GnRH neurons in vertebrate models.....	26
Zebrafish model system .....	27
HPG axis in ZF.....	28
Hypophysiotropic form of GnRH in ZF.....	30
GnRH3 neurogenesis in ZF .....	30
ZF as a model to study CHH.....	32
Aim of thesis .....	34
Materials and methods .....	36
Patients.....	37
Genetic analysis .....	38
DNA Purification from whole blood .....	39
Next-Generation-Sequencing (N.G.S.) screening.....	39
Design of the panel.....	39
Sample/Library Preparation .....	40
Sequencing using MiSeq <sup>®</sup> sequencer platform .....	41
Bioinformatic analysis.....	42
Sanger Sequencing.....	42
Amplification of the gene by PCR .....	43
Electroforesis on agarose gel.....	43
Purification of amplified fragment .....	43
Sequencing reaction .....	43
Analysis by automated DNA-sequencer .....	44
PROKR2 in vitro analysis.....	45
Creation of plasmids .....	46

Mutagenesis PCR .....	46
Enzymatic digestion with DpNI .....	47
Transformation of bacterial cells .....	48
PCR on colonies from plates .....	48
Maxiprep .....	48
Cell culture .....	49
Transfection Protocol .....	49
Fluorescence-activated cell sorting (FACS) .....	50
Western Blot assay .....	50
Protein quantification .....	51
Sodium Dodecyl Sulphate - PolyAcrylamide Gel Electrophoresis (SDS-PAGE) .....	51
Immunofluorescence assay .....	51
Radioimmunoassay (RIA) .....	52
IP-One ELISA .....	53
PROKR2 in vivo analysis .....	54
Maintenance of zebrafish .....	55
Real-Time qRT-PCR .....	56
Total RNA extraction .....	56
RT-PCR (Reverse Transcription-Polimerase Chain Reaction) .....	56
Real-Time PCR .....	56
Synthesis of probes for <i>In Situ</i> Hybridisation (ISH) .....	57
Cloning and transformation reaction .....	58
Isolation of plasmid DNA .....	58
Probes labelling and synthesis .....	59
RNA quantification .....	59
Whole mount <i>In Situ</i> Hybridisation (WISH) .....	59
Loss of function analysis .....	59
Generation of Tg:GnRH3-EGFP/ <i>prokr1b</i> <sup>ct814/ct814</sup> line .....	61
Results .....	63
Genetic analysis .....	64
CHH patients cohort composition .....	65
Genetic analysis of CHH variants .....	66
<i>PROKR2</i> variants .....	67
PROKR2 in vitro studies .....	70

Fluorescence-activated cell sorting (FACS) .....	71
Western Blot .....	72
Immunofluorescent assay.....	74
Functional studies .....	75
Gs-dependent signaling pathway.....	75
Gq-dependent signaling pathway .....	76
PROKR2 in vivo analysis .....	78
Bioinformatic analysis .....	79
Real-Time qRT-PCR .....	81
Whole-mount <i>In Situ</i> Hybridization.....	82
Knockdown experiments .....	84
Knockout of <i>prokr1b</i> .....	87
Discussion .....	89
Bibliography .....	98

## **List of acronyms**

**ARC:** Arcuate nucleus

**AVPV:** Anteroventral Periventricular nucleus

**CHH:** Congenital Hypogonadotropic Hypogonadism

**CP:** Cribiform Plate

**dpf:** days post-fertilization

**Hb:** Habenular Nucleus

**hpf:** hours post-fertilization

**HPG:** Hypothalamus-Pituitary Gonadal axis

**Hyp:** Hypothalamus

**KI:** Kinase domain

**KS:** Kallmann Syndrome

**M:** Meninges

**N.G.S.:** Next Generation Sequencing

**nCHH:** normosmic Congenital Hypogonadotropic Hypogonadism

**OB:** Olfactory Bulbs

**ON:** Olfactory Nucleus

**OP:** Olfactory Placodes

**OT:** Olfactory Tubercle

**POA:** Preoptic Area

**SP:** Signal Peptide

**TM:** Transmembrane domain

**TN:** Terminal Nerve

**VNN:** Vomeronasal Nerve

**ZF:** zebrafish



# *Abstract*

Congenital hypogonadotropic hypogonadism (CHH) is a rare disease characterized by delayed/absent puberty and infertility due to an inadequate secretion or action of gonadotrophin-releasing hormone (GnRH). CHH is genetically heterogeneous but, due to the infertility of affected individuals, most frequently emerges in a sporadic form, though numerous familial cases have also been registered. In around 50-60% of cases, CHH is associated with a variety of non-reproductive abnormalities, most commonly anosmia/hyposmia, which defines Kallmann syndrome (KS) by its presence. Broadly speaking, genetic defects that directly impact on hypothalamic secretion, regulation, or action of GnRH result in a pure neuroendocrine phenotype called normosmic CHH (nCHH), whereas genetic defects that impact of embryonic migration of GnRH neurons to the hypothalamus most commonly result in KS, though nCHH can also arise. CHH represents a difficult unresolved puzzle, although more than 25 genes have been described to be involved in CHH, molecular variants can explain only 35-45% of reported cases. These evidences raise in the last year the idea that CHH is an oligogenic complex genetic disease characterized by variable expressivity and penetrance<sup>1</sup>.

With the purpose to better understand the genetic component of CHH, the first part of this work was focused on genetic screening of the principal twelve genes involved in CHH on the largest cohort of Italian patients. Screening of a cohort of 512 CHH patients allows the identification of 204 total variants in 32.2% of clinical cases. The analysis of variants displays a oligogenicity of 4.6%, confirming the oligogenic nature of CHH. Between the genes that appeared more frequently involved in the identified allelic variant, *PROKR2* gene appears in 7.5% of the cases. Indeed we identified a total of 17 *PROKR2* allelic variants, being four novel variants (p.G70S, p.D99N, p.C208S, p.M278K). *PROKR2* gene is known to have an important and not fully understood role in GnRH neurons migration, and mutations of this gene in humans can cause KS or nCHH syndromes with a phenotypic heterogeneity of reproductive and olfactory defects.

Consequently we decided to focus the second part of this work on characterization of these variants *in vitro* and *in vivo* with the aim to better elucidate the role of prokineticin receptor 2 in CHH and GnRH neurons migration. *PROKR2* GPCR signal transduction pathways functionality was studied in the above mentioned 4 novel and in other 4 already described variants that lack extensive functional studies (p.R47W, p.M64V, p.R85H, p.P290S). The functional study revealed that these missense allelic variants can affect protein targeting and signaling pathways with variable degree. In particular p.G70S, p.C208S and p.P290S are the more compromised

with a general impairment for both protein trafficking and Gs/Gq intracellular transduction pathways, while p.R47W, p.M64V and p.R85H variants are mainly affected in their targeting to the cell membrane, even though with a still conserved activation. Interestingly, p.M278K and p.D99N variants showed a virtual lack of the Gs-pathway activation in the presence of a conserved response to the Gq-pathway stimulation. These findings indicate the need to evaluate the integrity of both *PROKR2*-dependent cAMP and IP intracellular accumulation for a more appropriate functional testing of novel identified allelic variants.

The final part of this work was focused on generating an *in vivo* model for studying the role of *PROKR2* in the migration of GnRH neurons using zebrafish animal model. Few data are available on literature about prokineticin receptors in zebrafish. Preliminary bioinformatics analysis revealed the presence of two well-conserved loci in the zebrafish genome, located on chr1, named *prokr1a*, and a predicted region on chr13 named *prokr1b*. To assess their expression during zebrafish development, we performed Real-Time qRT-PCR and whole mount *In Situ* Hybridization (WISH). For investigating the functional roles of *prokr1a* and *prokr1b*, knockdown experiments were performed injecting morpholino sequences. Downregulation of *prokr1b*, but not *prokr1a* affects the migration/architecture of GnRH3 neurons supporting the idea that *prokr1b* is the homologous gene of human *PROKR2*. To further analyze the impact of *prokr1b* on GnRH neurons migration, a ZF *prokr1b* knockout line was generated. Analysis of GnRH fibers network in zebrafish knockout line display the same migration defects observed during downregulation assay, confirming the role of *prokr1b* in the migrations of GnRH neurons.

In conclusion, in the present work we applied a multidisciplinary approach to better elucidate the genetic and molecular mechanisms involved in CHH, focusing on the role of *PROKR2* gene. Starting from genetic analysis we identified *PROKR2* variants that were pharmacologically characterized by *in vitro* experiments to evaluate how these variants can affect signaling pathway or receptor membrane translocation. Moreover, with expression and knockdown experiments, we identified the zebrafish *PROKR2* human ortholog and generate a new *in vivo* model, that will be important in order to unravel the precise role of the prokineticin pathway in the pathogenesis of CHH.

# *Introduction*

## **Congenital Hypogonadotropic Hypogonadism**

The central control of sexual maturation and reproduction resides in a complex anatomical and functional network of hypothalamic neurons, converging onto, and regulating the activity of GnRH gonadotropic neurons. These neuronal circuitries impact on the development, maturation and activity of GnRH neurons and ultimately regulate critical aspects of sexual differentiation, puberty onset, gonadal function and fertility<sup>2-4</sup>.

Congenital hypogonadotropic hypogonadism (CHH) is a disease with extremely variable phenotypic expression that affects the hypothalamic GnRH neuron, and includes two main groups of patients, those with olfactory defects (Kallmann syndrome, KS) and the normosmic patients with congenital hypogonadotropic hypogonadism (nCHH). The first case report came in 1856 when Maestre de San Juan described an individual with absence of olfactory structures in the brain and presence of small testes<sup>5</sup>. Approximately a century after Franz Josef Kallmann identified the hereditary nature of this disease<sup>6</sup> and Naftolin ascribed hypogonadism to a gonadotropin-releasing hormone (GnRH) deficiency<sup>7</sup>. CHH is more frequent in males (1:8000) than females (1:40000). Males frequently present with defective androgenization and growth at peripubertal age but micropenis and cryptorchidism may already be evident in the neonatal period, indicating a defective HPG activation during the prenatal development. Females generally present with primary amenorrhea and growth retardation. Additional neurological (e.g. anosmia, bimanual synkinesia, sensorineural hearing loss) and non-neurological defects (e.g. the midline or kidney defects, dental agenesis) may frequently co-exist and be linked to specific modes of inheritance. Biochemically, CHH patients present low or undetectable concentrations of circulating sex steroids and low/normal luteinizing hormone (LH) and follicle-stimulating hormone (FSH) serum levels, as a consequence of the impaired functionality of Hypothalamic-Pituitary-Gonadal (HPG) axis due to the GnRH deficiency.

## **The hypothalamic-pituitary-gonadal (HPG) axis**

The HPG axis plays a pivotal role in all vertebrates controlling many complex functions including growth, reproduction, osmoregulation, stress and metabolism. The physiological function of this axis is based on the pulsatile release of the GnRH by GnRH-neurons located in the hypothalamus. GnRH-neurons and olfactory system development are strictly connected;

during early stages of embryogenesis, GnRH-neurons arise outside of the brain in a niche at the border between respiratory epithelium and vomeronasal/olfactory from the neural crest and ectodermal progenitors. From these locations they start to migrate caudally in close association with developing sensory axons of the olfactory/vomeronasal/terminal nerve system to reach, passing through the cribriform plate, their final destination in the mediobasal hypothalamus<sup>8</sup>.

Once in the hypothalamus, functional GnRH-neurons detach from the olfactory axonal guides, and complete their differentiation extending axonal processes to the medial eminence through which pulsatile GnRH is secreted into circulation via the hypophyseal portal system. The GnRH interacts with its specific receptor, the GnRH-R, which is expressed on the membrane surface of the gonadotrope cells, thus stimulating the biosynthesis and secretion of the gonadotropins, luteinizing hormone (LH) and follicle-stimulating hormone (FSH). The two gonadotropins are then transported through the peripheral circulation to the gonads, where they stimulate either the steroidogenesis (estrogen, progesterone, and androgens) or the gametogenesis (oocytes and spermatozoa). The gonadal steroids, in turn, auto-regulate their own secretion through a feedback mechanism at the hypothalamus-pituitary level, decreasing the GnRH and gonadotropin secretion<sup>9</sup> (Figure 1).

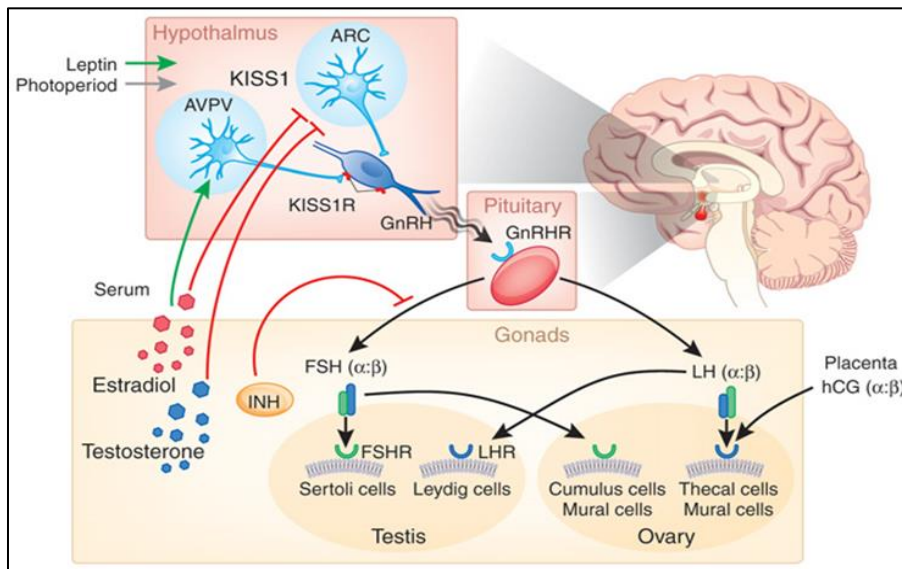


**Figure 1:** HPG axis illustration from Matzuk MM *et al.*, Nat Med. 2008.

The activity of the human GnRH-secreting neurons is present in the hypothalamus starting by the 10<sup>th</sup> week of gestational age, followed by the secretion of the two gonadotropins which are detectable from the 10<sup>th</sup>-13<sup>th</sup> weeks of gestation when the hypophyseal portal system has

developed. The secretion of the GnRH, and then LH and FSH, decline at mid-gestation due to the negative feedback exerted at the hypothalamus and pituitary levels by the surge of the placental steroid. After the delivery, due to the lack of the placental steroid negative feedback, GnRH and the gonadotropins rise and remain elevated for the first 12-24 months in the girls and for the first 6 months in boys, identifying the so called “minipuberty”. Subsequently, due to inhibitory mechanism so far not fully understood and maybe involving the neurotransmitters  $\gamma$ -aminobutyric acid (GABA) and the neuropeptide Y (NPY) the GnRH, LH and FSH levels decrease and remain suppressed till the beginning of the pubertal development<sup>10,11</sup>. Indeed, at puberty, the GnRH, and consequently the gonadotropins secretion resumes with a characteristic pulsatile manner, which is controlled by the GnRH pulse generator<sup>9</sup>.

Therefore, the normal GnRH development and pulse generation processes are essential for the integrity of the HPG axis and, by consequence, for normal reproductive function. Studies conducted in last two decades underline how all these processes are under the control of several genes.

## **Genetic of CHH**

### **a. Causal genes**

KS was originally described as caused by mutations in a specific X-chromosome gene, KAL-1<sup>12</sup>, with a consequent altered targeting of olfactory axons and migration of neurons producing GnRH, the key central regulator of the reproductive axis, but this genetic defect was soon found to be present in a minority of the patients. Thus, the causal event of the isolated CHH was often missing, and the classification of “idiopathic” CHH was consequently adopted. Nevertheless, the observation of familial cases with variable modes of inheritance (X-linked or autosomal dominant or recessive) soon indicated that CHH retains a highly heterogeneous genetic component. The application of conventional linkage studies to investigate the genetic basis has proven difficult, because most pedigrees tend to be of small size, since most patients remain infertile in the absence of therapeutic treatment. In the last decade, however, the knowledge on the pathogenesis of CHH has been profoundly deepened thanks to the utilization of animal and cellular models; these, together with the application of modern techniques of genetic investigation, brought evidence of previously unknown genetic determinants of CHH (either nCHH or KS). These new insights have played a significant role in disclosing the physiological

complexities of the HPG axis and therefore in elucidating the pathophysiology of CHH. Association with a multitude of candidate genes has nowadays been identified<sup>13</sup>. Some genes are determinant for the correct embryonic differentiation of the GnRH-secreting neurons or encode the signals essential for the correct migration of the GnRH neurons from their embryonic origin to the hypothalamus: the *ANOS1/KAL-1*; the receptor-ligand pair fibroblast growth factor receptor 1<sup>14,15</sup> and fibroblast growth factor 8<sup>16,17</sup> (*FGFR1/FGF8*); the nasal embryonic LH releasing hormone factor (*NELF*)<sup>18</sup>; the heparan sulfate 6-O-sulfotransferase1 (*HS6HST1*)<sup>19</sup>; the ligand–receptor complex prokineticin 2 and its receptor (*PROK2/PROKR2*)<sup>20-24</sup>; the chromodomain helicase DNA binding protein 7 (*CHD7*)<sup>25-29</sup>; the class 3 and 7 semaphorins *SEMA3A*<sup>30-32</sup>, *SEMA3E*<sup>33</sup> and *SEMA7A*<sup>32</sup>; the Sry-related HMG box factor 10 (*SOX10*)<sup>34,35</sup>; the WD repeat-containing protein 11 (*WDR11*)<sup>36,37</sup>, the fibroblast growth factors 17 (*FGF17*)<sup>38</sup>, the interleukin-17 receptor D (*IL17RD*)<sup>38</sup>, the protein sprouty homolog 4 (*SPRY4*)<sup>38</sup>, the dual specificity phosphatase 6 (*DUSP6*)<sup>38</sup>, the FEZ family zinc finger 1 (*FEZF1*)<sup>39</sup>. Other genes encode the elements of upstream signals contributing to the activation of GnRH neuron, such as the two ligand–receptor couples formed either by the *TAC3/TACR3*<sup>40-42</sup> (tachykinin 3 and its receptor also named neurokinin B, NKB, and/or neurokinin 3 receptor, NK3) or the *KISS1/KISS1R*<sup>43,44,41</sup> (kisspeptin1 and its receptor, previously known as GPR54). Finally, candidate genes for CHH also include the GnRH gene itself (*GnRH1*)<sup>45,46</sup> and its receptor (*GNRHR*)<sup>47,48</sup> (Figure 2).

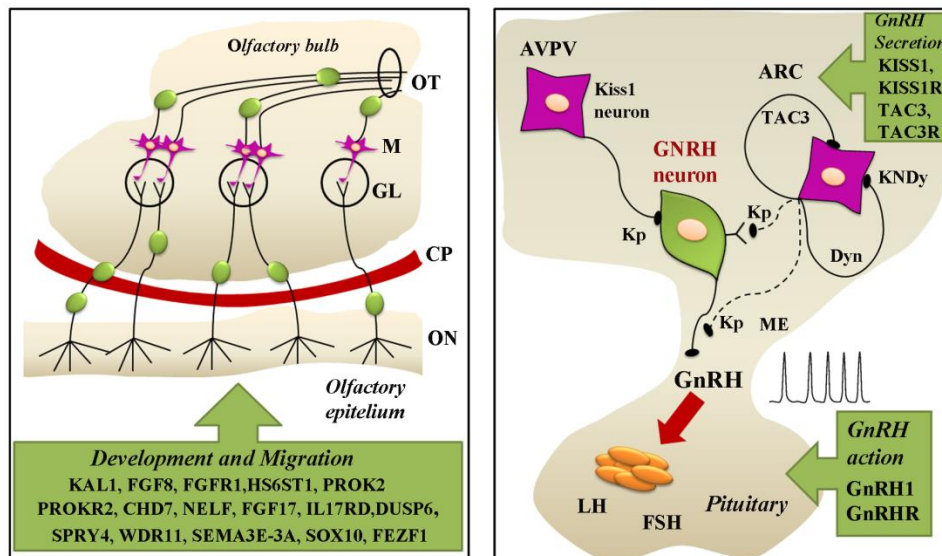


**Figure 2:** On the left, genes involved in development and migration of GnRH neurons. On the right, genes responsible for GnRH neurons secretion and release of GnRH hormone (from Vezzoli V. *et al.*, Minerva End. 2016).

Thus, from *KALI* in 1991, the first gene associated with KS<sup>49,50</sup> more than 25 genes have been identified as involved in CHH, although not all of them are equally involved in the pathogenesis of the CHH. Indeed, we can consider some of them as major genes, due to their more frequent or important involvement in the molecular pathogenesis of CHH.

***ANOS1/KALI:*** *KALI* gene, recently renamed *ANOS1*, is located in human on chromosome Xp22.3. The 14 exons that constitute the gene encode for anosmin-1, a 100 kDa extracellular matrix glycoprotein of 680 aminoacids. This protein is composed by an N-terminal cysteine-rich domain, followed by a whey acidic protein (WAP) domain, four fibronectin type III (FnIII) domains and a terminal histidine-rich region<sup>49,50</sup>. The fibronectin type III domain is essential to create a flat surface with a strong basic charge, enabling interactions between anosmin-1 and other components of the extracellular matrix<sup>51,52</sup>(Figure 3).

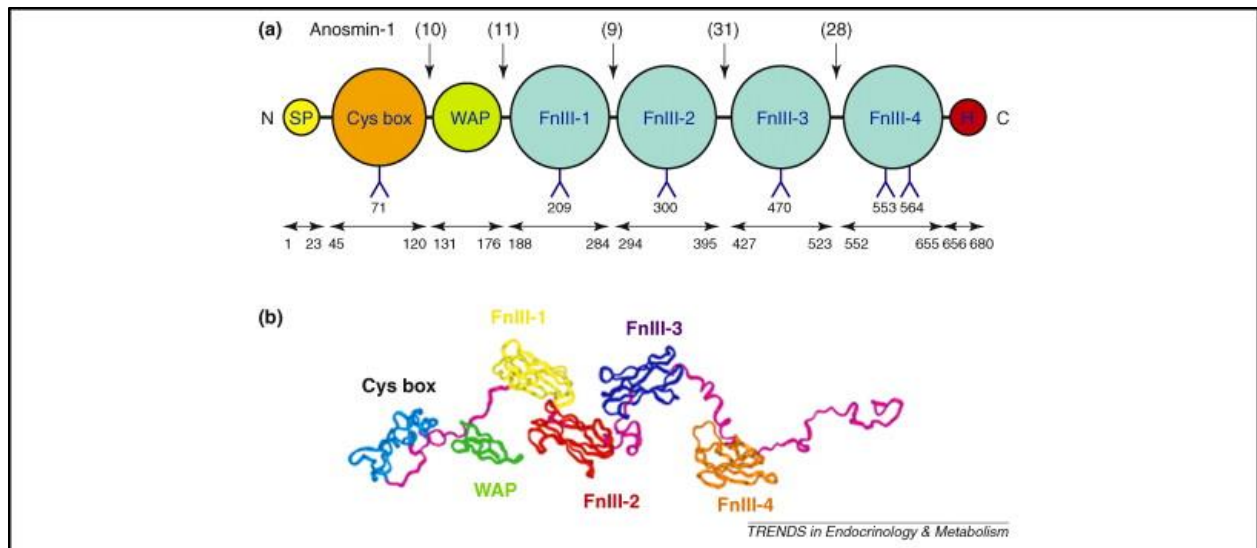


**Figure 3:** Anosmin-1 structure (from Hu Y. *et al.*, Trends Endocrinol Metab. 2010).

Anosmin-1 in human was detected in the olfactory system from week 5 onward restricted to the olfactory bulb presumptive region and later, to the primitive olfactory bulbs. Fundamental insights into the pathology of X-linked KS came from the post-mortem examination of a male 19-week-old human fetus carrying a chromosomal deletion encompassing the *KALI* gene. In this study, researchers reported that olfactory, vomeronasal and terminalis nerve fibers were not in contact with the brain neither were the GnRH neurons present in any area of the brain. Furthermore, they observed an abnormal accumulation of both nerve fibers and GnRH neurons in the upper nasal area, where they normally enter into the central nervous system<sup>53</sup> (Figure 4). These findings indicated that the causative defect primarily affects the migration of early olfactory axons, which takes place from the beginning of week 5 onward<sup>54</sup>. Sequentially, the lack of contact between the olfactory axons and the forebrain during week 6 would in turn prevent olfactory bulb differentiation<sup>55-57</sup>.

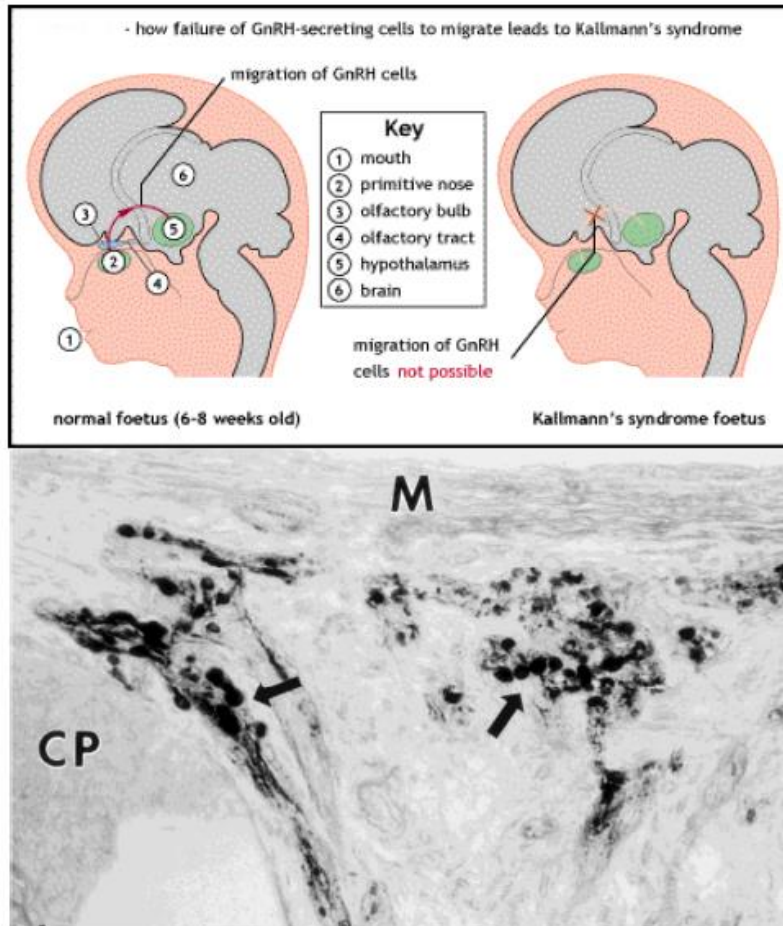


**Figure 4:** GnRH3 migration failure in a male fetus mutated for *KAL1*; CP= cribriform plate; M= meninges (from Schwanzel-Fukuda *et al.*, Nature 1989).

Genetic studies of KS patients reported that *KALI* gene abnormalities include missense and nonsense mutations, splice site mutations, intragenic deletions and submicroscopic chromosomal deletions involving the entire *KALI* gene<sup>58</sup>. All, but one<sup>59</sup>, patients harboring *KALI* mutations are presenting olfactory dysfunction of variable extents, moreover they often have a more complex phenotype<sup>60</sup> with a high incidence of renal agenesis and bimanual synkinesia defects that occurs respectively in 30%–40% and 75% of the patients<sup>20</sup>. Analysis of familial cases of KS reported that *KALI* is mutated in approximately 60% of these patients, while only 10%–15% of males mutated for this gene present sporadic KS, suggesting an X-linked mode of inheritance<sup>58</sup>.

***FGFR1*:** *FGFR1* gene, less frequently called *KAL2*, is located on chromosome 8p12. Its sequence contains 18 exons that translated generated a protein receptor belonging to the tyrosine kinase superfamily, that consists of four subtypes (named *FGFR1–4*) and seven FGFR isoforms.

These isoforms are able to specifically bind particular members of the 22 fibroblast growth factor (FGF) ligands. FGFR1 protein structure consists of three extracellular immunoglobulin-like loops (D1, D2 and D3), an acid box D1–D2 linker region that contains a stretch of negatively charged amino acids and a heparan sulphate-binding site, a transmembrane domain and an intracellular split tyrosine kinase domain<sup>61</sup> (Figure 5).

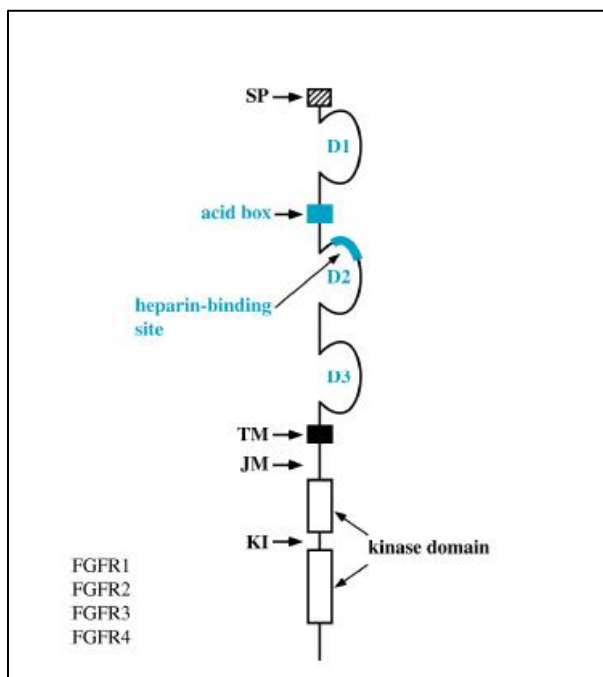


**Figure 5:** scheme representing structural domains of FGFR1.

Alternative splicing in the second half of the juxtamembrane D3 domain could generate two transmembrane isoforms of FGFR1 protein termed IIIb and IIIc<sup>62</sup>. The FGF ligand binding region is formed by the terminal membrane domains of D2 and D3. While D3 isoform determines ligand-binding specificity, the D1 domain can act as a potential competitive auto-inhibitor of the interaction between FGFR and FGF and HS folding back to interact with D2 in the FGF and heparan sulphate (HS) contact sites. FGFR1 signaling is based on dimerization and sub sequentially activation by autophosphorylation of receptor`s intracellular tyrosine kinase domains. These conformational changes in the receptor are induced by the bindings of FGFs, heparin and HS proteoglycan ligands<sup>63</sup>. *FGFR1* has been shown to play an essential role during embryogenesis, homeostasis and wound healing. Studies conducted during the development of central nervous system have underlined the critical role of FGF receptors and ligands in the

neurogenesis<sup>64</sup>. In the rostral forebrain, in particular *FGFR* and *FGF* affects the olfactory bulb development influencing, by consequence, the GnRH neuronal migratory activity<sup>65</sup>. In fact analysis of *Fgfr1*<sup>-/-</sup> knockout (KO) mice have shown aplasia in the olfactory bulbs<sup>65</sup>. Moreover *Fgfr1*<sup>-/-</sup> mice transfected with dominant negative *FGFR1* mutations exhibited an early onset together with a 30% decrease of hypothalamic GnRH neurons<sup>65</sup>. These results suggested that loss-of-function mutations in *FGFR1* result in a defect in GnRH neuron migration via the abnormal morphogenesis of the olfactory bulb, while specific gain-of function mutations in *FGFR1* cause craniosynostosis<sup>66</sup>. Since the first reported association between *FGFR1* loss-of function mutations and the dominant form of KS<sup>67</sup>, several *FGFR1* mutations have been identified in KS-affected individuals and in patients with nCHH, all of them occurred in the *FGFR1IIIc* isoform and spanned all of the functional domains of the receptor<sup>15,68</sup>. Clinically features of CHH patients with *FGFR1* defects includes, as for *KALI*, also non-reproductive and non-olfactory disorders<sup>60</sup>. Nevertheless analysis of these cases revealed a wide phenotypic variability in unrelated probands and mixed pedigrees. As a matter of fact, patients from the same family that shared an identical mutation exhibited the coexistence of KS, isolated hyposmia without hypogonadism, and nCHH<sup>15</sup>. The presence of modified genes, the involvement of multiple genes or an epigenetic mechanism was proposed as explanations for such different phenotypic expression of the same genetic defects<sup>69</sup>. It is accordingly evident that the precise quantitative regulation of *FGFR1* signaling is crucial for a normal development considering that both attenuated and increased signaling cause disparate phenotypes.

**HS6ST1:** *HS6ST1* gene is located on chromosome 2q21 and is composed by 2 exons. Its sequence encodes an enzyme of 411 aminoacids, whose function is to introduce a sulfate in the 6-O-position of the glucosamine sugar moiety within heparan sulfate (HS) (Figure 6).

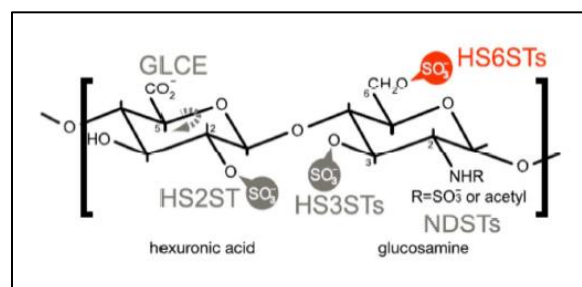


**Figure 6:** Chemical structure of HS. The red circle represents the sulfate residue introduced by HS6ST1 enzyme (from Tornberg J. *et al.*, Proc Natl Acad Sci U S A. 2011)

HS polysaccharides are components of the extracellular matrix and are essential for neural development due to their control in cell-to-cell communications<sup>70</sup>. In particular, this post-translational modification is important for the interaction and activation of the FGFR–FGF complex<sup>63</sup> and for the interaction between anosmin1 and the cell membrane<sup>64</sup>. Bülow and colleagues, in studies conducted using *C. elegans* model, demonstrated that overexpression of human *KALI* ortholog in specific worm interneurons causes axonal-branching defects<sup>71</sup>, and that this *kal-1* gain-of-function phenotype is suppressed by HS 6-O-sulfotransferase gene (*hst-6*)<sup>71,72</sup> suggesting the role of *HS6ST1* in the pathogenesis of nCHH/KS. Tornberg and coworkers support this thesis showing that all reported mutation founded sequencing the coding exons and flanking splice sites of the gene *HS6ST1* in a cohort of 338 GnRH-deficient patients affects residues that are highly conserved in HS6ST1. Moreover, they found that *HS6ST1* mutations recognized in patients with CHH reduce enzyme activity both *in vitro* and *in vivo*<sup>19</sup>. Clinically, patients carrying *HS6ST1* mutations could present a wide spectrum of severity of GnRH deficiency; this variability is also evident both within families that share the same genetic alteration<sup>19</sup>. Because *HS6ST1* mutation associated with CHH has not been described in the homozygous state and segregates as a complex trait with inheritance patterns that likely resulted from oligogenic interactions, it was proposed that the identified *HS6ST1* missense mutations might not be sufficient to cause disease, and suggested that *HS6ST1* represents an important gene for the neuroendocrine control of human reproduction.

***KISS1/KISS1R***: *KISS1* gene is located on chromosome 1q32 and encodes for a 145-amino acid kisspeptin 1. This precursor is cleaved in four products: kisspeptin 54 or metastatin the longest 54-amino acid peptide, and three minor products of 14, 13 and 10 residues called respectively kisspeptin 14, kisspeptin 13 and kisspeptin 10. All four peptides showed the same binding affinity and efficacy for receptor KISS1R; this leads to the hypothesis that the C terminal portion of the peptide is the important region for binding and activation of the receptor. *KISS1R*, previously known as *GPR54*, was mapped to chromosome 19p13.3. Translation of its sequence generates a 398 amino acids G protein-coupled receptor of 75KDa<sup>73</sup>. Expression analysis showed that while *KISS1R* is expressed in both the hypothalamus and pituitary, *KISS1* is restricted to hypothalamus<sup>73</sup>. Studies conducted on *Kiss1r* knockout mice demonstrate that KISS1R affects the processing or release of GnRH, but not the migration of GnRH neurons<sup>44,74</sup>. These knockout

mice represent a phenocopy of *Kiss1R*<sup>-/-</sup> human condition<sup>44</sup>, with normal GnRH neurons and hypothalamic content but almost absent sexual maturation. All mouse knockouts for *Kiss1R* and *Kiss1* described in literature recapitulate the human nCHH phenotype, confirming the crucial role of ligand-receptor couple KISS1/KISS1R as proximal regulators of GnRH release<sup>75</sup>. These findings support the role of *KISS1* as a tiny regulator of puberty and HPG axis. Indeed, its increased expression have been proposed to be one of the effector mechanisms at puberty<sup>76,77</sup> while downregulation mediates the HPG suppression observed in severe nutritional deprivations<sup>78</sup>. Moreover, KISS1 neurons are highly responsive to estrogens, and were demonstrated to be implicated in both positive and negative central feedback of sex steroids to GnRH production<sup>78</sup>. The role of *KISS1/KISS1R* was supported by observations of GnRH deficiency and failure to initiate or progress through puberty in CHH patients, carrying mutations in these genes<sup>79</sup>. Inactivation of mutations in *KISS1* and *KISS1R* shows an autosomal recessive pattern of inheritance.

***GNRHI***: Gonadotropin-releasing hormone (GnRH), located on chromosome 8p21-11.2, is encoded by the *GNRHI* gene. Composed by four exons and three introns, *Gnrhi* sequence translation generates a 92 amino acids pre-pro-protein (pre-pro-GnRH), including: a 23 amino acids signal sequence followed by two serine residues, the GnRH decapeptide, a GKR sequence and GAP 6 GnRH-associated peptide, a 56-amino acid peptide<sup>80</sup>. It plays a crucial role in the HPG axis, regulating the reproductive physiology. In particular its synthesis by hypothalamic neurons and pulsatile secretion into the hypothalamic-hypophyseal portal circulation controls the synthesis and release of the two gonadotropins exercised by anterior pituitary in both sexes<sup>80</sup>. *Gnrh1* KO mice exhibited anomalous tooth maturation and mineralization and a complete absence of GnRH synthesis that lead to infertility, sexually immaturity<sup>80,81</sup>. However, introduction of an intact GnRH gene into the genome of these mutant mice completely reversed the reproductive deficits<sup>82</sup>. Same was observed in humans where pulsatile GnRH administration reverted the delayed puberty phenotype in a male patient and his sister with homozygous mutation, affecting the peptide precursor pre-pro-GnRH<sup>45</sup>.

***GNRHR***: *GNRHR* is the receptor of *GNRHI*; its sequence is mapped on chromosome 4q21.2 and generates a 328-amino acid GPCR of 60 KDa. Its structure consists of an extracellular 35-amino

acid amino-terminal domain, and seven transmembrane domains and does not present a carboxy-terminal cytoplasmic tail<sup>80</sup>. Binding with its ligand, GnRH1 stimulates in the pituitary gonadotrope cells the beta isoform of Phosphoinositide phospholipase C, which mobilizes calcium and protein kinase, resulting ultimately in the activation of proteins involved in the synthesis and secretion of the gonadotropins LH and FSH. The GnRHR KO mouse model recapitulates clinical phenotype of CHH syndrome<sup>83,84</sup>, displaying reduced sexual organs, low gonadotropins and sex steroid levels, infertility, failure of sexual maturation and inability to respond to exogenous GnRH administration. Several human *GNRHR* loss of function mutations were described in CHH patients in the last 15 years<sup>47</sup>. Clinically, the phenotype of these individuals span a wide spectrum of defects ranging from fertile eunuch syndrome to the complete form of GnRH resistance, characterized by micropenis, cryptorchidism, very low gonadotropins levels and the absence of pubertal development. *GNRHR* mutations have been described in about 40–50% of familial nCHH cases, and in round 17% of sporadic nCHH<sup>85</sup>.

***TAC3/TAC3R***: *TACR3* or tachykinin receptors 3 gene is located on chromosome 4q25. It encodes for NK3R, a GPCR primarily expressed in the central nervous system that is activated when bound with its ligand Neurokinin B (NKB). NKB is a member of the tachykinin superfamily of neuropeptides, that also includes substance P and neurokinin A and is encoded by *TAC3* gene, located on chromosome 12q13–q21<sup>86</sup>. Its expression analysis showed a wider distribution in the central nervous system, in particular it is expressed in the arcuate nucleus of hypothalamic neurons that project to GnRH secreting ones<sup>86</sup>. Despite the overlapping expression of neurokinin B and kisspeptin in the arcuate nucleus, and the fact that both are downregulated by estrogens, suggesting similar roles for both in relaying feedback from sex steroids to GnRH production, studies in animal models indicates different functions. Indeed, experiments conducted in various species underline different ability between KISS and NKB in the stimulation of release of GnRH. In particular, kisspeptin can stimulate GnRH release in almost all species, while NKB cannot. Moreover, observation of KO mice for *NKB* or *KISS* revealed distinct phenotypes, with *NKB* KO mice with a normal fertility, whereas *KISS* KO mice displayed a CHH classic phenotype<sup>87-89</sup>. Clinical studies on humans revealed an association between mutation of *TACR3* and micropenis and cryptorchidism phenotypes in male patients,

demonstrating the importance of NKB/NK3R system for normal fetal gonadotrophin secretion<sup>40,87</sup>.

***PROK2 and PROKR2:*** *PROK2* and *PROKR2* are respectively ligand and receptors belonging to the family of prokineticins. This family is composed by two ligands *PROK1* and *PROK2* with similar affinities for their two receptors, namely *PROKR1* and *PROKR2*. Receptors operate as molecular switches to relay extracellular ligand-activation to intracellular heterotrimeric G proteins, and present a high conservation in their sequence (about 85%). Meanwhile, whilst *PROK1* and its receptor *PROKR1* expressions are mainly confined to gastrointestinal system where they promote gut motility, *PROK2* (locus 3p21.1) and *PROKR2* (locus 20p13) present a more specific neuroendocrine profile<sup>90,91</sup>. Indeed they are located in the arcuate nucleus, olfactory track and suprachiasmatic nucleus. *PROKR2*, as a member of the GPCR family, has an extracellular amino-terminal end, an intracellular carboxy-terminal domain and a central core formed by seven transmembrane  $\alpha$ -helical segments (TM1–TM7)<sup>90</sup>(Figure 7).

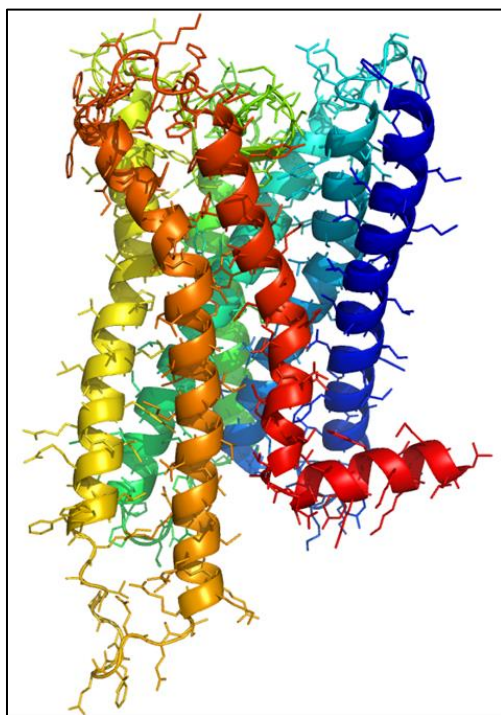


**Figure 7:** Structure of human *PROKR2* (gently provided by Prof. G. Kleinau, Leibniz-Institut für Molekulare Pharmakologie, Berlin).

*PROK2* gene encodes the protein Prokineticin 2, a peptide of 81 amino acids with pro-migratory activity that binds to its cognate G protein-coupled receptor (GPCR) *PROKR2*. Their molecular interaction activates the *PROKR2* downstream signal cascade via Gq and Gs<sup>92</sup>. Prokineticins were demonstrated to be involved in several physiological functions in neurogenesis, regulation of circadian rhythms, metabolism, angiogenesis, pain perception, muscle contractility, hematopoiesis, immune response, thermoregulation and energy expenditure<sup>93-96</sup>. Alteration of this system was found to be associated with several pathological conditions, including cancer<sup>97,98</sup>, immunological response<sup>99</sup>, mood disorder (anxiety/depression)<sup>100</sup>, and cardiomyopathy<sup>101</sup>. Analysis of knockout mice models for both ligand and receptor revealed the role of *PROK2* signaling in olfactory bulb (OB) morphogenesis and sexual maturation, suggesting *PROK2* and *PROKR2* as strong candidates for human GnRH deficiency<sup>102,103</sup>. Indeed, the homozygous *Prokr2* null mouse model results in KS phenotype, while the heterozygous mice do not show any important reproductive abnormality. The involvement of the *PROKR2*/*PROK2* pathway in the pathogenesis of the CHH was first described in 2006<sup>20</sup> and subsequently reported in several other patients series<sup>104,105</sup>. Pharmacologically, characterization of these variants demonstrate a variable impairment of their expression levels in heterologous cell system and a reduced activation of the Gq and Gs-dependent intracellular pathway<sup>22,24,106</sup>. Genetic analysis of *PROKR2* variants showed that the majority of them were found in heterozygous state, suggesting an autosomal dominant mode of inheritance due to either haploinsufficiency or a dominant-negative effect. Nevertheless, only the patients carrying homozygous mutations are displaying the most severe and penetrant clinical phenotypes<sup>20,24,107</sup>, while patients with heterozygous mutations are presenting a variable expressivity or incomplete penetrance of both the reproductive and olfactory phenotypes. Moreover, very recently, *PROKR2* variants, but not *PROK2*, have been also described in patients with combined pituitary hormone deficits<sup>108,109</sup>. Altogether, these data suggest an extensive role of *PROKR2* in the control of the entire neuroendocrine system. Notwithstanding knowledge about the precise molecular mechanisms of *PROKR2* in the neuroendocrine axis remains largely unexplored, underlying how further investigations are necessary.

b. Critical aspect in CHH phenomics and genomics

Since the two forms of the CHH, KS and nCHH, may exist in different relatives within unique familial settings, is supporting the idea that they may constitute variable phenotypic manifestations of largely common genetic defects. On such basis, a novel vision is now arising, in which CHH may be considered as a complex genetic disease characterized by variable expressivity, penetrance and modes of inheritance in which the inability to go through puberty represents the cardinal manifestation<sup>110</sup>. As in multifactorial complex diseases, the pathogenesis of CHH may include the influence of environmental factors, but also the concurrent involvement of SNPs or other genetic defects in two or multiple interacting genes. Indeed, the recent reports of patients carrying pathogenic rare variants in more than one gene have challenged the long-held view of a strictly monogenic disorder. Oligogenicity, which is as frequent as the biallelic defects in a single gene, may partially account for the phenotypic variability of isolated GnRH deficiency, as demonstrated in a North-American cohort<sup>69</sup>.

c. Open issues

The genetic analysis of all the so far known causative genes allows to identify a genetic cause in ~50% of the analyzed patients, leaving half of them still “idiopathic”<sup>111</sup>. This implies that new strategic and methodological advances are needed to cover this gap. Moreover, the recent demonstration of the oligogenic pathogenesis of the disease opens the question regarding how these genes are interacting between each other in determining the complex clinical phenotype. The use of specific animal models might be helpful in this respect.

## **GnRH neurons in vertebrate models**

Comparative endocrinology studies about GnRH neuronal development conducted on vertebrate organisms in the last fifteen years has greatly contributed to the current knowledge of the human reproductive axis. These experiments identified twenty four distinct forms of GnRH across fishes, amphibians and reptiles underlying the presence of two to three GnRH paralogous forms in all vertebrate species<sup>112-115</sup>. Consensus nomenclature adopted in the last decades classified GnRH genes basing on location and functions in three main groups called GnRH1, GnRH2 and GnRH3<sup>45,116-121</sup>. GnRH1 neurons are found, in vertebrates, prevalently in the preoptic area (POA) and the caudal hypothalamus, where they exert hormonal control of reproduction via its

regulation of gonadotrophin secretion from the pituitary gland. For this reason they are also called hypophysiotropic-GnRH form<sup>122</sup>. GnRH2 and GnRH3 are respectively located in midbrain tegmentum and terminal nerve/nasal compartment and, while they are indicated as not hypophysiotropic, recent findings seem to suggest an indirectly “neuromodulatory” action in reproductive neuroendocrine axis<sup>122,123</sup>. Among vertebrates, teleost fish represent one of the most heterogeneous groups with three GnRH isoforms in seabass and two in zebrafish (ZF)<sup>124</sup>. Despite these differences, ZF, with its characteristic of optical embryos transparency and amenability to genetic manipulation and imaging, has proved to be an ideal model organism for studying the early migration of GnRH neurons and the formation of the GnRH network<sup>125</sup>.

### **Zebrafish model system**

Zebrafish (*Danio rerio*) is a teleost fish native to Southeast Asia. Its unique combination of features makes zebrafish particularly well suited for experimental and genetic analysis of early vertebrate development. Zebrafish adults dimensions are tiny, thus many fishes can be housed in a small space. They have a relatively short generation time: an adult female reaches the sexual maturity in about three months, and it lays hundreds of eggs every few weeks per mating, generating a large progeny, suitable for genetic or experimental analysis. The fertilized embryos develop rapidly, making it possible to observe the entire course of early development in a short time. Somitogenesis begins at about 9 hpf (Hours Post-Fertilisation), at 24 hpf the zebrafish embryo has already formed all the major tissues and many organ precursors, such as a beating heart, circulating blood, nervous system, eyes and ears, all of which can be readily observed under a simple dissecting microscope. Larvae hatch by about 2.5 dpf (Days Post-Fertilisation) and they are swimming and feeding by 5–6 dpf<sup>126-128</sup>. A variety of tools and methodologies have been developed to exploit the advantages of the zebrafish system. Zebrafish embryos and early larvae are optically clear, allowing for direct, non-invasive observation or experimental manipulation at all stages of their development, such as whole mount *in situ* hybridization analysis of gene expression patterns with extraordinarily high resolution<sup>129</sup>. The externally developing embryos are readily accessible to experimental manipulation by techniques such as microinjection of biologically active molecules (RNA, DNA or antisense oligonucleotides), cell transplantation, fate mapping and cell lineage tracing<sup>130-133</sup>. The genome editing techniques such

as TALENs and CRISPR/CAS9 implemented in the last few years have deeply revolutionized the applications of ZF model, circumventing some limitations of knockdown technique<sup>134</sup>.

### HPG axis in ZF

HPG axis of ZF exhibits remarkable similarity to more evolved vertebrates, preserving the most important reproductive cells and hormones. In humans the triggering of HPG axis cascade of events begins in the hypothalamus by GnRH (gonadotropin releasing hormone) and kisspeptin (Kiss1) secreting neurons<sup>135</sup>. In non-mammalian vertebrates, such as teleosts, this process is conserved but in addition to *kiss1*, there exists a novel *kiss2* gene<sup>136-139</sup>. Researches conducted on ZF demonstrated a different distribution of these two kisspeptin genes in the brain. Kiss1 neurons are located in the ventral habenula, where they play a pivotal role in adaptive behaviors by regulating serotonergic and dopaminergic activities<sup>140,141</sup>, while Kiss2 fibers form a wide network projecting into the telencephalon, the mesencephalon, the hypothalamus and the pituitary where are directly in contact with GnRH3 neurons in the pars distalis<sup>142</sup>.

Despite these slight differences, both in human and ZF species Kisspeptin and GnRH hormones produced by these two neuronal population are essential for the release and fine regulation of the follicle stimulating hormone FSH (also called GTH-I in ZF) and luteinizing hormone, LH (GTH-II in ZF) by gonadotropic cells in the pituitary<sup>143,144</sup>. Indeed with a conserved mechanism kiss2 ZF hormone act on GnRH3 neurons stimulating the secretion of GnRH hormone that is the main regulator of the puberty onset<sup>137,145</sup>. ZF gonadotropins GTH-I and GHT-II produced by gonadotropic cells in response to the stimulation of the GnRH<sup>74,146-149</sup> mediate gametogenesis and steroidogenesis. In particular, FSH/GTH-I is responsible for spermatogenesis in male and folliculogenesis in female<sup>150,151</sup> while LH/GTH-II stimulate steroidogenesis in male acting on the Leydig cell in the testis and in oocyte maturation and growth<sup>149,152,153</sup> (Figure 8).

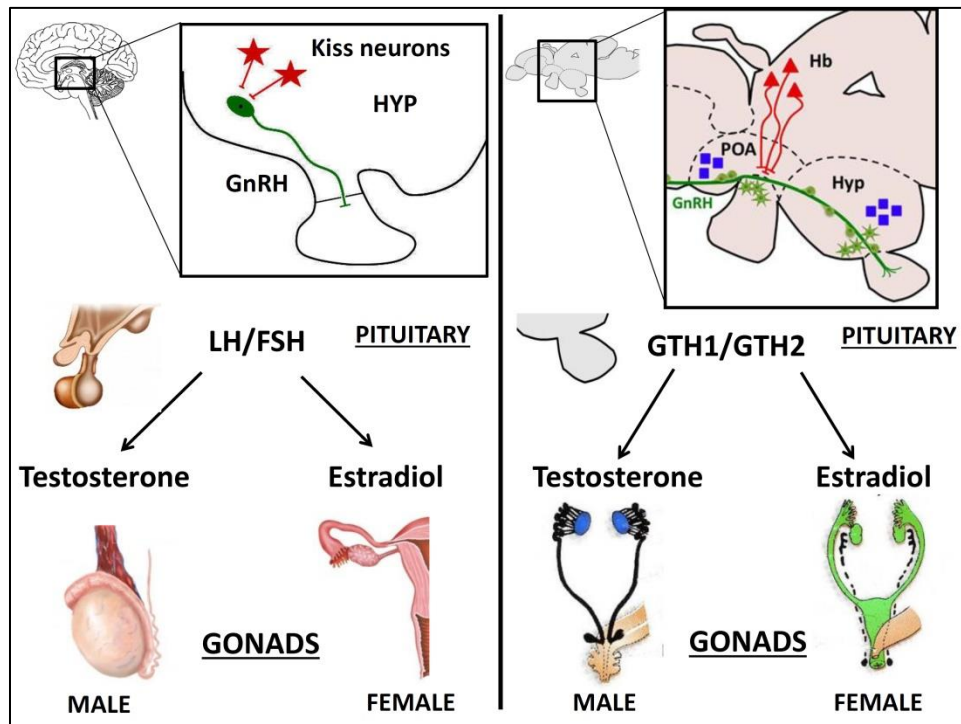


**Figure 8:** HPG axis in human (right) and zebrafish (left). In both organisms, Kiss neurons regulate, in the hypothalamus, GnRH neurons. In zebrafish there are two populations of Kiss neurons: kiss1 neurons (triangle in the figure) are localized in the habenular nucleus (Hb) while kiss2 (square) are more widely scattered in the hypothalamus (Hyp) and preoptic area (POA) (from Bonomi M. *et al.*, Handbook of Models of Human aging ed. 2, in press).

The analysis of GnRH-Gonadotrope-Vasculature architecture in ZF recently revealed a dual mode of gonadotropin regulation challenging the established model of delivery of GnRH3 hormone in this fish<sup>146</sup>.

Indeed in teleosts, a true median eminence has not been identified; instead, direct innervation of the endocrine cells (neuroglandular regulation) has been proposed as the predominant pathway by which the hypothalamus affects the gonadotropic cells<sup>154-159</sup>. Nevertheless using FSH:EGFP and LH:mCherry transgenic zebrafish line<sup>152</sup> Golan and colleagues observed that GnRH3 fibers formed multiple boutons upon reaching the pituitary, but most of these structures were located in the neurohypophysis rather than adjacent to gonadotropes. These GnRH3 boutons are structurally similar to the GnRH varicosities found in the mammalian median eminence and are considered as the release sites of this peptide in mammals<sup>160-163</sup> and in fish<sup>164</sup>. Moreover they found a close association between FSH cells and GnRH3 boutons, but only a fifth of the LH cells

were in contact with GnRH3 axons. These data suggest a more direct regulation of FSH cells rather than LH cells and a combination of neuroglandular and neurovascular delivery mode of GnRH3 hormone in ZF<sup>146</sup>.

#### Hypophysiotropic form of GnRH in ZF

*In vitro* and *in vivo* experiments revealed how hypophysiotropic neurons are dispersed in a loose continuum from olfactory region to hypothalamus. Zebrafish genome possesses only two form of *GNRH* (*gnrh2* and *gnrh3*) missing *GNRH1* mammalian orthologue gene. Expression of *gnrh2* gene is in midbrain tegmentum, identical to human counterpart, while for *gnrh3* is more widely observed in forebrain areas of terminal nerve, ventral telencephalon, POA, and hypothalamus. This expression in POA and hypothalamus, like mammalian GNRH1, and the high homology with human *GNRH1* (80%) suggest a role of *gnrh3* in the regulation of gonadotropins release in zebrafish. This hypothesis was confirmed by its ability to increase the mRNA level of the luteinizing hormone beta (*lhb*) in cultured primary pituitary cells. Moreover injection of kisspeptin-10, a molecule implicated in the pulsatile secretion of GnRH, into the flathead minnow (a fish belonging to the cyprinid family, as zebrafish) increased *gnrh3*, but not *gnrh2* secretion. These evidences demonstrated that in cyprinid fish that have only two forms of *gnrh*, *gnrh3* is the main hypophysiotropic form of GnRH<sup>165</sup>.

#### GnRH3 neurogenesis in ZF

The development of Tg(GnRH3:EGFP) transgenic line by Zohar group has allowed to study in details the embryonic origins of *gnrh3* neurons and their structures during ZF embryogenesis. Using this ZF line they observed that the first fluorescent signal is detectable at 24 hpf in olfactory regions<sup>118,166</sup>. Axons elongation begins at 26 hpf where, from *gnrh3* perikarya clusters located in olfactory placodes, projections begin to extend bilaterally dorsoventrally towards the pallium. This sprouting process continues in the following hours with some branches that arise from these axons and move dorsoventrally, whereas others caudoventrally. Between 32–36 hpf these projections meet caudally at midline to form the first commissure in the subpallium. New fibers arise from the somata around 40 hpf and elongate caudoventrally along the anterior and the optic commissures, to innervate the eyes. Concurrently a fourth set of axons starts its migration toward the hypothalamus. Later, at 48 hpf dorsocaudally axons end their route at the

midline forming a commissure in the pallium. Four distinct *gnrh3* fibers tracts are notable at this developmental stage (48 hpf) in the brain: in the pallium, in the subpallium, along the optic tract to the eyes and in the direction of the hypothalamus (Figure 9). Outside of the brain, *gnrh3* fibers were observed: in the retina, in the perikarya of the trigeminal ganglia and bilaterally along the spinal cord<sup>123,166</sup>.

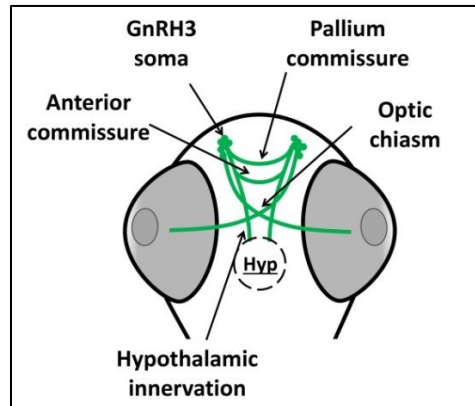


**Figure 9:** Schematic illustration of *gnrh3* fibers at 48 hpf. Four structures are recognizable at this developmental stage: pallium commissure, anterior commissure, optic chiasm and bilateral prolongations that reach hypothalamus (Hyp) (from Bonomi M. *et al.*, Handbook of Models of Human aging ed 2, in press).

These data suggest a common embryonic origin for both olfactory bulb(OB)-terminal nerves (TN) and preoptic area (POA)–hypothalamic GnRH neuronal populations<sup>166</sup>. This hypothesis was supported also by the migration of *gnrh3* somata, that consist of a bilateral stream of neurons moving from the olfactory region through the TN ganglion and ventral telencephalon to the ventral hypothalamus between 3 and 15 dpf. Indeed this migration path seems to use the preexisting vomeronasal-terminal nerves (VNN/TN) fibers as a scaffold, like mammals<sup>118</sup>. Finally, these results are reinforced by the evidence that laser ablation of the soma of *gnrh3* neurons in the nasal area during early development resulted in a complete lack of olfactory, terminal nerve, preoptic area, and hypothalamic *gnrh3* neurons<sup>167</sup>.

Recently, Zohar’s group generated a *gnrh3*<sup>-/-</sup> zebrafish line that harbors a deletion of 62 bp in the *gnrh3* gene<sup>168</sup>. Surprisingly, aside from an increasing of mRNA levels of pituitary gonadotropin genes (*fshb*, *lhb*, and *cga*) only during initial development, no GnRH3 neurogenesis or reproductive defects were observed in such *gnrh3* knockout line. Indeed, characterization of key components of the HPG axis downstream of *gnrh3*, performed in *gnrh3*<sup>-/-</sup> ZF, indicates a normal

gametogenesis and reproductive performance for both sexes<sup>168</sup>. These results seem to be in contrast with previous experiment where *gnrh3*-expressing cells laser ablation in the early phase of zebrafish development (4–6 dpf) leads to infertility<sup>167</sup>, thus opening a discussion about GnRH established role as key reproduction regulator in all species of vertebrates, including zebrafish. Nevertheless authors propose, basing also on knockdown data published in the past<sup>118,167</sup>, that development and correct migration of the *gnrh3* neurons remain fundamental to its appropriate function in ZF as it is demonstrated in humans. To explain the absence of phenotype observed in the *gnrh3*<sup>-/-</sup> ZF model, they postulated that gene knockout could trigger a compensatory mechanism which is not activated by gene knockdown or cells ablation due to different timing or duration of the elimination<sup>168</sup>.

### **ZF as a model to study CHH**

Zebrafish genome sequencing has demonstrated that zebrafish genome presents partial genome duplication. This is the consequence of a whole genome duplication event occurred during evolution in the ray-fin fish lineage, prior to the teleost radiation. After this divergence, the zebrafish genome has been resolving back to a diploid state again<sup>169</sup>. The result is that zebrafish could present two orthologues for the corresponding human gene. Despite this difference a genome analysis revealed that 71.4% of human genes has at least one zebrafish orthologue<sup>170</sup>. Moreover, 82% of human potential disease-related genes can be associated to at least one zebrafish orthologue, making zebrafish one of the most attractive and promising models for understanding the biological activity of human disease-related genes<sup>170</sup>. Due to these strong genome and anatomical conservations, ZF was used as a model for studying genes involved in CHH, such as *KALI* and *KISS1/KISS1R*.

*kalla/kal1b*. Two orthologs of human *KALI* gene were identified in ZF genome called *kalla* and *kal1b*. They present an homology in the amino acids sequences with human *KALI* of 75.5% and 66.5%, respectively. Both proteins shared the same domain structure with human *anosmin-1* that consist of: a cysteine-rich region at N-terminal followed by a whey acidic protein-like (WAP), four fibronectin type III domains, and a C-terminal histidine-rich region except for *anosmin-1b(kal1b)*, where this last domain is missing<sup>171</sup>. *In situ* hybridization experiments revealed for *kalla* transcript, a signal at 38 hpf in the olfactory bulbs, and a lower expression, in

midbrain, tectum, cerebellum, retina and spinal cord<sup>171</sup>. *kallb* mRNA seems to be expressed at later developmental stages (from 48 hpf) in the olfactory epithelium, in the rostral telencephalic area, the cerebral lobes and pronephric ducts<sup>171</sup>. Functional studies showed that downregulation of *kalla* transcript impairs proper axon fasciculation of olfactory neurons, and their terminal targeting at the olfactory bulbs. On GnRH system, *kalla* knockdown abolishes, in the hypothalamus, GnRH-immunoreactive cells, while for *kallb* only a limited reduction in *gnrh3* neurons was observed<sup>172</sup>, suggesting a specific role for *kalla* in the development of the endocrine GnRH system in zebrafish.

*kiss1/kiss2*. Studies conducted in ZF demonstrated that both *kiss1* and *kiss2* increase the number of GnRH3 neurons in zebrafish embryo. Patch clamp recording reveals that, while *kiss1* increases spike frequency and depolarizes membrane potential, *kiss2* exercises the opposite effect suppressing spike frequency and hyperpolarizing membrane potential; this demonstrates a regulatory role of *kiss1* on GnRH neurons<sup>173</sup>.

## *Aim of thesis*

Aim of this PhD work was to apply a multidisciplinary approach to better elucidate the genetic and molecular mechanisms involved in CHH, focusing in particular on the role of *PROKR2* gene.

For this purpose and thank to the availability in our laboratory of the largest Italian cohort of CHH patients (n=512), that was collected in collaboration with several Italian centers belonging to the “Società Italiana di Endocrinologia” (SIE), the “Società Italiana di Andrologia e Medicina della Sessualità” (SIAMS) and the “Società Italiana di Endocrinologia e Diabetologia Pediatrica” (SIEDP), we planned:

1. to perform an extensive genetic screening of this cohort by applying the NGS technique available in our laboratory;
2. to perform a pharmacological characterization of the *PROKR2* gene allelic variants identified in the cohort, in order to evaluate their pathogenic impact on protein membrane translocation and on activation of the principal intracellular pathways;
3. to generate an *in vivo* model of zebrafish, in order to investigate *PROKR2* functions during GnRH neurons migration.

# *Materials and methods*

## **Patients**

The largest biobank of Italian patients affected by CHH (n=512) was collected thanks to the “Network Italiano Ipogonadismo Centrale” (NICE) supported by: Società Italiana di Endocrinologia (SIE), Società Italiana di Andrologia e Medicina della Sessualità (SIAMS) and Società Italiana di Endocrinologia e Diabetologia Pediatrica (SIEDP). The institutional Ethic Committee approved the study and all patients gave their informed consent for the genetic investigations.

## *Genetic analysis*

## DNA Purification from whole blood

Genomic DNA was extracted from 3 ml of blood obtained from CHH patients after adding EDTA according to Gentra® Puregene® Kit Qiagen®. DNA obtained was then diluted to a final concentration of 25 ng/μl and stored at -20°C.

## Next-Generation-Sequencing (N.G.S.) screening

Genetic screening of genomic DNA samples obtained from CHH patients was performed using a multiplex-PCR approach (TruSeq Custom Amplicon, Illumina®). This technology represents the latest advancements to Illumina sequencing, aimed at optimizing data accuracy and research scalability. TruSeq Custom Amplicon (TSCA) is a fully customizable, amplicon-based assay for targeted resequencing. Typical sequencing workflow comprises: design of the panel of interested gene, sample/library preparation, cluster amplification, DNA sequencing, image analysis/base calling, read alignment, and variant discovery (Figure 10).

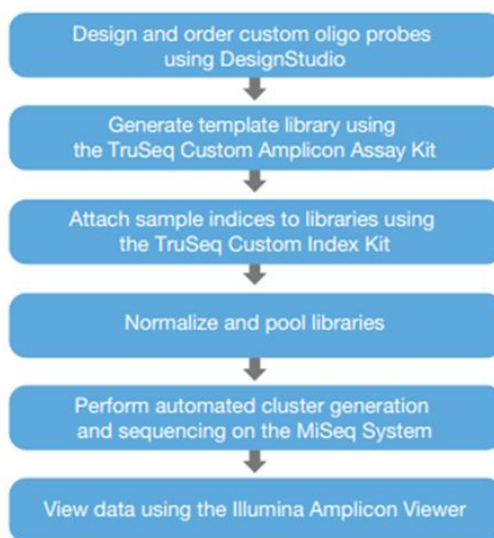


**Figure 10:** Flowchart for TruSeq Custom Amplicon, Illumina®. (adapted from Illumina website, [www.illumina.com](http://www.illumina.com)).

### Design of the panel

Panel of interested gene (*KALI*, *FGF8*, *FGFR1*, *TAC3*, *TAC3R*, *HS6ST1*, *GNRH*, *GNRHR*, *PROKR2*, *PROK2*, *KISS1*, and *KISS1R*) was designed using Illumina DesignStudio® software (<https://designstudio.illumina.com/>). This software is a free interface for custom probe design, providing dynamic feedback to select desired amplicons. Amplicon designs are generated

automatically using an algorithm that considers a range of factors, such as GC content, sequence similarity, presence of repetitive sequences, and possible underlying variants (SNPs). Once design is complete, it is possible to view candidate amplicons covering regions of interest as well as their design scores. For our study the amplicons were designed to cover the entire coding sequences of the mentioned selected genes and 25bp upstream and downstream of each exon.

### Sample/Library Preparation

According to Illumina TruSeq® DNA Sample Preparation Guide kit 250 ng of genomic DNA (gDNA) of each patient were used to prepare DNA library.

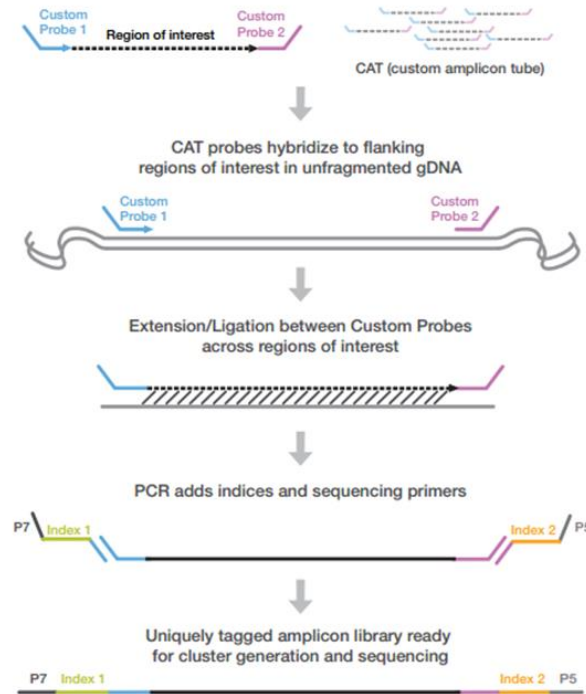


**Figure 11:** Flowchart for preparation of gDNA library. (adapted from Illumina website, [www.illumina.com](http://www.illumina.com)).

a. Hybridization of oligonucleotides pools to gDNA

During this passage a specific pools of oligonucleotides (CAT probes) hybridize to - flanking regions of interest in unfragmented gDNA.

b. Remove Unbound Oligos:

This process removes unbound oligos from genomic DNA using a size-selection filter. Two wash steps using SW1 (Stringent Wash 1) ensure complete removal of unbound

oligos. A third wash step using UB1(Universal Buffer 1) removes residual SW1 and prepares samples for the next step.

c. Extend and Ligate Bound Oligos:

This process connects the hybridized upstream and downstream oligos. A DNA polymerase extends from the upstream oligo through the targeted region, followed by ligation to the 5' end of the downstream oligo using a DNA ligase. The result is the formation of products containing the targeted regions of interest flanked by sequences required for amplification.

d. Amplify Libraries:

This step amplifies the extension-ligation products and add index 1 (i7) adapters, index 2 (i5) adapters, and sequences required for cluster formation.

e. Clean Up Libraries:

Uses of AMPure XP beads purify the PCR products from other reaction components.

f. Normalize Libraries:

This step normalizes the quantity of each library for balanced representation in pooled libraries. Only samples containing DNA require processing through the subsequent steps.

g. Pool Libraries:

Pooling libraries combines equal volumes of normalized libraries in a single tube. After pooling, dilute and denature the library pool before loading libraries for the sequencing run.

### Sequencing using MiSeq<sup>®</sup> sequencer platform

Sequencing was performed using Illumina MiSeq<sup>®</sup> sequencer platform. A single-use MiSeq Reagent Kit was used to perform sequencing run. Each MiSeq reagent kit includes a kit-specific flow cell type and Reagent Cartridge. The flow cell is a single-lane glass-based substrate on which clusters are generated and the sequencing reaction is performed (Figure 14 A). Reagent Cartridge is a single-use consumable consisting of foil-sealed reservoirs pre-filled with clustering and sequencing reagents sufficient for sequencing one flow cell (Figure 14 B).

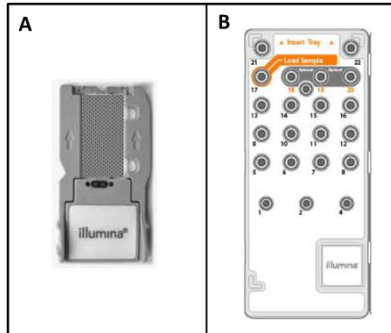


**Figure 14:** Illumina Flow cell©. **B:** Reagent Cartridge.

Before being ready to be loaded in MiSeq® Reagent Cartridge DNA library need to be denaturated.

### Bioinformatic analysis

Once completed the sequencing run, Illumina MySeq® generate a VCF (Variant Call Format) file. This file contain all variant found for each patients filtered for Minor Alleles Frequency (MAF) inferior to 1%.

### **Sanger Sequencing**

Variants identified through N.G.S. analysis have been confirmed by Sanger sequencing. This process consists of 4 steps:

1. Amplification of interested gene by PCR;
2. Electrophoresis on agarose gel of the amplified fragment;
3. Purification of PCR product;
4. Sequencing reaction;
5. Analysis by automated DNA-sequencer

### Amplification of the gene by PCR

For each gene, the reaction mix was prepared by the following protocol:

Template DNA	100 ng
Buffer 5X	5.0 $\mu$ l
Primer Forward (10 pmol)	1.25 $\mu$ l
Primer Reverse (10 pmol)	1.25 $\mu$ l
dNTPs mix (10Mm each)	0.5 $\mu$ l
Go Taq Promega <sup>TM</sup> (5U/ $\mu$ l)	0.25 $\mu$ l
DDW	Up to 25 $\mu$ l

The amplification of the fragment was performed in a Thermal Cycler

### Electrophoresis on agarose gel

Each PCR product is checked on 3% agarose gel that separates DNA fragments between 100 and 1000 base pair. Gels were prepared with TAE 1X buffer (0.04M Tris-acetate, 0.002M EDTA) and amended with the intercalating agent Midori Green (Bulldog Bio). Five  $\mu$ l of the sample were loaded and run onto the gel applying a 130mV voltage for around 30 minutes. In order to verify the presence of a PCR product, the gel is placed on an UV transilluminator that makes the bands visible; the molecular weight can be compared with molecular weight marker 100bp DNA Ladder (Euroclone).

### Purification of amplified fragment

In order to purify enzymes, nucleotides and salts from the previous reaction, purification of the remaining volume of PCR is performed by Amersham Biosciences, GFX<sup>TM</sup> PCR – DNA and Gel Band Purification Kit. Purification protocol was performed as recommended by the manufacturer.

### Sequencing reaction

Sanger sequencing is based on the selective incorporation of chain-terminating nucleotides by DNA polymerase during in vitro DNA replication. The sequencing reaction necessitates, a

single strand DNA as template, one DNA primer, and Big Dye Terminator mix 3.1 (Perkin Elmer) containing dNTPs, Amplitaq DNA Polymerase, MgCl<sub>2</sub> and modified di-deoxynucleotidetriphosphates (ddNTPs): these nucleotides that terminate DNA amplification, since lacking a 3'-OH group necessary for the formation of a phosphodiester bond between nucleotides; moreover, ddNTP are fluorescently labeled with different colours: Adenine: "HEK" green, Cytosine: "FAM" blue, Guanine: "NED" black and Thymine: "ROX" red. Amplitaq DNA Polymerase is characterized by two mutations, one in the active domain, that enables it to incorporate ddNTP in the DNA structure, and one in the N-terminus domain, which eliminates 3'-5' exonuclease activity.

Sequencing reactions of gene fragments were performed with both sense and antisense primers, in order to sequence the full length of the fragments. Then, sequence product is purified by ddNTPs and salts by CENTRI-SEP Spin Columns (Princeton Separations).

#### Analysis by automated DNA-sequencer

The principle of sequencer is based on capillary electrophoresis, where DNA molecules of different size migrate in solution under the influence of an electric field. The shorter the fragments are, the fastest they are absorbed on the chromatographic column; then, they are hit by a laser that will excite the fluorescent molecule bound to the ddNTP, releasing a signal that will be detected by the analyzer according to the four different colours. The analysis of the detected signals was done by the software ABI PRISM® 310 Genetic Analyzer (Perkin Elmer Applied Biosystem, Foster City, USA) and sequence analysis was performed by Sequencing Analysis Navigator (Perkin Elmer Applied Biosystem, Foster City, USA): the output is an electropherogram, a profile of peaks of different height and colour that identify the four DNA bases.

## ***PROKR2 in vitro analysis***

## Creation of plasmids

In order to perform functional studies, *PROKR2* wild-type (wt) sequence was ordered by Missouri S&T cDNA Resource Center, USA and inserted in SPRT-pcDNA3 plasmid (Figure 15).

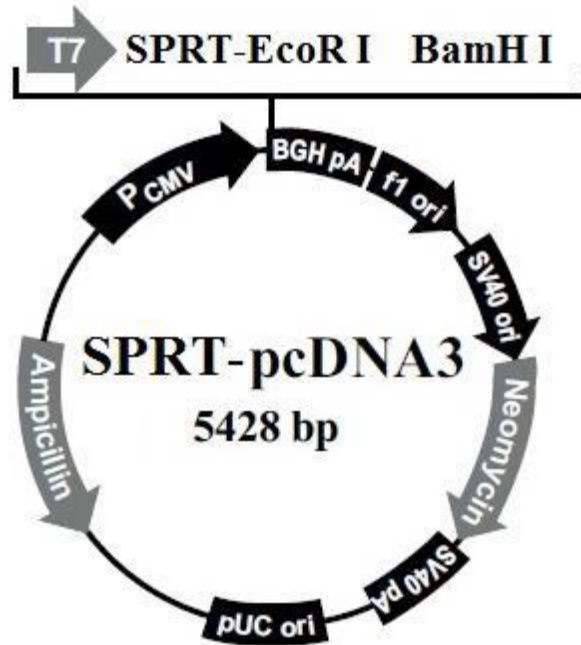


Figure 15: Schematic representation of SPRT-pcDNA3 vector.

SPRT-pcDNA3 vector includes, at the 5' end, a SPRT sequence which is translated in frame with the cloned protein at the N-terminal domain. This sequence includes a *signal peptide* (SP), for the secretion of the delivery of the protein to the cytoplasmatic membrane, and a *rhodopsin tag* (RT), a 20-AA peptide derived from bovine rhodopsin.

### Mutagenesis PCR

Plasmids containing the 8 variants of *PROKR2* gene identified in our study by genetic analysis were generated by mutagenesis of SPRT-pcDNA3-*PROKR2* plasmid. The mutant constructs were produced using QuickChange™ Site-Directed Mutagenesis Kit (Stratagene). *Pfu Turbo*® DNA polymerase, which has a high proofreading activity, amplifies both strands starting from synthetic oligonucleotides, of which one contains the mutation of interest (Table 1). Primer pairs were 40 bp and designed in order to have same T<sub>m</sub>.

The sense primer carries the mutation at half of the total length, and can bind specifically to the target sequence. The antisense primer is always WT and has a 20 bp-overlap with the coupled sense primer.

The PCR products were checked by loading on 1% agarose gel with 1µl Gel Loading 6X, and run applying a constant voltage of 130 Volt for 30'. Gel was then placed on a UV transilluminator and the interest band was identified by comparison with molecular weight 1kb DNA Ladder (Invitrogen).

<b>R47W</b>	<b>FW:</b> GGATGAGGATGAGGACATGACCAAGACCTGGACCTTCTTC <b>REV:</b> GGTCTTGGTCATGTCCTCATCCTCACCATAGGGAGGTCAT
<b>M64V</b>	<b>FW:</b> CGTCATTGGCATTGCACTGGCAGGCATCGTGCTGGTCTGC <b>REV:</b> GATGCCTGCCAGTGCAATGCCAATGACGATCTTGGCTGCG
<b>G70S</b>	<b>FW:</b> GGCAGGCATCATGCTGGTCTGCGGCATCAGTAACTTTGTC <b>REV:</b> GATGCCGCAGACCAGCATGATGCCTGCCAGTGCAATGCCA
<b>R85H</b>	<b>FW:</b> GCTGCCCTCACCCGCTATAAGAAGTTGCACAACCTCACCA <b>REV:</b> GCAACTTCTTATAGCGGGTGAGGGCAGCGATAAAGACAAA
<b>D99N</b>	<b>FW:</b> TCTGCTCATTGCCAACCTGGCCATCTCCA ACTTCCTGGTG <b>REV:</b> GAGATGGCCAGGTTGGCAATGAGCAGATTGGTGAGGTTG
<b>C208S</b>	<b>FW:</b> TATTGTCAAGAGCCAGGAGAAGATCTTCAGTGGCCAGATC <b>REV:</b> GAAGATCTTCTCCTGGCTCTTGACAATAAAGAGGACCGTT
<b>M278K</b>	<b>FW:</b> TGCCGCAGGAAGACGGTCTGGTGCTCAAGTGCATTCTCA <b>REV:</b> TGAGCACCAGGACCGTCTTCTGCGGCAGCGCAGCCGCTT
<b>P290S</b>	<b>FW:</b> TCTCACGGCCTATGTGCTGTGCTGGGCATCCTTCTACGGT <b>REV:</b> TGCCAGCACAGCACATAGGCCGTGAGAATGCACATGAGC

**Table 1:** Primers used for mutagenesis of *PROKR2*.

#### Enzymatic digestion with DpnI

PCR products were then digested with Dpn I (New England Biolabs) which, binding methylated sequence Gm6ATC, degrades WT templates in the reaction (*E. coli* DNA is indeed methylated) and leaves neo-synthesized DNA that contain the mutation.

Seventeen  $\mu$ l of PCR products are digested for 2 hours at 37° C, with 10 units of Dpn I (1 $\mu$ l) and 2 $\mu$ l of NEB 4 buffer (50mM Potassium acetate; 20mM Tris-acetate; 10mM Magnesium acetate; 1mM DTT pH=7,9 at 25 °C) (New England Biolabs).

### Transformation of bacterial cells

*E. coli* competent cells were transformed by One Shot® TOP10 (Invitrogen) as recommended by the manufacturer.

### PCR on colonies from plates

6 colonies from selective LB agar plates were selected, grown in LB added with ampicillin 50mg/ml for 5 hours at 37°C, at 170 rpm. Then, a PCR following the same protocol reported in “Amplification of the gene by PCR” using T7 and 741R primers indicated in Table 2. The clones were then verified by sequencing in order to verify that further mutations were not inserted by random mutagenesis in the DNA, as described in the section " Sequencing reaction”, while the primers used for the different reactions are the following:

<b>Primer T7</b>	TAATACGACTCACTATAGGG
<b>247Fw</b>	AAGTTGCGCAACCTCACC
<b>495Fw</b>	AATTATCAAACGGCCTCC
<b>724Fw</b>	TGCTATGCCAGGATCTCC
<b>741Rev</b>	GGAGATCCTGGCATAGCA
<b>930Fw</b>	TACCTCACTGCCTTCTACGTGG
<b>1130Rev</b>	TTCAGCCTGATACAGTCC

**Table 2:** primers used for the sub-cloning of *PROKR2* gene.

### Maxiprep

In order to obtain highest yield of plasmidic DNA (around hundreds of  $\mu$ g) of the selected clone, the DNA was extracted by PureYield™ Plasmid Maxiprep System (Promega), following the manufacturer’s instructions. Plasmidic DNA was then quantified by spectrophotometer.

## Cell culture

For *in vitro* studies were used two cellular lines HEK 293 and COS7. HEK 293 is for Human embryonic kidney cells 293, a specific cell line originally derived from human embryonic kidney cells grown in tissue culture. COS (an abbreviation for CV-1 in Origin with SV40 genes) cells are a laboratory cell line derived in the 1960s from African Green Monkey, (*Cercopithecus aethiops*) kidney tissue. Both cells lines grow adherently to glass and plastic in culture and were maintained at 37 °C and 5% CO<sub>2</sub> in a complete growth medium DMEM+GlutaMAX™-I (Dulbecco's Modified Eagle's Medium, Gibco) additioned with 10% FBS (fetal bovine serum, Gibco), 1% Pen:Strep and 1% Fungizone.

### Transfection Protocol

Cells were transfected with FuGENE® HD transfection reagent (Promega) following the manufacturer's instructions. The FuGENE® HD Transfection Reagent is a nonliposomal formulation designed to transfect DNA into a wide variety of cell lines with high efficiency and low toxicity. Following protocol is divided for COS7 and HEK293 cells and for FACS, Western Blot, Immunofluorescence, Radioimmuno and Elisa assays.

Day 1:

- Plate  $2 \times 10^6$  HEK 293 cells in 100mm Petri dishes;
- Plate  $2 \times 10^6$  COS7 cells were in 100mm Petri dishes;

Day 2:

- Split HEK 293 in a 6-well dishes seeding  $2 \times 10^5$  cells/well for FACS analysis;
- Split HEK 293 in a 6-well dishes seeding  $2 \times 10^5$  cells/well for Western Blot analysis;
- Split HEK 293 in a 96-well dishes seeding  $2 \times 10^5$  cells/well for RIA analysis;
- Split HEK 293 in a 96-well dishes seeding  $2 \times 10^4$  cells/well for IP1-ELISA analysis;
- Split COS7 in a 6-well dishes seeding  $4 \times 10^4$  cells/well for Immunofluorescence analysis;

Day 3:

- Mix 93,5 µl DMEM+GlutaMAX™-I (Dulbecco's Modified Eagle's Medium, Gibco), 2,5 µg of plasmidic DNA;
- Add to the mix 4µl di FuGENE® and incubate for 15 minutes.

- Add 100 ul of the mix to cultured cells.

Day 4:

- Aspire cells medium;
- Add 2 ml of new DMEM+GlutaMAX™-I (Dulbecco's Modified Eagle's Medium, Gibco) additioned with 10% FBS (fetal bovine serum, Gibco), 1% Pen:Strep and 1% Fungizone.

Day 5:

Functional study. Every experiment was conducted as a duplicate and repeated twice. Cells transfected with SPRT-pcDNA3 vector (empty vector) were used as negative control.

### **Fluorescence-activated cell sorting (FACS)**

Fluorescence-activated cell sorting (FACS) is a specialized type of flow cytometry. It provides a method for sorting a heterogeneous mixture of biological cells into two or more containers, one cell at a time, based upon the specific light scattering and fluorescent characteristics of each cell. It is a useful scientific instrument as it provides fast, objective and quantitative recording of fluorescent signals from individual cells. HEK 293 cells were transfected according to previous protocols and analyzed using FACScalibur™ Flow Cytometer - 3 Colors. Analysis was conducted on not-permealized HEK 293 using MAb anti-RT primary antibody gently provided by Dr. Sabine Costagliola (IRIBHM, ULB, Bruxelles, Belgium).

### **Western Blot assay**

The Western Blot (sometimes called protein immunoblot) is a widely used analytical technique used in molecular biology, immunogenetics and other molecular biology disciplines to detect specific proteins in a sample of tissue homogenate or extract. Protein were extracted from HEK 293 cells using RIPA buffer (10mM Tris-HCl pH 7.5, 500 mM NaCl, 0,1% SDS, 1% NP40, 1% sodium deoxycholate, 2 mM EDTA, 2 mM Na<sub>2</sub>VO<sub>4</sub>, 2 mM Na<sub>4</sub>P<sub>2</sub>O<sub>7</sub>, 2mM NaF).

### Protein quantification

For protein quantification we used Thermo Scientific™ Pierce™ BCA Protein Assay. A detergent-compatible formulation based on bicinchoninic acid (BCA) for the colorimetric detection and quantitation of total protein. This method combines the well-known reduction of  $\text{Cu}^{+2}$  to  $\text{Cu}^{+1}$  by protein in an alkaline medium (the biuret reaction) with the highly sensitive and selective colorimetric detection of the cuprous cation ( $\text{Cu}^{+1}$ ) using a unique reagent containing bicinchoninic acid. The purple-colored reaction product of this assay is formed by the chelation of two molecules of BCA with one cuprous ion. This water-soluble complex exhibits a strong absorbance at 562nm that is nearly linear with increasing protein concentrations over a broad working range (20-2000 $\mu\text{g/mL}$ ). A standard curve was used to determine the protein concentration of each sample.

### Sodium Dodecyl Sulphate - PolyAcrylamide Gel Electrophoresis (SDS-PAGE)

SDS-PAGE is a technique used in molecular biology to separate biological macromolecules, usually proteins according to their electrophoretic mobility. Mobility is a function of the length, conformation and charge of the molecule. A chemical denaturant (sodium dodecyl sulfate or SDS) is added to turn the molecule into an unstructured linear chain whose mobility depends only on its length and mass-to-charge ratio. In most proteins, the binding of SDS to the polypeptide chain imparts an even distribution of charge per unit mass, thereby resulting in a fractionation by approximate size during electrophoresis.

For signal development we used Thermo Scientific™ Pierce™ ECL Plus Western Blotting Substrate, an highly sensitive, nonradioactive, enhanced acridan-based chemiluminescent/chemifluorescent substrate for the detection of horseradish peroxidase (HRP) on immunoblots. The reaction of the acridinium ester intermediates with peroxide produces a prolonged chemiluminescence, which can be visualized on X-ray film or an imaging system.

### **Immunofluorescence assay**

Immunofluorescence (IF) technique uses the specificity of antibodies to their antigen to target fluorescent dyes to specific biomolecule targets within a cell, and therefore allows visualization of the distribution of the target molecule through the sample. Indirect IF uses two antibodies. The

primary antibody is unconjugated and a fluorophore-conjugated secondary antibody directed against the primary antibody is used for detection.

COS7 cells were grown in 6-wells plates and transfected according to transfection protocols previously described. MAb anti-RT was used as primary antibody and Anti-Mouse IgG whole molecule-FITC produced in goat as secondary antibody. Pictures of microscope slides were taken using Nikon C2<sup>+</sup>®.

### **Radioimmunoassay (RIA)**

Radioimmunoassay (RIA) is an *in vitro* assay that measures the presence of an antigen with very high sensitivity. Any biological substance for which a specific antibody exists can be measured at nanomolar and picomolar concentrations. The target antigen is labeled radioactively and bound to its specific antibodies (a limited and known amount of the specific antibody has to be added). Sample is then added in order to initiate a competitive reaction of the labeled antigens from the preparation, and the unlabeled antigens from the serum-sample, with the specific antibodies. The competition for the antibodies will release a certain amount of labeled antigen. This amount is proportional to the ratio of labeled to unlabeled antigen. A binding curve can then be generated which allows the amount of antigen to be derived. For cAMP determinations, culture medium was removed 48 h after transfection and replaced by Krebs-Ringer-HEPES buffer for 30 min. Thereafter, cells were incubated for 60 min in fresh Krebs-Ringer-HEPES buffer supplemented with 25 M phosphodiesterase inhibitor Rolipram (Laboratory Logeais, Paris, France) and various concentrations of highly purified PROK2 10-7M (Fitzgerald Industries International). At the end of the 1-h incubation, the medium was discarded and replaced with 0.1 M HCl. The cell extracts were dried in a vacuum concentrator, resuspended in water, and diluted appropriately for cAMP evaluations by RIA according to the method of Brooker *et al.*<sup>174</sup>. Duplicate samples were assayed in all experiments. Results are expressed in picomoles of cAMP/ml. Concentration-effect curves were fitted with the Prism computer program (GraphPad Software, Inc., San Diego, CA), and EC50 values were determined.

## **IP-One ELISA**

For this experiment we used Cisbio IP-One ELISA assay kit®. This assay has been designed to monitor the activation of Phospholipase C (PLC) coupled receptors, which carry information within the cell. the activation triggers the release of D-myo-inositol 1,4,5 trisphosphate (IP3) resulting in a transient increase of intracellular Ca<sup>2+</sup>. The IP3 lifetime within the cell is very short (less than 30 sec) before it is transformed into IP2 and IP1. When LiCl is added to the culture medium, the degradation of IP1 into myo-inositol is inhibited, and IP1 can therefore accumulate in the cell. Then, after receptor activation, IP1 can be precisely quantified using the IP-One assay.

Every experiment was conducted as a duplicate and repeated twice. For each well the OD (optical Density) at 620 nm were subtract from the OD at 450 nm. Average was calculated from duplicates of each standard, sample and NSB (nonspecific binding).

Average net OD = Average bound OD – Average NSB OD

Calculate % B/BO = divide the net OD for each standard and sample by standard CO net OD and multiply by 100

## *PROKR2 in vivo analysis*

## Maintenance of zebrafish

Breeding fish were maintained at 28°C on a 14 hours light/10 hours dark cycle. They are bred in 3-5 litre tanks in three different systems (Figure 16). Embryos were collected by natural spawning and staged according to what described by Kimmel and colleagues<sup>126</sup>. They are raised in an incubator at 28°C in fish water with 0,1% Methylene Blue in petri dishes.



**Figure 16:** ZebTEC Active Blue Stand Alone® system present in our lab (Tecniplast™).

Stock solution for fish water: 34 g of Instant Ocean Sea Salt dissolved in 1 l of deionised H<sub>2</sub>O.

Fish water: 50 ml of stock solution in 10 l of deionised H<sub>2</sub>O.

We used the following zebrafish lines:

wild type (wt):

- AB strain: obtained from Wilson lab, University College London

transgenic and knockout lines:

- Tg:GnRH3-EGFP strain provided by Gothilf lab, Tel-Aviv University, Tel-Aviv
- *prokr1b*<sup>ct814/ct814</sup> knockout strains provided by Prober lab, Caltech Institute, US-CA.

## **Real-Time qRT-PCR**

Real-Time qRT-PCR (Real-Time Quantitative Reverse Transcription PCR) is used for the detection and quantification of RNA targets. This technique use fluorescent reporter molecules (SYBR™ Green) to monitor the production of amplification products during each cycle of the PCR. Before the Real-Time PCR, this technique requires the extraction of RNA from tissues and then its retrotranscription in cDNA.

### Total RNA extraction

Total RNA is extracted from embryos of different developmental stages using the TRIzol™(Thermo Fisher Scientific). Total RNA were extracted from pools of 20 embryos for each developmental stage using TRIzol™ Reagent and resuspended the in 20–50 µl of RNase-free water, 0.1 mM EDTA, or 0.5% SDS solution.

### RT-PCR (Reverse Transcription-Polimerase Chain Reaction)

The reaction was carried out following the protocol of SuperScript ® III First-Strand Synthesis System for RT-PCR (Invitrogen).

### Real-Time PCR

Real-time analysis was performed using ABI PRISM™ 7900HT Fast Real-Time PCR System. For each developmental stage 50 ngr of cDNA were used. Elongation factor 1-alpha 1 (eEF1a1) gene was used as endogenous control. Quantification of the targets were normalized using the comparative CT method (also known as the  $\Delta\Delta CT$  method), after ensuring that the targets and endogenous control had similar or relatively equivalent PCR efficiencies. Each experiment was conducted as a triplicate and repeated three times.

The following primers were used:

<i>prokr1a</i> FW	5' TTGTGCTTTGTGTCTCCATTAAC 3'
<i>prokr1a</i> REV	5' TTATCCAGACCCCAAATATAAGC 3'
<i>prokr1b</i> FW	5' AGGTTTTGTGCGCCTCAGTTAAT 3'
<i>prokr1b</i> REV	5' CGACCCACACTCCTGTGATCAAA 3'
<i>eef1a</i> FW	5' CTGGTGTCTCAAGCCTGGTA 3'
<i>eef1a</i> REV	5' ACTTGACCTCAGTGGTTACATTGG 3'

### Synthesis of probes for *In Situ* Hybridisation (ISH)

To perform an *in situ* hybridisation assay we synthesised two probes: a RNA antisense probe and a control RNA sense probe that is identical to endogenous transcript and consequently should not bind to the mRNA during the hybridisation, the last one is necessary to verify the specificity of the RNA–antisense probe. In order to synthesised the probes we designed two primers to amplify a 500 bp long sequence for *GnRH3*, *prokr1a* and *prokr1b* . Then we performed a RT-PCR reaction on total RNA extracted from 26 hpf (hours post fertilisation) embryos.

The following primers were used:

<i>prokr1a</i> FW	5'GGTACATGGCTATCGTTCACC 3'
<i>prokr1a</i> REV	5'CCTAACGCTCACAAAGCACA 3'
<i>prokr1b</i> FW	5'ATATGGCCATCGTTCATCCT 3'
<i>prokr1b</i> REV	5'CAGAACGATCCGCTTGAAGT 3'
<i>GnRH3</i> FW	5' AGCATGGAGTGGAAAGGAAG 3'
<i>GnRH3</i> REV	5' AGCCCATCTGTTCCTTCAGT 3'

## Cloning and transformation reaction

The RT-PCR product was cloned in the pCR<sup>®</sup>II-TOPO<sup>®</sup> vector (Figure 17) following manufacturer's instructions of TOPO TA Cloning<sup>®</sup> kit (Invitrogen), that provide for the cloning of PCR product in the plasmidic vector and then its bacteric transformation using One Shot<sup>®</sup> TOP10 (Invitrogen) competent cells. pCR<sup>®</sup>II-TOPO<sup>®</sup> vector has two promoters Sp6 and T7 in order to synthesise the antisense and sense probes (Figure 17.).

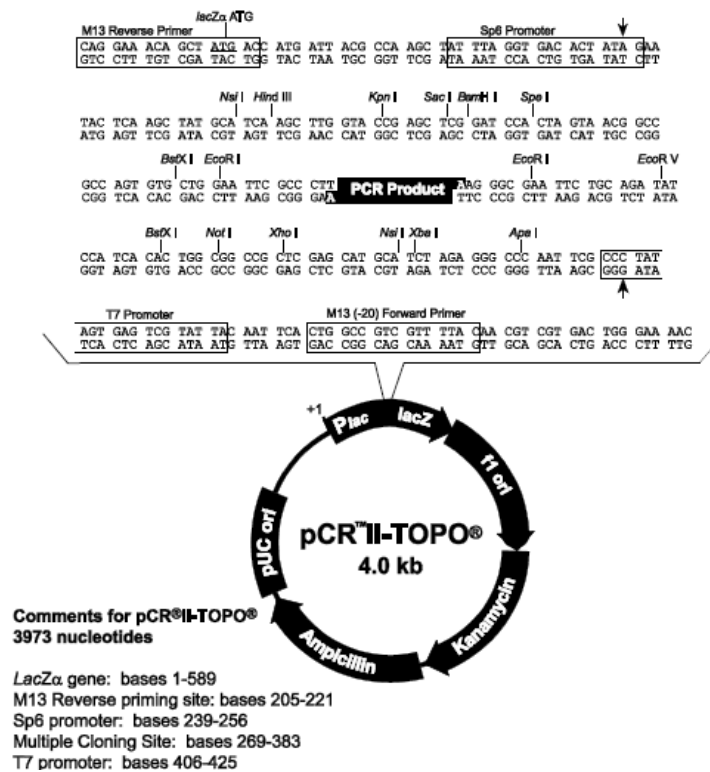


**Figure 17:** schematic representation of the pCR<sup>®</sup>II-TOPO<sup>®</sup> vector. (from TOPO<sup>®</sup> TA Cloning<sup>®</sup> Kit user manual Invitrogen).

## Isolation of plasmid DNA

Recombinant colonies were screened and preparation of plasmid was performed using PureYield<sup>™</sup> Plasmid Maxiprep System (Promega) according to the manufacturer's instructions. The extracted plasmidic DNA was run on 1% agarose gel. The preparation was verified by DNA sequencing on both strands in order to understand the insert orientation and so to decide the restriction enzymes to linearise the plasmid in order to perform the probes synthesis

### Probes labelling and synthesis

The linearized plasmids were then used as templates for antisense and sense digoxigenin-UTP labelling and for *in vitro* riboprobe synthesis following the DIG RNA Labeling Kit (SP6/T7; Roche) manufacturer's instructions.

### RNA quantification

Probes were run on 1% agarose gels and scanned using a Typhoon 9220 Imager (Amersham Pharmacia Biotech, UK) using Typhoon Scanner Control Software (release 2.0). Densitometric quantitation of the bands was performed using Windows ImageQuant 5.1 Software.

## **Whole mount *In Situ* Hybridisation (WISH)**

Embryos at the appropriate stage were fixed in 4% paraformaldehyde (PFA)/ phosphate buffered saline (PBS) over night at 4°C; then they were dechorionated and the embryos were dehydrated in 100% methanol and stored at -20°C until processed for whole mount *in situ* hybridisation as described by Jowett and colleagues<sup>175</sup>.

## **Loss of function analysis**

We tested two different antisense morpholino oligonucleotides (MOs) for both *prokr1a* and *prokr1b*. All of them were splice-blocking MO synthesised by Gene Tools LLC (Oregon, USA). The morpholino sequences are the following:

*prokr1a*SPL1: 5' ATTTAAGACAAGCACTCACCTGTCC 3'

which corresponds to the putative exon 1/ intron 1 boundary of zebrafish *prokr1a*;

*prokr1a*SPL2: 5' TGTACCTGTTGAATACAGAACGTGA 3'

which targets the putative intron 1/exon 2 boundary of zebrafish *prokr1a*;

*prokr1b*SPL1: 5' AGTATGTAAATCCCCTGACCTGTC 3'

which corresponds to the putative exon 1/ intron 1 boundary of zebrafish *prokr1b*;

*prokr1b*SPL2: 5' TATACCTGAACACAGAGACCACAGT 3'

which corresponds to the putative intron 1/exon 2 boundary of zebrafish *prokr1b*;

Morpholinos were dissolved in Danieau's solution (58 mM NaCl; 0,7 mM KCl; 0,4 mM MgSO<sub>4</sub>·H<sub>2</sub>O; 0,6 mM Ca(NO<sub>3</sub>)<sub>2</sub>; 5 mM Hepes pH 7.2) at 2 mM concentration and stored at –80°C.

Embryos were microinjected at the 1–4 cells stage and Rodamin dextran (Molecular Probes) was usually co-injected as a tracer. As a negative control we injected standard control morpholino (*ctrl*-MO) that targets human  $\beta$ -globin gene. This oligo has not been reported to have other targets or generate any phenotypes in any known test system except human  $\beta$ -thalassemic hematopoietic cells.

*Ctrl*-MO: 5' CCTCTTACCTCAGTTACAATTTATA 3'

About 40 embryos are aligned on the edge of a slide that is placed in a 100 mm petri dish. The microinjections were performed by the “Micromanipulator 5171” (Eppendorf) and the microinjector “Cell Tram Oil” (Figure 18).



**Figure 18:** microinjection equipment.

After injection embryos were raised in fish water at 28°C and observed up to the stage of interest. Imaged embryos after 24 hpf were treated with PTU 1X (1-Phenil-2-thiourea, SIGMA; stock PTU 10X 0.015 g of PTU powder in 50 ml of fish water) to inhibit pigment formation (Westerfield, 1995). For a better observation the injected embryos are anaesthetized using tricaine 1X (Ethyl 3-aminobenzoate methanesulfonate salt, SIGMA; stock tricaine 25X 0.08 g in 20 ml of distilled H<sub>2</sub>O) in fish water and PTU 1X. Injected embryos (morphants) were embedded at 48 hpf in UltraPure™ Low Melting Point Agarose (Thermo Fisher Scientific) and photographed using confocal laser scanning microscope Nikon C2<sup>+</sup>® with 20X lens.

### **Generation of Tg:GnRH3-EGFP/*prokr1b*<sup>ct814/ct814</sup> line**

To generate Tg:GnRH3-EGFP/*prokr1b*<sup>ct814/ct814</sup> line we crossed Tg:GnRH3-EGFP line with *prokr1b*<sup>ct814/ct814</sup> fish obtaining Tg:GnRH3-EGFP/*prokr1b*<sup>ct814/wt</sup> line. Fish generated by this mating (F1 generation) were raised, screened at 24 hpf for EGFP and incrossed generating F2 generation. Fin clipping were performed in order to isolate genetic material from individual fish for the purpose of genotyping. A small amount of tissue is clipped from the end of the tail in order to extract DNA which will be used for further analysis such as PCR.

Procedure:

- Fish were anesthetized by immersion in 0.02% MS-222 (tricaine) at neutral pH until gill movement is slowed. Stock preparation is 4g/L buffered to pH 7 in sodium bicarbonate (at 2:1 bicarb to MS-222). The dosage for adult anesthesia is 168ug/ml or 4.2ml stock solution in 100 ml water. The anesthetized fish is then transferred immediately onto a petri dish or clean surface using a plastic spoon. The fin is clipped with a razor blade, surgical scissors or scalpel at a point not greater than halfway between the tip of the fin and the point where the scales end. No more than 50% of the fin area were removed.
- Fish are then immediately transferred to a container with fresh system water and monitored continuously until they are recovered and the ability to right themselves.
- Tissue removed were put in a labeled 1.5 ml Eppendorf containing 50 µl lysis buffer (10 mM Tris pH 8, 2 mM EDTA, 0.2% Triton X-100, 200 µg/ml Proteinase K).

- Samples were put at 55 °C overnight.
- To inactivate proteinase K sample were heated at 95 °C for 15 minutes.

Genomic DNA was used as template for PCR.

*prokr1b*<sup>ct814/ct814</sup> fish contains a 1 bp deletion (nucleotide 12 of the open reading frame: 5'-C-3'), which results in a change in reading frame after amino acid 4 and a premature stop codon after amino acid 13 compared to 396 amino acids for the WT protein.

Primer used for genotyping are the following:

<i>prokr1b</i> Gen FW	5' TGAGCGTAATGCTAATGGTCT 3'
<i>prokr1b</i> Gen REV	5'CCAGAGTGGCGATAAACACA 3'

PCR products were purified and sequenced in the same way described in Sanger sequencing section to identify Tg:GnRH3-EGFP/*prokr1b*<sup>ct814/ct814</sup> fish.

At 48 hpf fish were embedded in UltraPure™ Low Melting Point Agarose (Thermo Fisher Scientific) and photographed using confocal laser scanning microscope Leica TCS SP8® with 20X and 40X lens.

# *Results*

## *Genetic analysis*

## CHH patients cohort composition

Genetic analysis was performed on a cohort of 512 CHH patients composed by 38% affected by Kallmann Syndrome (KS) and 62% normosmic CHH. For KS patients, 24% were female and 76% male, while for nCHH 75% male and 25% female (Figure 19).

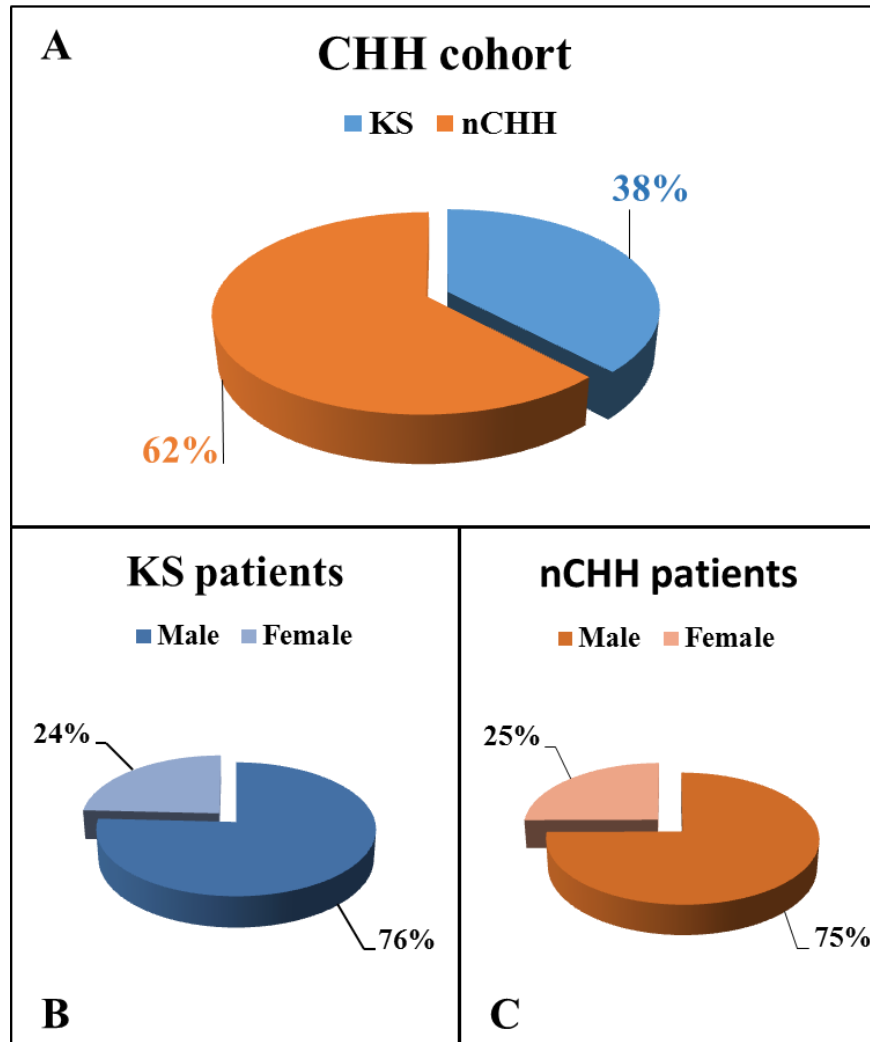


**Figure 19:** Chart A represent KS and nCHH patients composition of CHH cohort analyzed while B and C represents sex imbalance for single pathologies.

## Genetic analysis of CHH variants

Genetic analysis revealed the presence of variants in 32.2% of patients. A total of 204 variants were identified in our cohort, the majority of them (140) were missense variants (Table 3).

	KS	nIHH	Total
<i>Missense</i>	52	88	140
<i>Nonsense</i>	8	5	13
<i>Frameshift</i>	11	11	22
<i>Deletions</i>	4	3	7
<i>Insertions</i>	2	1	3
<i>Others</i>	7	12	19
<i>Total</i>	84	120	204

**Table 3:** genetic variants identified in CHH cohort divided for type of mutations.

Analysis of variants displayed that 23.8% were monoallelic, 3.8% biallelic and 4.6% were digenic (Figure 20).

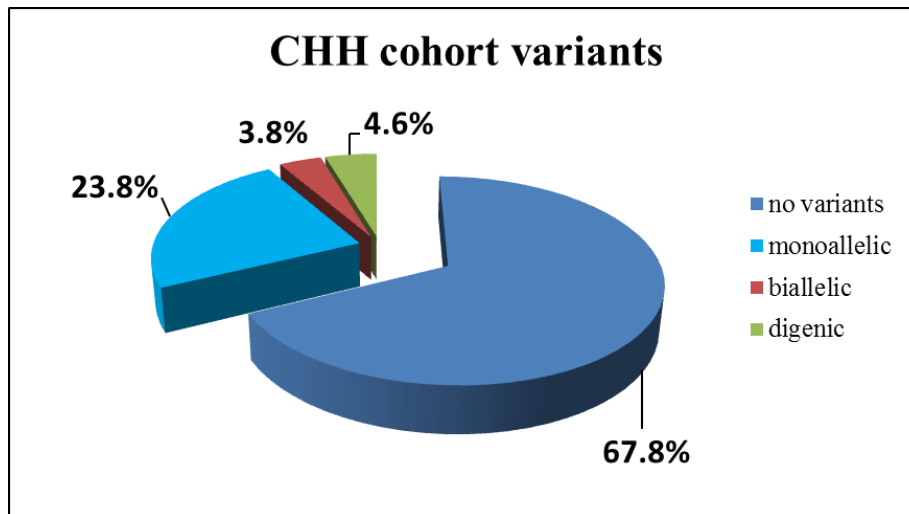


**Figure 20:** Chart representing variants distribution among CHH cohort. No variants: patients with no mutation on analyzed genes; monoallelic: patients carrying variants on one allele; biallelic: patients with mutation on both alleles of a single gene; digenic: patients carrying mutation on more than one gene.

Variants distribution among genes showed that *FGFR1*, *PROKR2*, *GNRHR*, *KALI* and *TACR3* genes resulted the most mutated in our cohort with 12.5%, 7.5%, 6.3%, 5.6% and 4.8% of

patients carrying rare variants, respectively. No mutations were founded in *HS6ST1* gene (Figure 21).

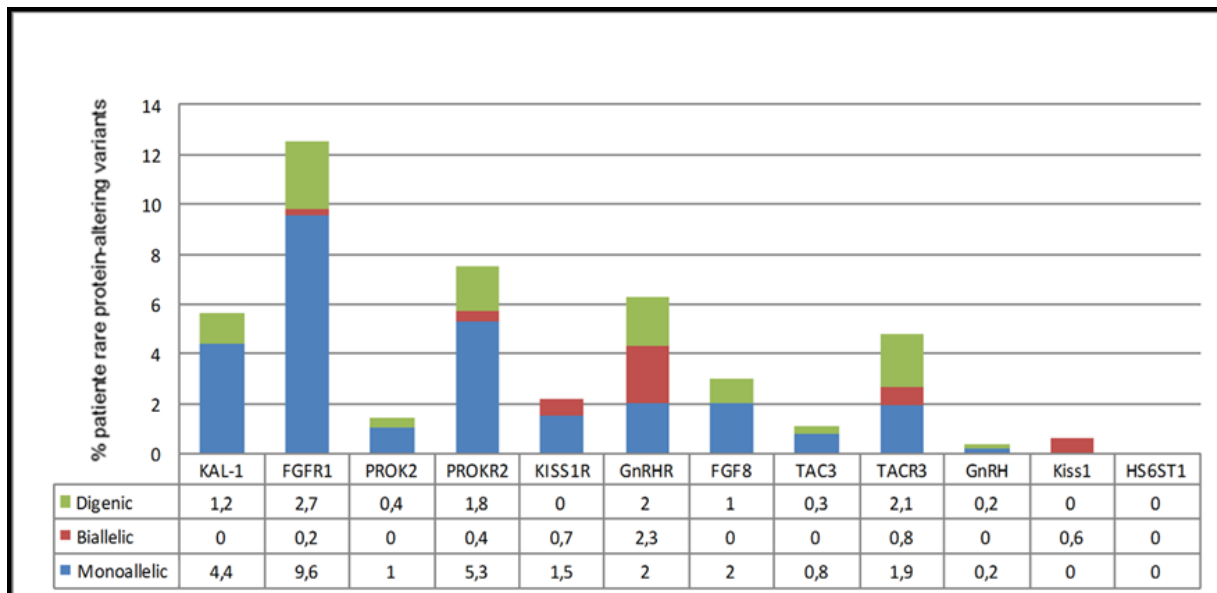


**Figure 21:** Chart representing variants distribution among genes analyzed.

### ***PROKR2* variants**

Genetic screening of *PROKR2* gene in our CHH cohort allowed the identification of 17 variants in 35 patients. 15 variants were missense and 2 frameshift mutations; these two led to premature stop codon. Moreover, we found only one variant in homozygous state (p.R85H) in a KS and in a nCHH patients, whereas the majority were found in heterozygous state (Table 4).

Variants	rs/CM	M.A.F.	Bibliography Ref.
p.R47W	rs768088473	N/A	N/A
p.M64V	CM111638	N/A	Sykiotis (2010) Proc. Natl. Acad. Sci.
p.G70S**	rs764674615	N/A	N/A
p.R85H	rs74315418	MAF< 0.01	Dodé (2006) PLoS Genet; Abreu (2012) Mol Endocrinol.; Caronia (2011) N. Engl. J. Med.;
p.V158I	rs368732206	0.0002 (ExAC)	Sarfati (2013) Eur. J. Endocrinol.; Libri (2013) J. Clin, Endocrinol. Metab.;
p.L173R	rs74315416	MAF=0.004	Dodé (2006) PLoS Genet.; Avbelj Stefanija (2012) Hum. Mol. Genet.;
p.C208S**	N/A	N/A	N/A
p.R268C	rs78861628	MAF: 0.01	Dodé (2006) PLoS Genet; 1000 Genomes Project (2010) Nature; Berg (2013) Genet. Med.;
p.M278K**	N/A	N/A	N/A
p.P290S	rs149992595	0.0001071 (ExAC)	Dodé (2006) PLoS. Genet. ; Miraoui (2013) Am. J. Hum. Genet. ; Monnier (2009) Hum. Mol. Genet. ;
p.D99N**	rs773364376	N/A	N/A
p.T260M	rs370738961	0.00006 (ExAC)	Sykiotis (2010) Proc Natl Acad Sci USA; Libri (2013) J Clin Endocrinol.;
p.V331M	rs117106081	MAF: 0.012	Dodé (2006) PLoS Genet.; 1000 Genomes Project (2010) Nature ; Berg (2013) Genet. Med.;
p.V334M	rs371564610	0.00002 (ExAC)	Sarfati (2013) Eur. J. Endocrinol.; Libri (2013) J. Clin. Endocrinol. ;
p.R357W	rs375036628	N/A	Cole (2008) J. Clin. Endocrinol. ; Miraoui (2013) Am. J. Hum. Genet. ; Sbai (2014) FASEB J. ;
p.H20MfsTer24 (c.58delC)	rs587777834	N/A	Dodé (2006) PLoS Genet. ; Libri (2013) J. Clin. Endocrinol. ; Miraoui (2013) Am. J. Hum. Genet. ;
p.N15TfsX30 (c.43_44insCTTTA)	rs776060323	N/A	Libri (2013) J. Clin. Endocrinol. Metab.

**Table 4:** *PROKR2* variants identified in KS and nCHH populations. \*\* indicated novel identified variants.

Pharmacological studies of some of these *PROKR2* variants (p.V158I, p.V334M, p.N15TfsX30) were previously performed in our lab (Libri DV *et al*, 2013). Thus, in the present thesis, we focused on four novel *PROKR2* variants (p.G70S, p.D99N, p.C208S and p.M278K) and four previously reported variants (p.R47W, p.M64V, p.R85H and p.P290S) that were identified in our

CHH cohort. All these PROKR2 variants were characterized by specific *in vitro* studies. An analysis of selected variants using the most known *in silico* software to predict potential effect of sequence alterations, revealed that p.R47W and p.M64V are the more tolerated, while for the majority of software the other variants are considered as disease-causing (Table 5).

Variant	Exon	Domain	SIFT (cut off: 0,05)	PROVEAN (cut off: -2,5)	POLYPHEN	MUTATION TASTER
p.R47W	1	ECL1	TOLERATED (0,071)	NEUTRAL (-1,66)	BENIGN (0,001)	POLYMORPHISM
p.M64V	1	TM1	TOLERATED (0,083)	NEUTRAL (-1,27)	BENIGN (0,118)	DISEASE CAUSING
p.G70S	1	TM1	DAMAGING (0,009)	DELETERIOUS (-4,73)	PROBABLY DAMAGING (1,000)	DISEASE CAUSING
p.R85H	1	ICL1	DAMAGING (0,000)	DELETERIOUS (-4,23)	PROBABLY DAMAGING (1,000)	DISEASE CAUSING
p.D99N	1	TM2	DAMAGING (0,000)	DELETERIOUS (-4,53)	PROBABLY DAMAGING (1,000)	DISEASE CAUSING
p.C208S	2	ECL2	DAMAGING (0,000)	DELETERIOUS (-8,82)	PROBABLY DAMAGING (1,000)	DISEASE CAUSING
p.M278K	2	TM6	DAMAGING (0,007)	DELETERIOUS (-3,39)	POSSIBLY DAMAGING (0,545)	DISEASE CAUSING
p.P290S	2	TM6	DAMAGING (0,000)	DELETERIOUS (-7,29)	PROBABLY DAMAGING (1,000)	DISEASE CAUSING

**Table 5:** disease causing prediction analysis using SIFT, PROVEAN POLYPHEN and MUTATION TASTER software.

## ***PROKR2 in vitro studies***

To characterize the selected PROKR2 variants identified in our cohort we cloned them and wild-type *PROKR2* sequence into SPRT-pcDNA3 plasmid (see Materials and Methods). The presence of a rhodopsin tag at N-Terminal of all the engineered plasmids allowed us to detect and measure protein levels in FACS assay and Western Blot, by using a specific antibody against this rhodopsin Tag (kindly provided by Dr.Sabine Costagliola, IRIBHM, ULB, Bruxelles).

### Fluorescence-activated cell sorting (FACS)

FACS assay were conducted on non- permeabilized HEK 293T cells to measure the amount of receptor expressed on the cell membrane.

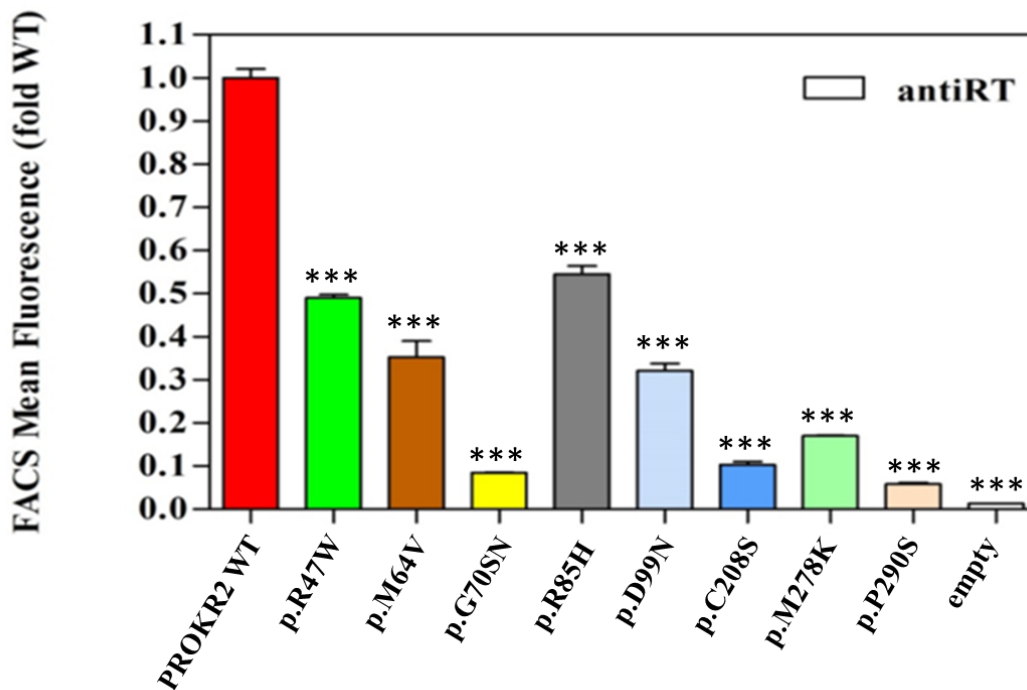


**Figure 22:** Chart representing the expression of PROKR2 receptor variants on HEK293T not-permeabilized cells. All value were calculated as fold of PROKR2 WT. \*\*\*= P<0,001 (One-way-ANOVA).

Results display a statistically significant reduced expression of the prokineticin receptor on the membrane for all variants (Figure 22). In particular, p.R47W, p.M64V, p.D99N and p.R85H variants display a moderate reduction (from 30% to 50%) in respect to PROKR2 WT, while the

remaining variants (p.G70S, p.C208S and p.P290S) expressed really low levels of the receptors on cell membrane (Table 6).

<b>Variant</b>	<b>Expression: (fold of wt)</b>	<b>Variant</b>	<b>Expression: (fold of wt)</b>
<b>PROKR2 WT</b>	1,00	<b>D99N</b>	0,321
<b>R47W</b>	0,490	<b>C208S</b>	0,103
<b>M64V</b>	0,352	<b>M278K</b>	0,170
<b>G70S</b>	0,085	<b>P290S</b>	0,058
<b>R85H</b>	0,545	<b>pcDNA3</b>	0,014

**Table 6:** Recapitulatory expression of PROKR2 variants revealed by FACS analysis. All numbers were expressed as fold of PROKR2 WT

## Western Blot

To better assess expression of PROKR2 variants we performed a Western Blot assay on total lysates from HEK 293T transfected cells. Densitometric analysis showed that monomeric form of PROKR2 is expressed at comparable levels for all the variants (Figure 23).

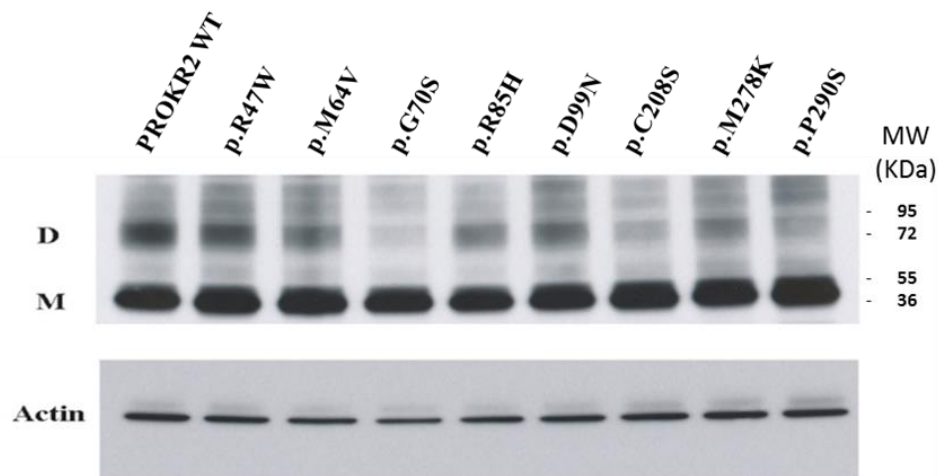


**Figure 23:** Western Blot of PROKR2 WT and variants. On the bottom, Actin levels were measured and used to normalize PROKR2 monomeric protein levels.

Interestingly, our antibody detected for all samples a different specific signal at higher molecular weight than PROKR2 monomer (72-95KDa). In a recent work, it was proposed that PROKR2 exists as a dimer *in vivo*<sup>176</sup> thus, basing on this paper, we hypothesized that the protein giving this signal could be the dimeric form of PROKR2. A subsequent densitometric analysis of this signal revealed low intensity levels for p.G70S and p.C208S (Figure 24 B).

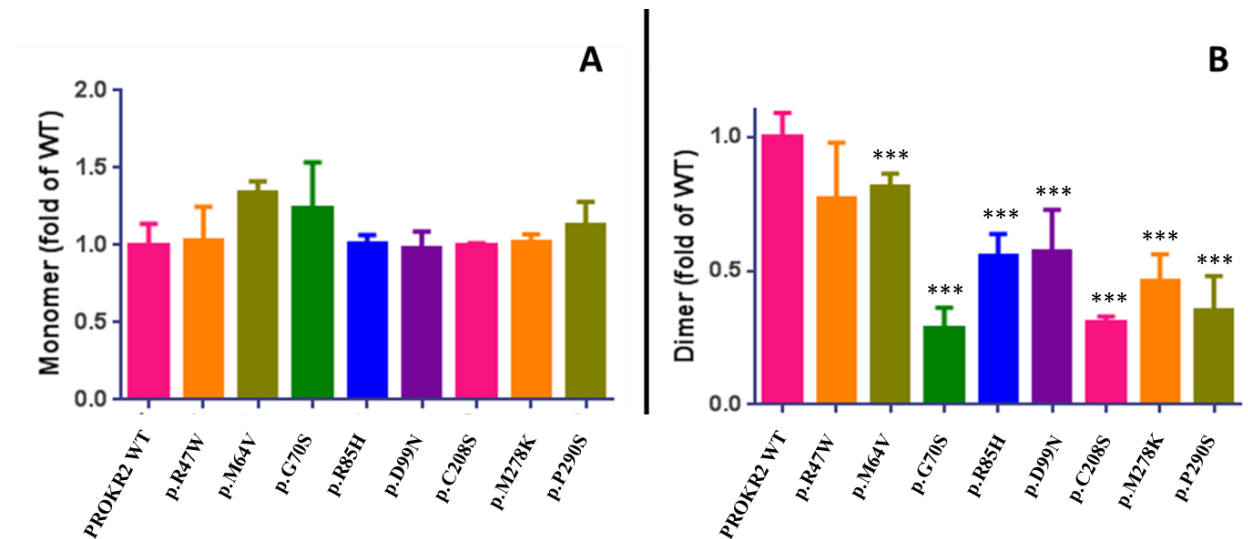


**Figure 24:** Expressions levels of PROKR2 monomeric and dimeric form. **A:** monomers are similar to wild type; **B:** supposed PROKR2 dimeric form signal. Both data sets were normalized on respective wild-type level. \*\*\*= $P < 0,001$  (One-way-ANOVA).

## Immunofluorescent assay

To evaluate intracellular localization of the proteins generated by PROKR2 variants, we performed an immunofluorescence assay on permeabilized COS7 cells fixed at 48 hours post-transfection.

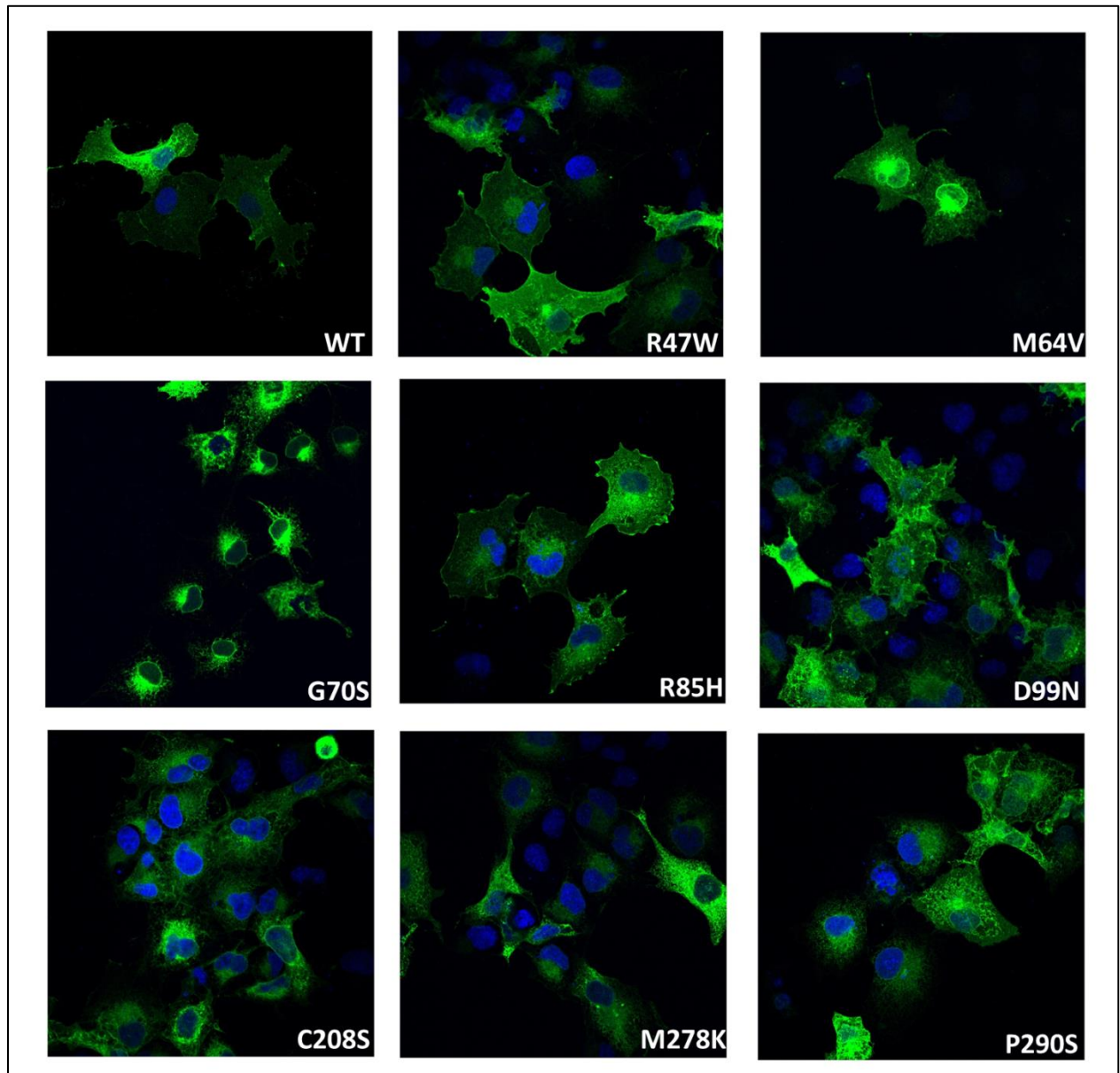


**Figure 25:** Immunofluorescence conducted on permeabilized COS7 cells. Green signal represent PROKR2, blue are cellular nucleus colored with DAPI.

Observing the distribution of PROKR2 signals is possible to note how p.G70S, p.C208S, p.M278K and p.P290S variants present strong intracellular signals compared to WT protein (Figure 25), suggesting a difficult receptor membrane-trafficking of these PROKR2 variants.

## Functional studies

To assess the impact of our variants on intracellular signaling pathways of PROKR2, HEK293T cells were transfected with pcDNA3/SPRT-PROKR2-variants plasmids and stimulated with increasing doses of human PROK2 ligand. The PROKR2 is coupled either to the Gs-dependent or the Gq-dependent signaling pathways, and, as we firstly demonstrated<sup>24</sup>, it is important to evaluate both during the characterization of the PROKR2 allelic variants. Thus, either the levels of cAMP and IP1 (a metabolite of PIP2-calcium pathway) were measured for all the tested variants.

### Gs-dependent signaling pathway

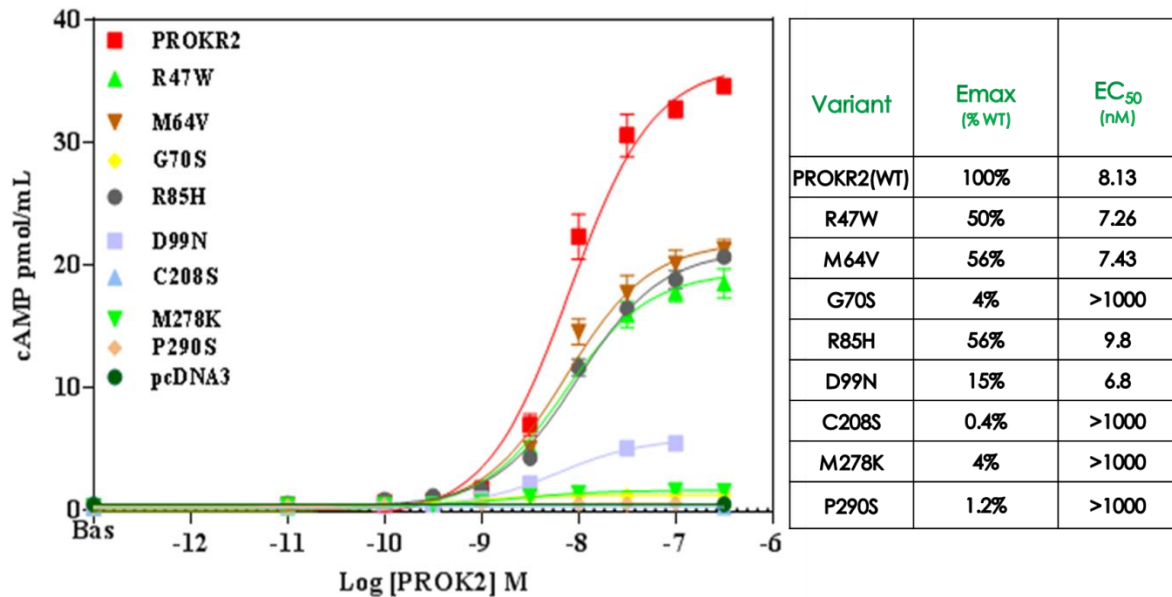


**Figure 26:** Chart on the left represents values of cAMP measured in HEK293T cells transfected with PROKR2 variants after stimulation with PROK2 ligand. Table on the right displays the Emax (as percentage of PROKR2 WT) and EC<sub>50</sub> calculated using GraphPad Prism 5<sup>®</sup>.

Cells lysate were collected, and intracellular cAMP levels were measured using radioimmunoassay (RIA) technique. Concentration-effect curves were constructed using GraphPad Prism 5<sup>®</sup>.

Analysis of chart and table reported underline how PROKR2 variants could be arbitrary divided for their functionality in three groups (Figure 26) :

- p.R47W, p.M64V and p.R85H showed a reduction of their Emax to about 50% of PROKR2 WT.
- p.D99N showed a strong reduction of the Emax of around 15% of the WT.
- p.G70S, p.C208S, p.M278K and p.P290S present a virtual absent response in terms of cAMP accumulation.

All active variants present EC<sub>50</sub> values comparable with the PROKR2 WT.

Gq-dependent signaling pathway

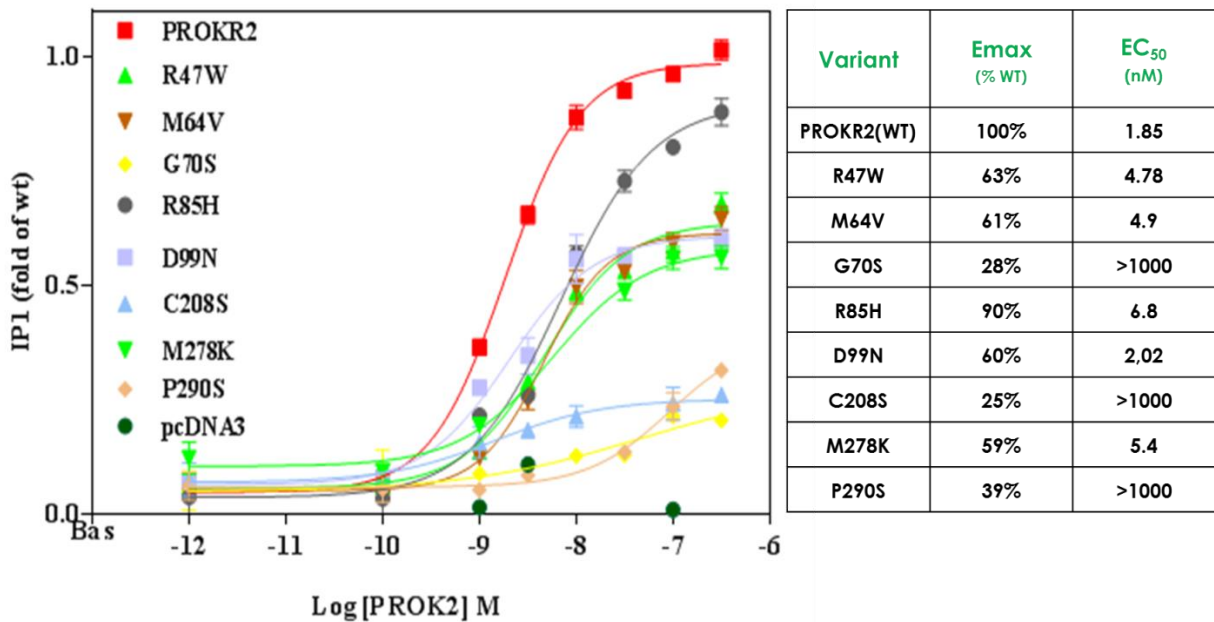


**Figure 27:** Chart and table show IP1 levels of PROKR2 WT and variants. Emax (as percentage of PROKR2 wild-type) and EC<sub>50</sub> were calculated using GraphPad Prism 5<sup>®</sup>.

Gq-pathway activity was estimated using IP-One ELISA assay kit CISBIO<sup>®</sup>. Intracellular IP1 accumulation was measured after stimulation with increasing doses of PROK2 ligand. Similarly to Gs-pathway analysis, it is possible to divide PROKR2 variants in three groups based on the levels of the Emax they achieved. The p.R85H variant showed a pharmacological profile comparable to PROKR2 WT, while p.M278K, p.R47W, p.M64V and p.D99N variants present about a 40% reduction of their Emax compared to WT receptor. Variants p.G70S, p.C208S and

p.P290S showed the strongest reduction of their IP1 Emax, between 60 and 75% of the WT (Figure 27).

## ***PROKR2 in vivo analysis***

## Bioinformatic analysis

Bioinformatics analysis conducted aligning human *PROKR2* nucleotide sequence with ZF genome using Blastn™ alignment revealed the presence of two possible homologous sequence inside the zebrafish genome localized on Chr.1 and Chr. 13 respectively named *prokr1a* (NM\_001173406.1) and *prokr1b* (NM\_001173407).

Alignment of protein sequences of Prokr1a and Prokr1b with human *PROKR2* revealed a high degree of similarity (Figure 28)

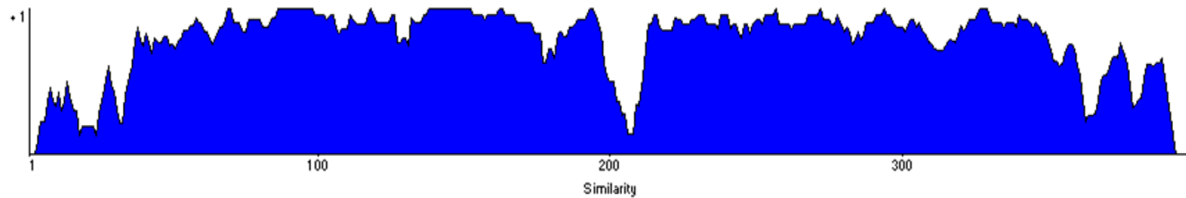


**Figure 28:** Similarity is a score of how similar each amino acid (or groups of amino acids) is across the whole alignment.

The identity percentage of the two ZF protein sequences compared to human *PROKR2* is about 70% for both with Prokr1b that displays a slightly higher value (77,3%) in respect to Prokr1a (72,3%) (Figure 29).



**Figure 29:** Alignment of protein sequences of Prokr1a, Prokr1b and PROKR2.

Synteny analysis performed using Genomicus web server (<http://www.genomicus.biologie.ens.fr/genomicus>) revealed a good conservation of blocks of genes between mammals' chromosomes, but no shared synteny between mammal and fish (Figure 30).

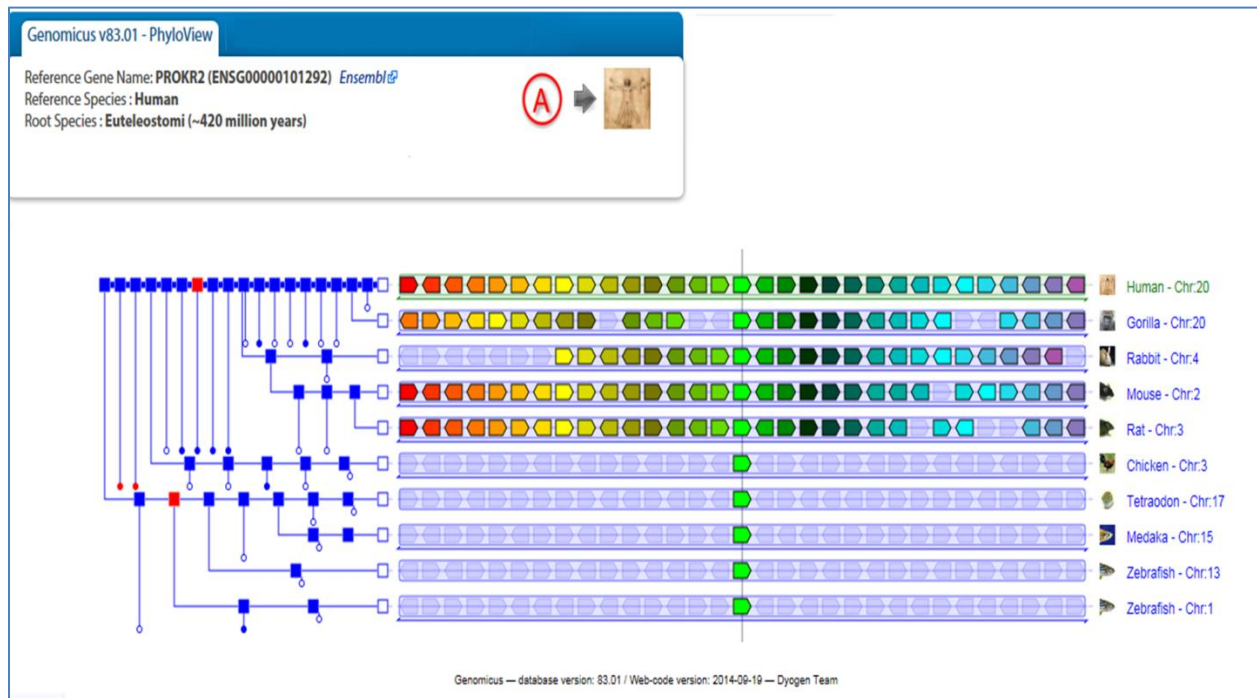


**Figure 30:** synteny describes the physical co-localization of genetic loci on the same chromosome within an individual or species.

## Real-Time qRT-PCR

To evaluate expression of *prokr1a* and *prokr1b* during early developmental stages of ZF, we performed Real-Time qRT-PCR on RNA extracted from ZF embryos.

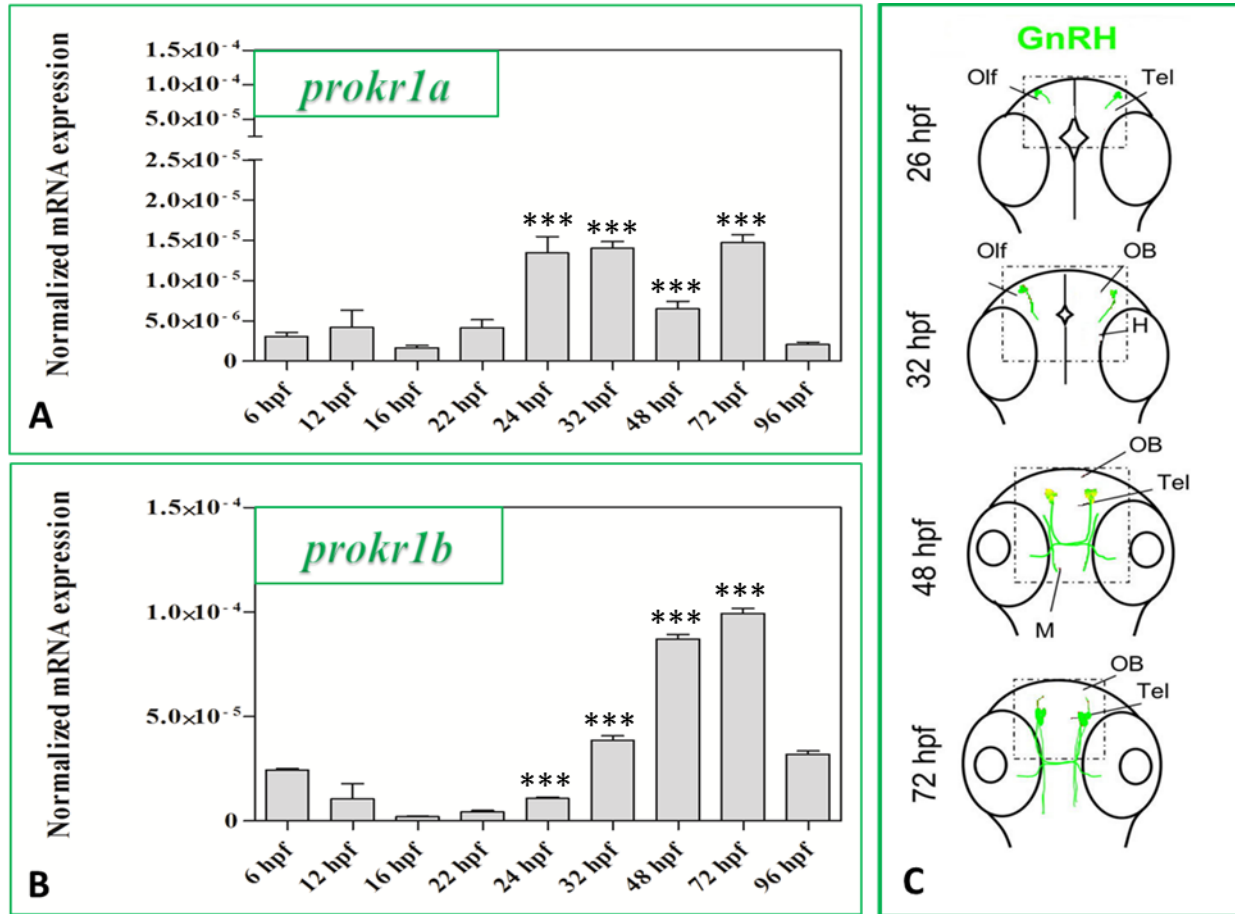


**Figure 31:** Real-Time qRT-PCR analysis displaying the expression levels of *prokr1a* (A) and *prokr1b* (B). Figure C is a representation of the migration pattern of GnRH (adapted from Palevitch O. , *et al*, Dev Dyn. 2009). \*\*\*= $P < 0,001$  (One-way-ANOVA).

Results displayed that *prokr1b* (Figure 31 B) has higher expression level compared to *prokr1a* (Figure 31 A). More interestingly, expression of *prokr1b* start to increase at 24 hours post fertilization (hpf) until 72 hpf, seeming to be consistent with the migration pattern of GnRH3 fibers described in literature<sup>166</sup> (Figure 31 C).

## **Whole-mount *In Situ* Hybridization**

To characterize the spatial expression a whole mount *In Situ* Hybridization (WISH) were conducted on fixed embryos at different developmental stages.

Results revealed for *prokr1b* a signal in the olfactory placode (OP) from 36 hpf to 72 hpf (Figure 32 B1-B6) that is comparable to the GnRH3 signal (Figure 32 C1-C6). Otherwise, *prokr1a* displays only a feeble signal in midbrain-hindbrain junction at 36 hpf and 48 hpf (Figure 32 A1-A4) and later at 72 hpf in the liver (Figure 32 A5-A6).

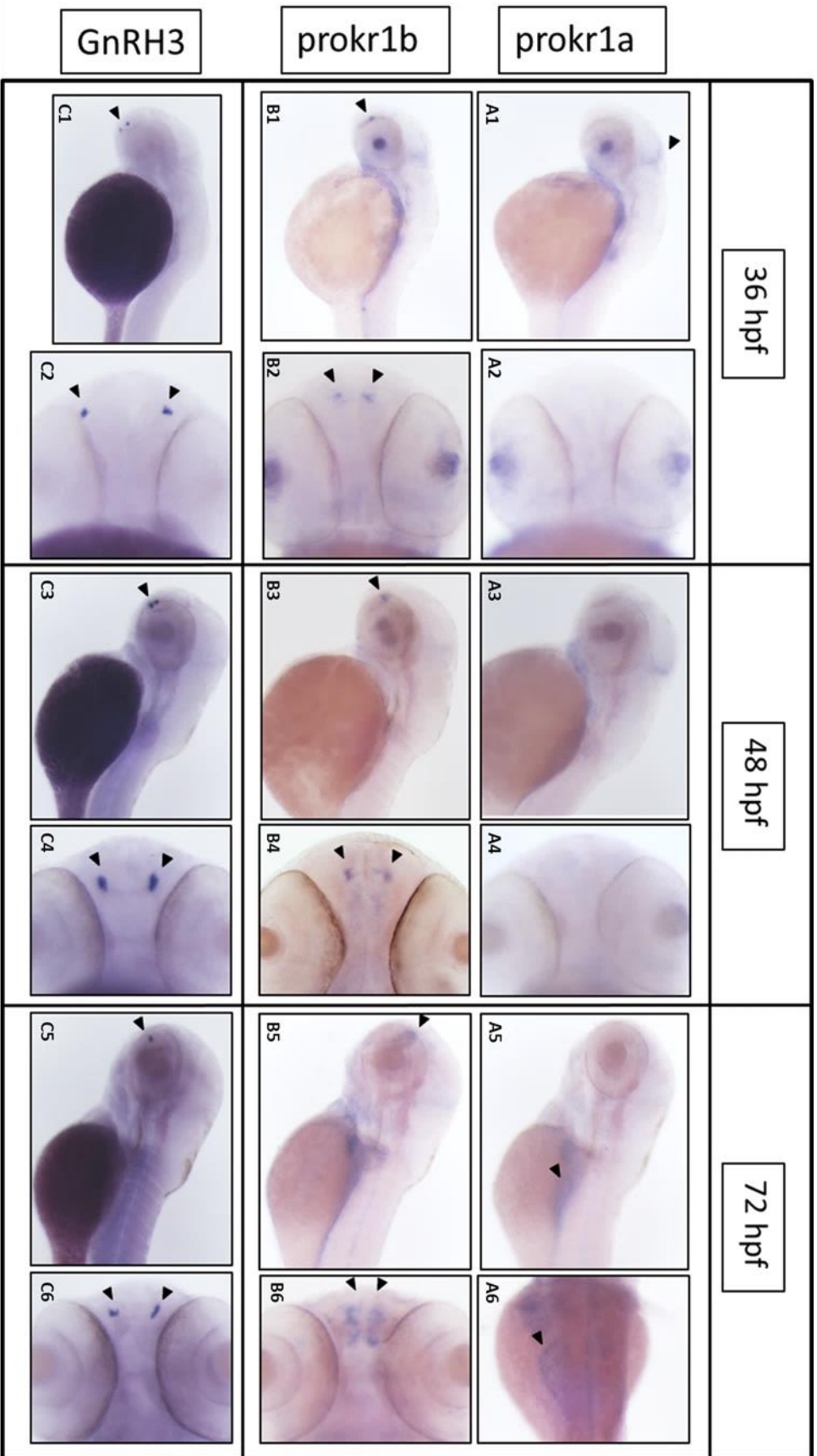


**Figure 32:** WISH experiments conducted on ZF embryos at 36, 48 and 72 hpf. Lateral view of embryos: A1, B1, C1, A2, B2, C2, A5, B5 and C5. Ventral view: A2, B2, C2, A4, B4, C4, A6 and C6. A6 is a dorsal view of the body. Black arrows indicates the signal.

## Knockdown experiments

To further characterize the role of *prokr1a* and *prokr1b* gene in the migration of GnRH3 neurons along ZF development, we performed knockdown experiments.

Two morpholino sequences for *prokr1a* and *prokr1b* were designed and ordered on Gene Tools LLC website (<http://www.gene-tools.com/>). Sequences were tested injecting different doses of each morpholino sequences in ZF embryos at one-cell stage. Total RNA was extracted from injected embryos at 24 hpf, retrotranscribed and a RT-PCR were performed to assess the specificity of morpholino sequences (Figure 33).

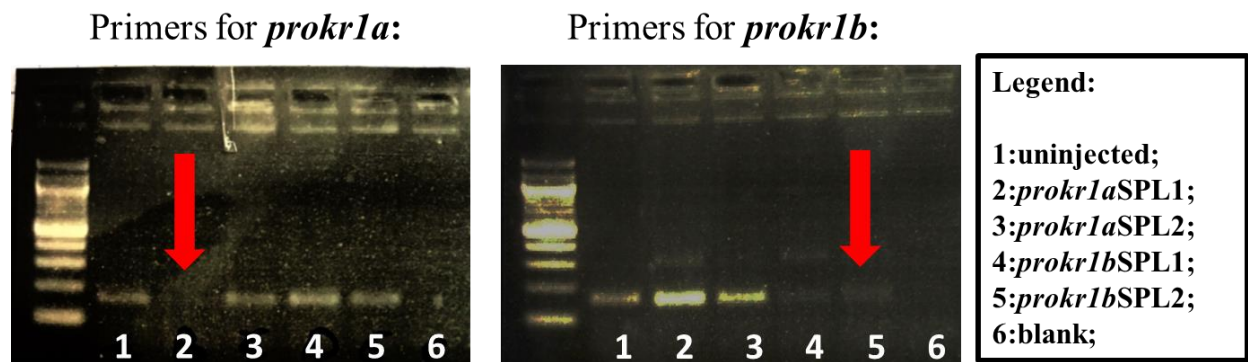


**Figure 33:** RT-PCR on uninjected and injected embryos. Red arrows indicate morpholino sequences able to downregulate their target gene.

As showed in the figure above, *prokr1aSPL1* and *prokr1bSPL2* downregulate specifically expression only of *prokr1a* and *prokr1b* respectively.

Knockdown effect of *prokr1a* and *prokr1b* genes were evaluated taking advantage of Tg:GnRH3-EGFP ZF transgenic line (gently provided by prof. Yoav Gothilf, Tel-Aviv University, Tel-Aviv; see Materials and Methods for the procedure). Pictures of liveTg:GnRH3-EGFP embryos taken at 48 hpf developmental stages using Nikon C2<sup>+</sup>™ Confocal Laser Scanning Microscope (CLSM) display a GnRH3 fibers network composed by: two GnRH3 somas detectable close to olfactory placodes and branch of axons departing from these perikarya that form a pallium commissure and cross at the level of the optic chiasm to innervate retina (Figure 34 A).

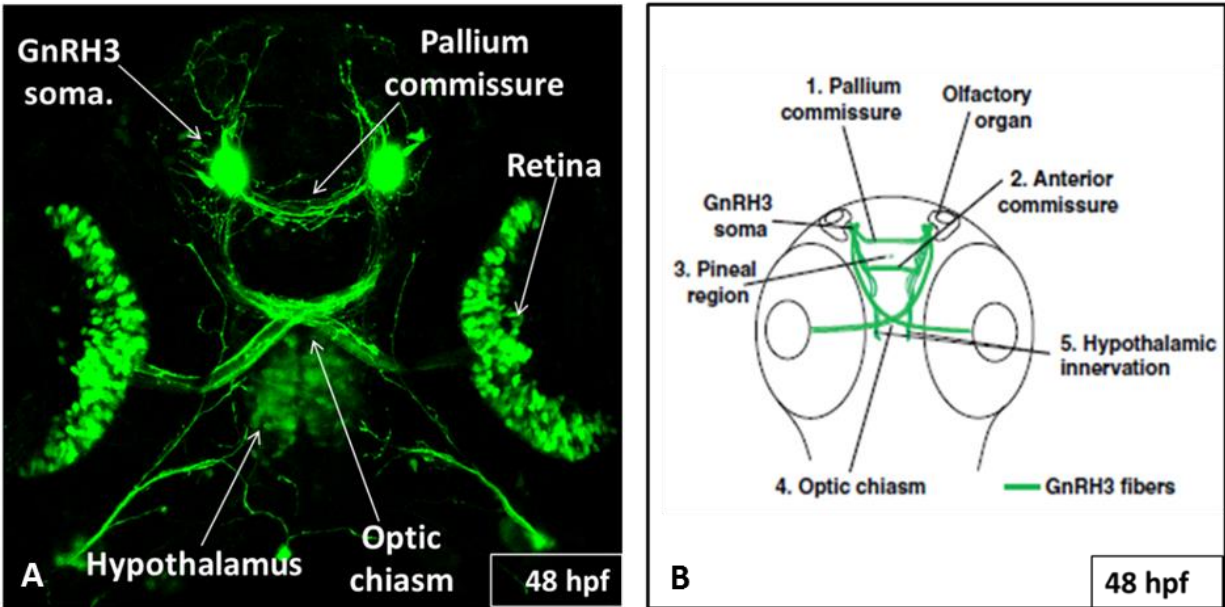


**Figure 34:** **A** ventral view of head of ZF Tg:GnRH3-EGFP living embryos at 48 hpf, taken using confocal laser-scanning microscope. **B** GnRH3 network at 48 hpf described in literature (adapted from Abraham *et al.*, Gen Comp Endocrinol. 2009)

Transgenic fish were injected with *prokr1a*SPL1, *prokr1b*SPL2 and Ctrl-MO (a morpholino sequence without target inside ZF genome, used as control for off-target effects). Pictures were collected at 48 hpf developmental stage using a Nikon C2<sup>+</sup>™ CLSM.

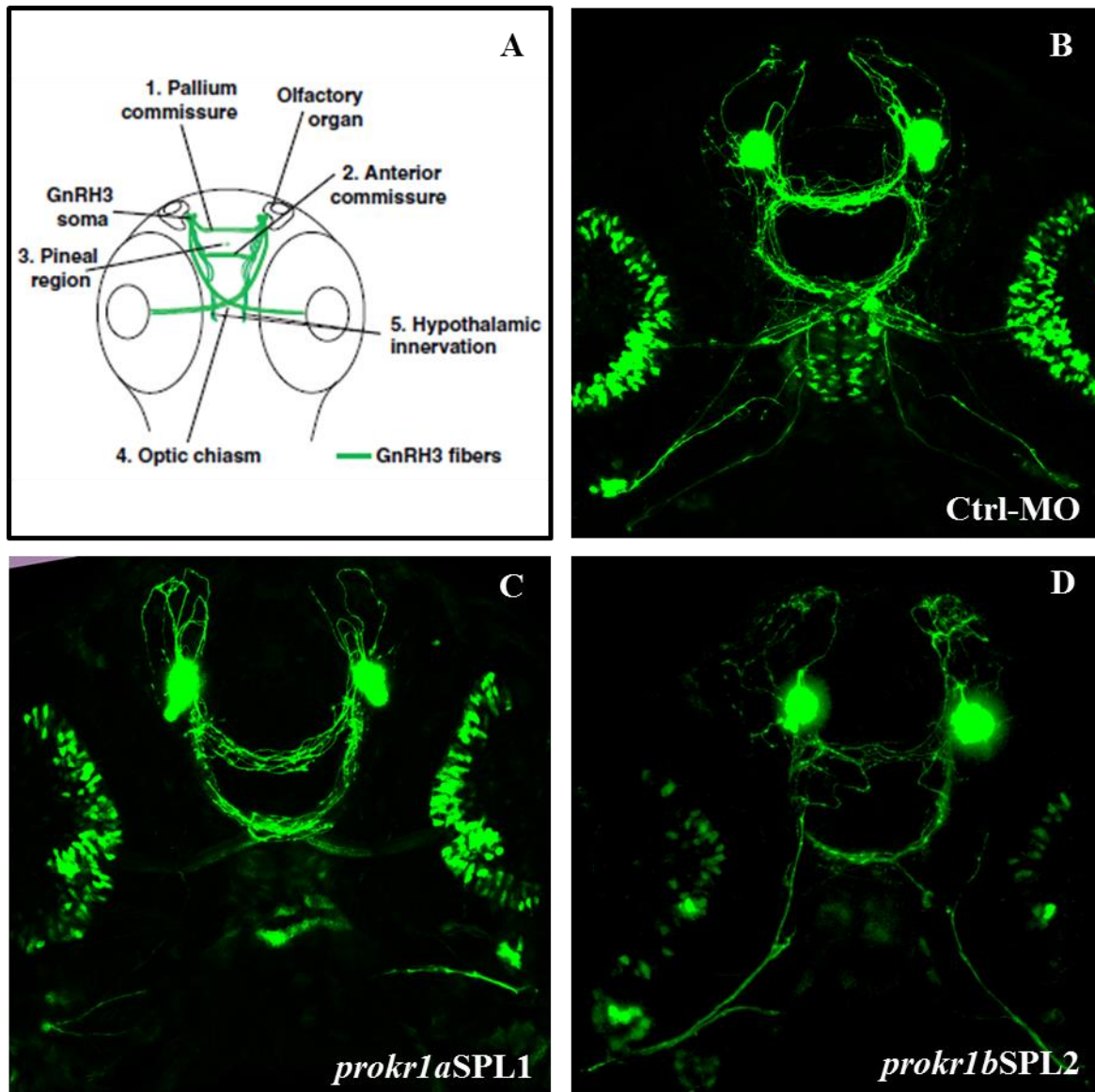


**Figure 35:** A: ZF GnRH3 network at 48 hpf described on literature (adapted from Abraham *et al.*, Gen Comp Endocrinol. 2009). B: Tg:GnRH3-EGFP embryos at 48 hpf injected with Ctrl-MO morpholino; C: Tg:GnRH3-EGFP embryos at 48 hpf injected with *prokr1aSPL1* morpholino; D: Tg:GnRH3-EGFP embryos at 48 hpf injected with *prokr1bSPL2* morpholino.

Analysis of pictures revealed that in embryos injected with *prokr1aSPL1* morpholino (Figure 35 C) GnRH3 network seems to be comparable with uninjected (Figure 34 A) or Ctrl-MO (Figure 35 B). On the contrary, injected embryos *prokr1bSPL2* showed alterations in the normal architecture of GnRH3 network (Figure 35 D). In particular GnRH3 fibers departing from GnRH somas seem to be less in number, and their route looks generally disorganized, especially at level of pallium commissure and optic chiasm. Moreover, no fibers innervate retina and signal in this

location and in the hypothalamus the signal looks faint (Figure 35 D). All these defects are noticeable comparing *prokr1b*SPL2 injected embryos both with Ctrl-MO and *prokr1a*SPL1 injected embryos.

### Knockout of *prokr1b*

To confirm the defects observed during *prokr1b* knockdown experiments, we crossed *prokr1b*<sup>ct814/ct814</sup> (provided by prof. David Prober, Caltech Institute, US-CA, see Materials and Methods) with Tg:GnRH3-EGFP. Fish of *prokr1b*<sup>ct814/ct814</sup> KO line contains a mutation in *prokr1b* gene that generate a frameshift and a premature stop codon at amino acid 13. The resulting protein is composed only by 13 of 396 amino acids of the normal WT protein, lacking fundamental structural domains.

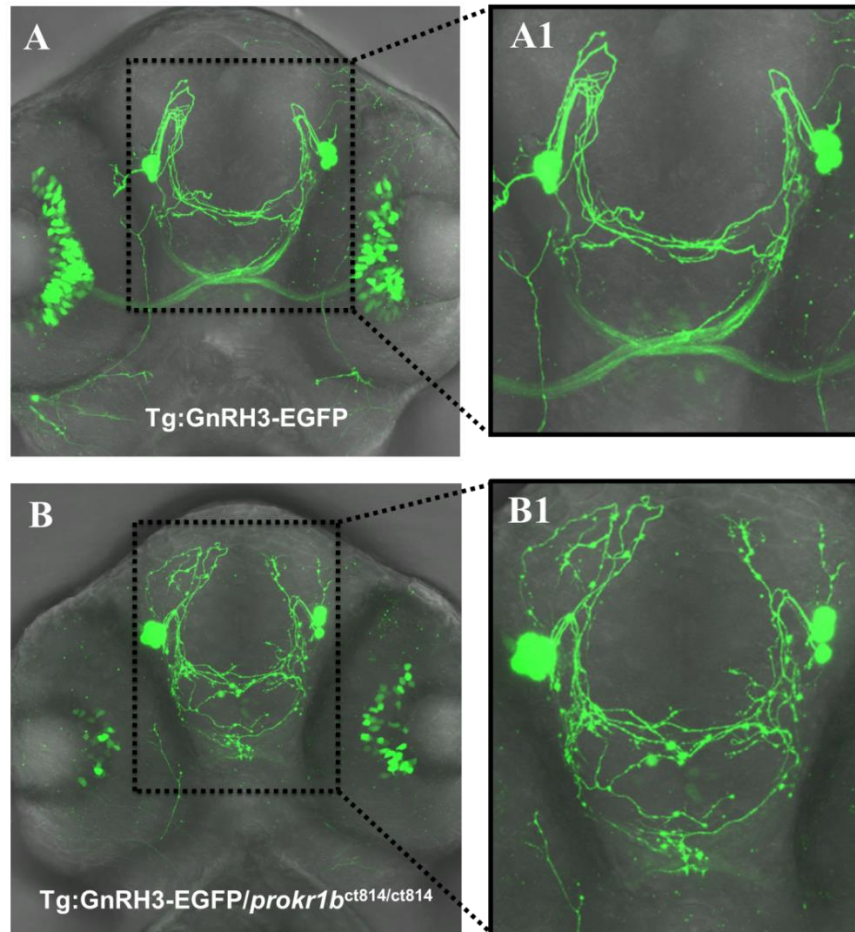


**Figure 36:** Pictures are ventral view of head of 48 hpf living embryos taken using confocal laser scanning microscope (Leika TCS SP8®). **A:** Tg:GnRH3-EGFP embryos. **B:** Tg:GnRH3-EGFP/*prokr1b*<sup>ct814/ct814</sup> embryos. **A1:** detail of GnRH3 fiber network of Tg:GnRH3-EGFP. **B1:** detail of GnRH3 fiber network of Tg:GnRH3-EGFP/*prokr1b*<sup>ct814/ct814</sup>.

Pictures of Tg:GnRH3-EGFP/*prokr1b*<sup>ct814/ct814</sup> embryos at 48 hpf display alterations in GnRH3 network (Figure 36 B-B1), similarly to what observed for *prokr1b*SPL2 morpholino injection (Figure 35 D), with a general disorganization of the fibers at the level of GnRH3 somata and pallium commissure. Moreover, there is clearly a lack of signal at the level of optic chiasm were GnRH3 fibers usually cross and a reduced fluorescence in the retina of Tg:GnRH3-EGFP/*prokr1b*<sup>ct814/ct814</sup> ZF embryos compared to Tg:GnRH3-EGFP (Figure 35A-A1).

# *Discussion*

During this PhD project, we conducted a genetic screening of 12 CHH-related genes on 512 CHH patients. This study represents a genetic screening conducted on the largest CHH cohort. Data analysis shows the presence of 204 variants in 32.2% of clinical cases, 140 of them (67.8%) were missense variants. Examination of variants distribution in the cohort underlined how in our clinical records *FGFR1* resulted the most frequently involved gene with 12.5% of patients carrying allelic variants on this gene, followed by *PROKR2* (7.5%), *GNRHR* (6.3%), *KALI* (5.6%) and *TACR3* (4.8%). These percentages are consistent with results presented in other studies<sup>12,14,38,40,59,69,177</sup>. Calculation of oligogenicity rate, represented by patients carrying digenic mutations, in our cohort display a value of 4.6% which is even higher if compared to 2.5% estimated by Sykiotis and colleagues<sup>69</sup>. Thus, the present study, that is including the largest cohort ever sequenced for multiple genes, is confirming the conceptual shifting of CHH from monogenic to oligogenic disease. Moreover, our study is also confirming that oligogenicity is strictly dependent from the number of genes analyzed and sample size. Indeed, passing from 8 genes screened in 397 CHH patients (Sykiotis) to 12 genes in 512 patients in the present study, the rate of oligogenicity increases from 2.5% to 4.6%. Nevertheless, oligogenicity doesn't give us information about molecular mechanisms by which oligogenic interactions cause isolated GnRH deficiency. Two hypotheses have been proposed: one is that mutations could act independently during different developmental stages, such that their additive effects compromise the ontogeny of GnRH neurons and/or pituitary gonadotropes sufficiently to impair sexual maturation and fertility. Otherwise, mutations may have a synergistically effect on the same ligand/receptor pair or signaling pathway. It is impossible to unequivocally distinguish between these two models; this is because the precise role of the known disease genes in the regulation of GnRH biology still requires further elucidations<sup>69</sup>.

Among the genes involved in CHH, we focused our attention on the *PROKR2* gene, which is one of the most frequently involved gene in our series, and which still presents many open issues regarding its involvement in the pathogenesis of CHH. Prokineticin pathway is known to have an important role during GnRH neurons migrations. The association between *PROKR2* and CHH came by the work of Matsumoto and colleagues in 2006, where they described that homozygous *Prokr2* KO mice, but not heterozygous, displayed abnormal development of the olfactory bulb and reproductive system, a phenotype that remind to KS<sup>103</sup>. These firsts indications suggested that *PROKR2* was a gene associated to KS and that only defects on both alleles could affect

GnRH migration and, by consequence, lead to KS. Nevertheless genetic screening conducted during the last years revealed that mutations on *PROKR2* gene were found both in KS and nCHH patients and mostly in heterozygous state<sup>22,178,179</sup> bringing to a reconsideration of its pathogenetic mechanisms. Furthermore, *in vitro* studies of reported missense mutations demonstrated a deleterious effect on *PROKR2* signaling in transfected cells, but the same mutations have been also found in apparently unaffected individuals<sup>20,180</sup>. Taken together, these data underline how *PROKR2* role in the pathogenesis of CHH and the functional impact of missense *PROKR2* variants has not been fully characterized. Genetic screening conducted in our cohort identified 17 *PROKR2* rare variants (Minor allele frequency, MAF<0.01) in 37 patients. Similarly to other studies present in literature, the majority of patients (35) presented variants in heterozygous state; only two, one KS and one nCHH, presented p.R85H variant in homozygous state. Moreover, among 37 CHH patients affected by mutation in *PROKR2*, 11 displayed anosmia (KS) but 26 had a normal sense of smell (nCHH), confirming that mutations in *PROKR2* are not exclusively associated to KS. Interestingly, we identified 4 novel variants in our cohort (p.G70S, p.D99N, p.C208S and p.M278K). All 4 variants were single-nucleotide polymorphism (SNPs) missense variants. To better elucidate the molecular mechanisms by which missense mutation affect the signaling of *PROKR2*, we conducted *in silico* and *in vitro* experiments on these novel variants and p.R47W, p.M64V, p.R85H and p.P290S, 4 already reported variants which lack extensive functional studies. *In silico* analysis of chosen variants using software for prediction of the possible impact of an amino acid substitution on the structure and function of a human protein (Sift, Provean, Polyphen and MutationTaster) resulted in a unanimously deleterious effect verdict for all 4 novel variants and for p.R85H and p.P290S, suggesting an important role of these amino acids residues for the protein integrity. Indeed, algorithms of these prediction softwares are mainly based on alignment and comparison of amino acid sequences of the selected protein between multiple species to identify the most conserved, and thus more important, amino acids. Same analysis conducted on p.R47W and p.M64V predicted a tolerated effect for both, even though MutationTaster software signaled a possible disease causing effect for p.M64V. *PROKR2* is a class A member of GPCR; as explained in the introduction, this receptor is an integral membrane protein consisting of 7 trans-membrane domains coupled with G proteins. Its 3D structure was modeled on crystal structures of rhodopsin and  $\beta$ 2-adrenergic, two G protein-coupled receptors belonging to the same subfamily of *PROKR2*<sup>106</sup>. When a ligand

binds to the extracellular domain of GPCR, it causes a conformational change in the GPCR, which allows it to activate an associated G protein and triggering intracellular pathways. There are two principal signal transduction pathways involving the G protein–coupled receptors: the cAMP signal pathway (Gs-pathway) and the phosphatidylinositol signal pathway (Gq-pathway)<sup>181,182</sup>. Previous *in vitro* studies have demonstrated how missense variants can affect both receptor membrane-trafficking and signaling activation of PROKR2 differently or selectively<sup>24,106,183</sup>. Basing on these evidences, we structured our study evaluating receptor membrane-targeting and intracellular Gs/Gq pathways activation of identified *PROKR2* variants.

### Receptor membrane-trafficking

FACS assay performed on not-permeabilized HEK293T cells transfected with *PROKR2* variants plasmids revealed reduced membrane expression levels of the receptor for all variants. This impairment is more severe in the case of p.G70S, p.C208S, p.M278K and p.P290S variants with expression values comprised between 5%-17% respect to *PROKR2* wild-type (WT) levels. For the remaining 3 variants, p.R47W, p.M64V and R85H, expression levels indicate that 50% of the protein reach cellular surface. To assess that these variable membrane expression was not due to different transfection efficiency of *PROKR2* variants plasmids, we performed a Western Blot assay. Densitometric analysis of monomeric forms (45 kDa) of *PROKR2* WT compared to *PROKR2* variants displayed similar intensity levels validating FACS data. Interestingly, Western Blot analysis revealed another band at an apparent molecular mass approximately twice than the monomer (72–95 kDa). A band with the same molecular mass was already described in Marsango and colleagues article in 2011 as dimeric form of *PROKR2*<sup>176</sup>. Differently from previous densitometric analysis, results revealed a different intensity among variants with p.G70S, p.C208S and p.P290S that displays the lowest intensity, suggesting a possible impairment in dimerization process for these variants. To evaluate intracellular localization, we conducted an immunofluorescence assay. Images obtained displayed a membrane fluorescent signal comparable to *PROKR2* WT for p.R47W, p.M64V, p.R85H and p.D99N. On the contrary, a strong intracellular signal close to the nucleus was observed for p.G70S, p.C208S, p.M278K and p.P290S. The localization of intracellular signal suggests, for these variants, a detainment in Golgi or endoplasmic reticulum. These data are in accordance with FACS analysis and confirm a strong alteration in membrane-trafficking for p.G70S, p.C208S, p.M278K and p.P290S variants.

### Intracellular Gq/Gs pathway

Evaluation of intracellular signaling process in chosen variants display a strong impairment of both Gs/Gq-pathways for p. G70S, p.C208S and p.P290S variants that, in the case of Gs-pathway, is a total absence of cAMP accumulation. Differently, variants p.R47W, p.M64V and p.R85H present for both assays an Emax levels that are about 50%, indicating a reduced functionality for both signaling pathways. Interestingly, p.D99N and p.M278K variants showed a differential activation of intracellular pathways with Gs pathway strongly impaired, and Gq-pathways that retain half of the functionality compared to PROKR2 WT.

Thus, altogether, analysis of the data obtained by our FACS, cAMP and IP1 assays allowed us to arbitrarily divide variants on three main groups, basing on the functionality of membrane trafficking and intracellular pathways.

<b>Mutation</b>	<b>Membrane expression (fold of WT)</b>	<b>Gs-pathway activation (Emax %WT)</b>	<b>Gq-pathway activation (Emax %WT)</b>
<b>WT</b>	<b>1</b>	<b>100%</b>	<b>100%</b>
<b>p.R47W</b>	<b>0.49</b>	<b>50%</b>	<b>63%</b>
<b>p.M64V</b>	<b>0.35</b>	<b>56%</b>	<b>61%</b>
<b>p.R85H</b>	<b>0.54</b>	<b>56%</b>	<b>91%</b>
<b>p.D99N</b>	<b>0.32</b>	<b>15%</b>	<b>60%</b>
<b>p.M278K</b>	<b>0.17</b>	<b>4%</b>	<b>59%</b>
<b>p.G70S</b>	<b>0.08</b>	<b>4%</b>	<b>28%</b>
<b>p.C208S</b>	<b>0.1</b>	<b>0.4%</b>	<b>25%</b>
<b>p.P290S</b>	<b>0.06</b>	<b>1.2%</b>	<b>39%</b>

**Table 7:** Comparison between membrane expression levels (FACS) and Gs/Gq pathways activation. Red color represent variants with strong impairment of both membrane-trafficking and intracellular pathways. Green variants with mild impairment for both processes and yellow variants that present a strong impairment for Gs but not for Gq pathways.

Looking at these results, the nature of amino acids substitution and domain localization, we postulated a pathogenic effect for each single variants analyzed. Variants p.R47W and p.M64V and p.R85H presented a moderate membrane expression and are able to maintain at least 50% of

their intracellular pathway functionality (Green in Table 7). For p.M64V, this could be due to the fact that both methionine and valine are hydrophobic amino acids, so substitution doesn't involve changes in the charge and could not impact on protein stability. Moreover, their side chains are less reactive, and rarely are involved in protein functionality. These observations are in accordance with data reported in literature. Indeed, a study conducted in 2012 showed how this variant was found associated with p.L173R, a variant known to be deleterious and prevalent among GnRH-deficient patients of diverse geographic and ethnic origins<sup>184</sup>. Therefore, is it possible that p.M64V mutation alone isn't enough to lead to a CHH clinical phenotype, and that patients affected by this amino acid substitution presented a mutation in another CHH-related gene not investigated in our genetic analysis. Variant p.R85H is located on the first intracellular loop (ICL1) of PROKR2 protein. Abreu and colleagues demonstrated in a previous work how this protein domain is important for receptor function<sup>185</sup>. In this work, they analyze several arginine 85 variants reported on literature demonstrating how these mutations interfere only modestly with IP1 and p42/p44 MAPK signaling pathways<sup>185</sup>. Results obtained by our assay on R85H confirm literature data and, in addition, demonstrate that also Gs-pathway is less affected by this mutation. Analysis of p.G70S, p.C208S and p.P290S variants displayed both a strong impairment of membrane-trafficking and lowest (or absent) activation of Gs/Gq pathways (red in Table 7). Intracellular detainment observed in immunofluorescence assay could suggest a folding problem for these variant proteins, that could not overcome endoplasmic reticulum (ER) quality-control system<sup>186</sup>. In particular, cysteine residues substituted in p.C208S is localized in extracellular loop 2 (ECL2); this amino acid is involved in disulfide bridge with cysteine 128, a strongly conserved amino acid residue in GPCRs<sup>187</sup>. Interestingly, p.D99N and p.M278K display a different impairment of intracellular pathways, maintaining a moderate activation of Gq-pathways and a strong reduction of Gs-pathways (yellow in Table 7). For p.M278K, the different nature of methionine, a nonpolar hydrophobic residue, and lysine, that is polar and hydrophilic, could lead to a different conformation of  $\alpha$ -helices and, by consequence, their interaction could modify for example hydrophobic interface between transmembrane domain 5 and 6 (TM5 and TM6), two domains that were shown to be involved in regulation, spatial arrangements and activity of prokineticin receptor 2 dimers<sup>188</sup>.

*In vitro* analysis conducted during this PhD allowed to better evaluate the impact of *PROKR2* missense variants identified during our genetic screening. Moreover, these results confirm, at the

same time, what postulated in a previous work conducted in our lab, that assessment of the impact of *PROKR2* variants on both the cAMP and IP pathways could help to avoid absolving mutations that selectively compromise one signaling branch leaving the other intact, and thereby to avoid erroneously predicting a reduced risk of disease in the variant-carrying progeny of such patients<sup>24</sup>.

To better characterize the role of the *PROKR2* in the CHH pathogenesis and to overcome the limits of the KO mouse model, which is not perfectly fitting with the human phenotype, we decided to generate a new animal model. Thus, the last part of this project was focused on elucidating the role of *PROKR2* on GnRH neurons ontogeny processes, taking advantage of the ZF model which, as extensively demonstrated by studies conducted by Zohar group, displays a high conservation degree of GnRH neurogenesis processes respect to humans<sup>125,166,167</sup>. These evidences, together with advantages offered by this model such as fast development, embryo and larvae transparent and the availability of Tg-GnRH3-EGFP transgenic line, make ZF a highly effective model for studying GnRH neuronal development<sup>125</sup>. Few data were available in literature about prokineticin receptors in ZF, so our study started performing a bioinformatic analysis. BLAST alignment tools identified two sequences: *prokr1a* located on Chr. 1 and *prokr1b* located on Chr. 13. Alignment of protein sequences of these two genes displayed for both of them an identity about 70% with human *PROKR2*. However these information together with synteny analysis didn't provide clear information about the orthologs of human *PROKR2* gene in ZF. The possible presence in ZF of two co-orthologs in contrast to a single copy gene in humans and other mammals is not uncommon. Indeed teleost lineage, to which ZF belong, experienced an additional whole genome duplication soon after divergence from tetrapods<sup>189,190</sup>. To better elucidate if *prokr1a* and *prokr1b* genes are respectively orthologs of human *PROKR1* and *PROKR2*, or they are both co-orthologs of either *PROKR1* or *PROKR2*, we evaluated the expression of these two genes along ZF embryo development. Real-Time qRT-PCR analysis displays different expression levels for the two genes along ZF early developmental stages. Comparison of *prokr1a* and *prokr1b* expression pattern revealed that *prokr1b* is the most expressed and, most interestingly, it exhibits an increase at 24 hpf that culminate at 72 hph. This time window can be comparable with migration time of GnRH3 neurons described on literature by Abraham and colleagues<sup>125</sup> suggesting a possible role for *prokr1b* during this process. Following WISH experiments, performed to measure spatial expression patterns of mRNA,

support this thesis. Indeed only *prokr1b* showed a signal close to olfactory placodes that is similarly to what obtained using GnRH3 probe. It is interesting to note that this signal does not overlap exactly the GnRH3 signal, suggesting that in ZF *prokr1b* could not be expressed by GnRH neurons like observed in mice for *Prokr2*<sup>102,178</sup>. Since it is known that human *PROKR2* is involved in the migration of GNRH neurons, these spatial and temporal overlapping of *prokr1b* could indicate a role of this gene during migration of GnRH neurons. To better assess functions of *prokr1a* and *prokr1b* genes, we conducted knockdown experiments in ZF model. Results obtained revealed that downregulation of *prokr1b* (*prokr1b*SPL2) produced defects in the GnRH3 fibers network that looked, at 48 hpf, generally disorganized if compared to *prokr1a* and control injected fishes. Nevertheless, observation of discrepancies between knockdown (via antisense) and knockout (via genetic inactivation) phenotypes in ZF has recently started a debate on zebrafish community, questioning the validity of morpholino knockdown technique<sup>191,192</sup>. In order to confirm the function of *prokr1b* during GnRH3 ontogeny and avoid possible misleading interpretation due to toxicity or off-target effect of antisense injection, we generated *prokr1b* knockout model (Tg:GnRH3-EGFP/*prokr1b*<sup>ct814/ct814</sup>). Examination of GnRH3 neurons network in this embryo revealed a general misrouting of fibers similar to what observed in *prokr1b* knockdown fish. Moreover, a detailed analysis of Tg:GnRH3-EGFP/*prokr1b*<sup>ct814/ct814</sup> phenotype, showed the presence in pallium commissure of small dots not noticed before. GnRH3 somata migration process is described to start in ZF at 72 hpf (Abraham 2010) excluding that these small dots are GnRH3 cells. Instead, similar sphere-shaped structures were described by Matsumoto and colleagues in the axons of *Prokr2*<sup>-/-</sup> mice as tangles of GnRH fibers<sup>103</sup>, suggesting that the small dots observed could represent the same structure. Taken together these results confirm the important role of *prokr1b* during GnRH3 neurons migration and establishing it as the ZF orthologous of human *PROKR2*. Moreover the use of ZF *prokr1b* KO model in conjunction with knockdown experiments of other CHH-related genes, as well as crosses with existing mutant lines for other genes important for GnRH neurogenesis (i.e. *anos1a/sa1160* or *kissr1*<sup>-/-</sup>, *kissr2*<sup>-/-</sup><sup>193</sup>) could provide many new information regarding the early establishment of the forebrain GnRH system, the factors controlling this complex developmental event, and its functional significance.

In conclusion, in the last thirty years we have reached a better comprehension of the GnRH neurons processes and perturbations that lead to CHH condition. Nevertheless, the large amount

of idiopathic patients testifies that we are far from fully elucidating these mechanisms. The large numbers of gene identified and phenotypic heterogeneity of individual affected by CHH reflect the complexity of GnRH system. Only a deep characterization of genes involved in GnRH neurons processes combining genetic screening, *in vitro* and *in vivo* model could allow us to solve this complex puzzle. In this PhD project, we tried to apply this multidisciplinary approach: screening the largest cohort of patients we better assess the oligogenic component of CHH and identified new variants in *PROKR2* gene. Using *in vitro* assays we were able to study these variants and explain how defects in the sequences could affect folding, cell-membrane translocation and signaling pathways of PROKR2. Lastly we identified the ZF orthologous gene of human *PROKR2* (*prokr1b*), characterized its role during GnRH neurons development and generated a ZF knockout model Tg:GnRH3-EGFP/*prokr1b*<sup>ct814/ct814</sup>, which will be important to better characterize the contribution of the prokineticin pathway in the pathogenesis of CHH.

# *Bibliography*

- 1 Marino, M. & Moriondo, V. Central hypogonadotropic hypogonadism: genetic complexity of a complex disease. 2014, 649154, doi:10.1155/2014/649154 (2014).
- 2 Cariboni, A., Maggi, R. & Parnavelas, J. G. From nose to fertility: the long migratory journey of gonadotropin-releasing hormone neurons. *Trends in neurosciences* 30, 638-644, doi:10.1016/j.tins.2007.09.002 (2007).
- 3 Garaffo, G. et al. Profiling, Bioinformatic, and Functional Data on the Developing Olfactory/GnRH System Reveal Cellular and Molecular Pathways Essential for This Process and Potentially Relevant for the Kallmann Syndrome. *Frontiers in endocrinology* 4, 203, doi:10.3389/fendo.2013.00203 (2013).
- 4 Morelli, A. et al. Metabolic syndrome induces inflammation and impairs gonadotropin-releasing hormone neurons in the preoptic area of the hypothalamus in rabbits. *Molecular and cellular endocrinology* 382, 107-119, doi:10.1016/j.mce.2013.09.017 (2014).
- 5 Maestre de San Juan, A. Falta total de los nervios olfatorios con anosmia en un individuo en quien existia una atrofía congénita de los testículos y miembro viril. *Siglo Medico* 131 (1856).
- 6 Kallmann, F., Schoenfeld, WA, Barrera, SE. The genetic aspects of primary eunuchoidism. *Am J Mental Defic* 48 (1944).
- 7 Naftolin, F., Harris, G. W. & Bobrow, M. Effect of purified luteinizing hormone releasing factor on normal and hypogonadotrophic anosmic men. *Nature* 232, 496-497 (1971).
- 8 Forni, P. E. & Wray, S. GnRH, anosmia and hypogonadotropic hypogonadism--where are we? *Frontiers in neuroendocrinology* 36, 165-177, doi:10.1016/j.yfrne.2014.09.004 (2015).
- 9 Wierman, M. E., Kiseljak-Vassiliades, K. & Tobet, S. Gonadotropin-releasing hormone (GnRH) neuron migration: initiation, maintenance and cessation as critical steps to ensure normal reproductive function. *Frontiers in neuroendocrinology* 32, 43-52, doi:10.1016/j.yfrne.2010.07.005 (2011).
- 10 Blogowska, A., Rzepka-Gorska, I., Krzyzanowska-Swiniarska, B., Zoltowski, S. & Kosmowska, B. Leptin, neuropeptide Y, beta-endorphin, gonadotropin, and estradiol levels in

girls before menarche. *Gynecological endocrinology : the official journal of the International Society of Gynecological Endocrinology* 17, 7-12 (2003).

11 Waldhauser, F., Weissenbacher, G., Frisch, H. & Pollak, A. Pulsatile secretion of gonadotropins in early infancy. *European journal of pediatrics* 137, 71-74 (1981).

12 Bonomi, M. et al. New understandings of the genetic basis of isolated idiopathic central hypogonadism. *Asian journal of andrology* 14, 49-56, doi:10.1038/aja.2011.68 (2012).

13 Vezzoli, V. et al. The complex genetic basis of congenital hypogonadotropic hypogonadism. *Minerva endocrinologica* 41, 223-239 (2016).

14 Dode, C. et al. Loss-of-function mutations in *FGFR1* cause autosomal dominant Kallmann syndrome. *Nature genetics* 33, 463-465, doi:10.1038/ng1122 (2003).

15 Pitteloud, N. et al. Mutations in fibroblast growth factor receptor 1 cause both Kallmann syndrome and normosmic idiopathic hypogonadotropic hypogonadism. *Proceedings of the National Academy of Sciences of the United States of America* 103, 6281-6286, doi:10.1073/pnas.0600962103 (2006).

16 Falardeau, J. et al. Decreased *FGF8* signaling causes deficiency of gonadotropin-releasing hormone in humans and mice. *The Journal of clinical investigation* 118, 2822-2831, doi:10.1172/jci34538 (2008).

17 Trarbach, E. B. et al. Nonsense mutations in *FGF8* gene causing different degrees of human gonadotropin-releasing deficiency. *The Journal of clinical endocrinology and metabolism* 95, 3491-3496, doi:10.1210/jc.2010-0176 (2010).

18 Xu, N. et al. Nasal Embryonic LHRH Factor (NELF) Mutations in Patients with Normosmic Hypogonadotropic Hypogonadism and Kallmann Syndrome. *Fertility and sterility* 95, 1613-1620.e1611-1617, doi:10.1016/j.fertnstert.2011.01.010 (2011).

19 Tornberg, J. et al. Heparan sulfate 6-O-sulfotransferase 1, a gene involved in extracellular sugar modifications, is mutated in patients with idiopathic hypogonadotropic hypogonadism. *Proceedings of the National Academy of Sciences of the United States of America* 108, 11524-11529, doi:10.1073/pnas.1102284108 (2011).

- 20 Dode, C. et al. Kallmann syndrome: mutations in the genes encoding prokineticin-2 and prokineticin receptor-2. *PLoS genetics* 2, e175, doi:10.1371/journal.pgen.0020175 (2006).
- 21 Leroy, C. et al. Biallelic mutations in the prokineticin-2 gene in two sporadic cases of Kallmann syndrome. *European journal of human genetics : EJHG* 16, 865-868, doi:10.1038/ejhg.2008.15 (2008).
- 22 Cole, L. W. et al. Mutations in prokineticin 2 and prokineticin receptor 2 genes in human gonadotrophin-releasing hormone deficiency: molecular genetics and clinical spectrum. *The Journal of clinical endocrinology and metabolism* 93, 3551-3559, doi:10.1210/jc.2007-2654 (2008).
- 23 Abreu, A. P., Kaiser, U. B. & Latronico, A. C. The role of prokineticins in the pathogenesis of hypogonadotropic hypogonadism. *Neuroendocrinology* 91, 283-290, doi:10.1159/000308880 (2010).
- 24 Libri, D. V. et al. Germline prokineticin receptor 2 (PROKR2) variants associated with central hypogonadism cause differential modulation of distinct intracellular pathways. *The Journal of clinical endocrinology and metabolism* 99, E458-463, doi:10.1210/jc.2013-2431 (2014).
- 25 Ogata, T. et al. Kallmann syndrome phenotype in a female patient with CHARGE syndrome and CHD7 mutation. *Endocrine journal* 53, 741-743 (2006).
- 26 Jongmans, M. C. et al. CHD7 mutations in patients initially diagnosed with Kallmann syndrome--the clinical overlap with CHARGE syndrome. *Clinical genetics* 75, 65-71, doi:10.1111/j.1399-0004.2008.01107.x (2009).
- 27 Kim, H. G. et al. Mutations in CHD7, encoding a chromatin-remodeling protein, cause idiopathic hypogonadotropic hypogonadism and Kallmann syndrome. *American journal of human genetics* 83, 511-519, doi:10.1016/j.ajhg.2008.09.005 (2008).
- 28 Marcos, S. et al. The prevalence of CHD7 missense versus truncating mutations is higher in patients with Kallmann syndrome than in typical CHARGE patients. *The Journal of clinical endocrinology and metabolism* 99, E2138-2143, doi:10.1210/jc.2014-2110 (2014).

- 29 Balasubramanian, R. et al. Functionally compromised CHD7 alleles in patients with isolated GnRH deficiency. *PNAS* 111, 17953-17958, doi:10.1073/pnas.1417438111 (2014).
- 30 Hanchate, N. K. et al. SEMA3A, a gene involved in axonal pathfinding, is mutated in patients with Kallmann syndrome. *PLoS genetics* 8, e1002896, doi:10.1371/journal.pgen.1002896 (2012).
- 31 Young, J. et al. SEMA3A deletion in a family with Kallmann syndrome validates the role of semaphorin 3A in human puberty and olfactory system development. *Human reproduction* (Oxford, England) 27, 1460-1465, doi:10.1093/humrep/des022 (2012).
- 32 Kansakoski, J. et al. Mutation screening of SEMA3A and SEMA7A in patients with congenital hypogonadotropic hypogonadism. *Pediatric research* 75, 641-644, doi:10.1038/pr.2014.23 (2014).
- 33 Cariboni, A. et al. Dysfunctional SEMA3E signaling underlies gonadotropin-releasing hormone neuron deficiency in Kallmann syndrome. *The Journal of clinical investigation* 125, 2413-2428, doi:10.1172/jci78448 (2015).
- 34 Pingault, V. et al. Loss-of-function mutations in SOX10 cause Kallmann syndrome with deafness. *American journal of human genetics* 92, 707-724, doi:10.1016/j.ajhg.2013.03.024 (2013).
- 35 Vaaralahti, K. et al. De novo SOX10 nonsense mutation in a patient with Kallmann syndrome and hearing loss. *Pediatric research* 76, 115-116, doi:10.1038/pr.2014.60 (2014).
- 36 Kim, H. G. et al. WDR11, a WD protein that interacts with transcription factor EMX1, is mutated in idiopathic hypogonadotropic hypogonadism and Kallmann syndrome. *American journal of human genetics* 87, 465-479, doi:10.1016/j.ajhg.2010.08.018 (2010).
- 37 Quaynor, S. D. et al. The prevalence of digenic mutations in patients with normosmic hypogonadotropic hypogonadism and Kallmann syndrome. *Fertility and sterility* 96, 1424-1430.e1426, doi:10.1016/j.fertnstert.2011.09.046 (2011).

- 38 Miraoui, H. et al. Mutations in FGF17, IL17RD, DUSP6, SPRY4, and FLRT3 are identified in individuals with congenital hypogonadotropic hypogonadism. *American journal of human genetics* 92, 725-743, doi:10.1016/j.ajhg.2013.04.008 (2013).
- 39 Kotan, L. D. et al. Mutations in FEZF1 cause Kallmann syndrome. *American journal of human genetics* 95, 326-331, doi:10.1016/j.ajhg.2014.08.006 (2014).
- 40 Topaloglu, A. K. et al. TAC3 and TACR3 mutations in familial hypogonadotropic hypogonadism reveal a key role for Neurokinin B in the central control of reproduction. *Nature genetics* 41, 354-358, doi:10.1038/ng.306 (2009).
- 41 Young, J. et al. TAC3 and TACR3 defects cause hypothalamic congenital hypogonadotropic hypogonadism in humans. *The Journal of clinical endocrinology and metabolism* 95, 2287-2295, doi:10.1210/jc.2009-2600 (2010).
- 42 Gianetti, E. et al. TAC3/TACR3 mutations reveal preferential activation of gonadotropin-releasing hormone release by neurokinin B in neonatal life followed by reversal in adulthood. *The Journal of clinical endocrinology and metabolism* 95, 2857-2867, doi:10.1210/jc.2009-2320 (2010).
- 43 de Roux, N. et al. Hypogonadotropic hypogonadism due to loss of function of the KiSS1-derived peptide receptor GPR54. *Proceedings of the National Academy of Sciences of the United States of America* 100, 10972-10976, doi:10.1073/pnas.1834399100 (2003).
- 44 Seminara, S. B. et al. The GPR54 gene as a regulator of puberty. *The New England journal of medicine* 349, 1614-1627, doi:10.1056/NEJMoa035322 (2003).
- 45 Bouligand, J. et al. Isolated familial hypogonadotropic hypogonadism and a GNRH1 mutation. *The New England journal of medicine* 360, 2742-2748, doi:10.1056/NEJMoa0900136 (2009).
- 46 Chan, Y. M. et al. GNRH1 mutations in patients with idiopathic hypogonadotropic hypogonadism. *Proceedings of the National Academy of Sciences of the United States of America* 106, 11703-11708, doi:10.1073/pnas.0903449106 (2009).

- 47 de Roux, N. et al. A family with hypogonadotropic hypogonadism and mutations in the gonadotropin-releasing hormone receptor. *The New England journal of medicine* 337, 1597-1602, doi:10.1056/nejm199711273372205 (1997).
- 48 Layman, L. C. et al. Mutations in gonadotropin-releasing hormone receptor gene cause hypogonadotropic hypogonadism. *Nature genetics* 18, 14-15, doi:10.1038/ng0198-14 (1998).
- 49 Franco, B. et al. A gene deleted in Kallmann's syndrome shares homology with neural cell adhesion and axonal path-finding molecules. *Nature* 353, 529-536, doi:10.1038/353529a0 (1991).
- 50 Legouis, R. et al. The candidate gene for the X-linked Kallmann syndrome encodes a protein related to adhesion molecules. *Cell* 67, 423-435 (1991).
- 51 Hu, Y., Gonzalez-Martinez, D., Kim, S. H. & Bouloux, P. M. Cross-talk of anosmin-1, the protein implicated in X-linked Kallmann's syndrome, with heparan sulphate and urokinase-type plasminogen activator. *The Biochemical journal* 384, 495-505, doi:10.1042/bj20041078 (2004).
- 52 Soussi-Yanicostas, N. et al. Anosmin-1, defective in the X-linked form of Kallmann syndrome, promotes axonal branch formation from olfactory bulb output neurons. *Cell* 109, 217-228 (2002).
- 53 Schwanzel-Fukuda, M., Bick, D. & Pfaff, D. W. Luteinizing hormone-releasing hormone (LHRH)-expressing cells do not migrate normally in an inherited hypogonadal (Kallmann) syndrome. *Brain research. Molecular brain research* 6, 311-326 (1989).
- 54 Bossy, J. Development of olfactory and related structures in staged human embryos. *Anatomy and embryology* 161, 225-236 (1980).
- 55 Pearson, A. A. The development of the nervus terminalis in man. *The Journal of comparative neurology* 75, 39-66, doi:10.1002/cne.900750104 (1941).
- 56 Stout, R. P. & Graziadei, P. P. Influence of the olfactory placode on the development of the brain in *Xenopus laevis* (Daudin). I. Axonal growth and connections of the transplanted olfactory placode. *Neuroscience* 5, 2175-2186 (1980).

- 57 Gong, Q. & Shipley, M. T. Evidence that pioneer olfactory axons regulate telencephalon cell cycle kinetics to induce the formation of the olfactory bulb. *Neuron* 14, 91-101 (1995).
- 58 Bianco, S. D. & Kaiser, U. B. The genetic and molecular basis of idiopathic hypogonadotropic hypogonadism. *Nature reviews. Endocrinology* 5, 569-576, doi:10.1038/nrendo.2009.177 (2009).
- 59 Sato, N. et al. Clinical assessment and mutation analysis of Kallmann syndrome 1 (KAL1) and fibroblast growth factor receptor 1 (FGFR1, or KAL2) in five families and 18 sporadic patients. *The Journal of clinical endocrinology and metabolism* 89, 1079-1088, doi:10.1210/jc.2003-030476 (2004).
- 60 Trarbach, E. B., Silveira, L. G. & Latronico, A. C. Genetic insights into human isolated gonadotropin deficiency. *Pituitary* 10, 381-391, doi:10.1007/s11102-007-0061-7 (2007).
- 61 Groth, C. & Lardelli, M. The structure and function of vertebrate fibroblast growth factor receptor 1. *The International journal of developmental biology* 46, 393-400 (2002).
- 62 Mohammadi, M. et al. Structures of the tyrosine kinase domain of fibroblast growth factor receptor in complex with inhibitors. *Science (New York, N.Y.)* 276, 955-960 (1997).
- 63 Ibrahimi, O. A., Zhang, F., Hrstka, S. C., Mohammadi, M. & Linhardt, R. J. Kinetic model for FGF, FGFR, and proteoglycan signal transduction complex assembly. *Biochemistry* 43, 4724-4730, doi:10.1021/bi0352320 (2004).
- 64 Gonzalez-Martinez, D. et al. Anosmin-1 modulates fibroblast growth factor receptor 1 signaling in human gonadotropin-releasing hormone olfactory neuroblasts through a heparan sulfate-dependent mechanism. *The Journal of neuroscience : the official journal of the Society for Neuroscience* 24, 10384-10392, doi:10.1523/jneurosci.3400-04.2004 (2004).
- 65 Hebert, J. M., Lin, M., Partanen, J., Rossant, J. & McConnell, S. K. FGF signaling through FGFR1 is required for olfactory bulb morphogenesis. *Development* 130, 1101-1111 (2003).

- 66 Hu, Y. & Bouloux, P. M. Novel insights in FGFR1 regulation: lessons from Kallmann syndrome. *Trends in endocrinology and metabolism: TEM* 21, 385-393, doi:10.1016/j.tem.2010.01.004 (2010).
- 67 Dode, C. & Hardelin, J. P. Kallmann syndrome: fibroblast growth factor signaling insufficiency? *Journal of molecular medicine (Berlin, Germany)* 82, 725-734, doi:10.1007/s00109-004-0571-y (2004).
- 68 Trarbach, E. B. et al. Novel fibroblast growth factor receptor 1 mutations in patients with congenital hypogonadotropic hypogonadism with and without anosmia. *The Journal of clinical endocrinology and metabolism* 91, 4006-4012, doi:10.1210/jc.2005-2793 (2006).
- 69 Sykiotis, G. P. et al. Oligogenic basis of isolated gonadotropin-releasing hormone deficiency. *Proceedings of the National Academy of Sciences of the United States of America* 107, 15140-15144, doi:10.1073/pnas.1009622107 (2010).
- 70 Inatani, M., Irie, F., Plump, A. S., Tessier-Lavigne, M. & Yamaguchi, Y. Mammalian brain morphogenesis and midline axon guidance require heparan sulfate. *Science (New York, N.Y.)* 302, 1044-1046, doi:10.1126/science.1090497 (2003).
- 71 Bulow, H. E., Berry, K. L., Topper, L. H., Peles, E. & Hobert, O. Heparan sulfate proteoglycan-dependent induction of axon branching and axon misrouting by the Kallmann syndrome gene kal-1. *Proceedings of the National Academy of Sciences of the United States of America* 99, 6346-6351, doi:10.1073/pnas.092128099 (2002).
- 72 Bulow, H. E. & Hobert, O. Differential sulfations and epimerization define heparan sulfate specificity in nervous system development. *Neuron* 41, 723-736 (2004).
- 73 Kotani, M. et al. The metastasis suppressor gene KiSS-1 encodes kisspeptins, the natural ligands of the orphan G protein-coupled receptor GPR54. *The Journal of biological chemistry* 276, 34631-34636, doi:10.1074/jbc.M104847200 (2001).
- 74 Messenger, S. et al. Kisspeptin directly stimulates gonadotropin-releasing hormone release via G protein-coupled receptor 54. *Proceedings of the National Academy of Sciences of the United States of America* 102, 1761-1766, doi:10.1073/pnas.0409330102 (2005).

- 75 Chan, Y. M., Broder-Fingert, S. & Seminara, S. B. Reproductive functions of kisspeptin and Gpr54 across the life cycle of mice and men. *Peptides* 30, 42-48, doi:10.1016/j.peptides.2008.06.015 (2009).
- 76 Rance, N. E. Menopause and the human hypothalamus: evidence for the role of kisspeptin/neurokinin B neurons in the regulation of estrogen negative feedback. *Peptides* 30, 111-122, doi:10.1016/j.peptides.2008.05.016 (2009).
- 77 O'Rahilly, S. & Farooqi, I. S. in *Endotext* (eds L. J. De Groot et al.) (MDText.com, Inc., 2000).
- 78 Castellano, J. M. et al. KiSS-1/kisspeptins and the metabolic control of reproduction: physiologic roles and putative physiopathological implications. *Peptides* 30, 139-145, doi:10.1016/j.peptides.2008.06.007 (2009).
- 79 Lippincott, M. F., True, C. & Seminara, S. B. Use of genetic models of idiopathic hypogonadotropic hypogonadism in mice and men to understand the mechanisms of disease. *Experimental physiology* 98, 1522-1527, doi:10.1113/expphysiol.2013.071910 (2013).
- 80 Limonta, P. & Manea, M. Gonadotropin-releasing hormone receptors as molecular therapeutic targets in prostate cancer: Current options and emerging strategies. *Cancer treatment reviews* 39, 647-663, doi:10.1016/j.ctrv.2012.12.003 (2013).
- 81 Tiong, J., Locastro, T. & Wray, S. Gonadotropin-releasing hormone-1 (GnRH-1) is involved in tooth maturation and biomineralization. *Developmental dynamics : an official publication of the American Association of Anatomists* 236, 2980-2992, doi:10.1002/dvdy.21332 (2007).
- 82 Mason, A. J. et al. The hypogonadal mouse: reproductive functions restored by gene therapy. *Science (New York, N.Y.)* 234, 1372-1378 (1986).
- 83 Wu, S., Wilson, M. D., Busby, E. R., Isaac, E. R. & Sherwood, N. M. Disruption of the single copy gonadotropin-releasing hormone receptor in mice by gene trap: severe reduction of reproductive organs and functions in developing and adult mice. *Endocrinology* 151, 1142-1152, doi:10.1210/en.2009-0598 (2010).

- 84 Pask, A. J. et al. A novel mouse model of hypogonadotrophic hypogonadism: N-ethyl-N-nitrosourea-induced gonadotropin-releasing hormone receptor gene mutation. *Molecular endocrinology* 19, 972-981, doi:10.1210/me.2004-0192 (2005).
- 85 Valdes-Socin, H. et al. Reproduction, smell, and neurodevelopmental disorders: genetic defects in different hypogonadotropic hypogonadal syndromes. *Frontiers in endocrinology* 5, 109, doi:10.3389/fendo.2014.00109 (2014).
- 86 Pinto, F. M. et al. mRNA expression of tachykinins and tachykinin receptors in different human tissues. *European journal of pharmacology* 494, 233-239, doi:10.1016/j.ejphar.2004.05.016 (2004).
- 87 Sandoval-Guzman, T. & Rance, N. E. Central injection of senktide, an NK3 receptor agonist, or neuropeptide Y inhibits LH secretion and induces different patterns of Fos expression in the rat hypothalamus. *Brain research* 1026, 307-312, doi:10.1016/j.brainres.2004.08.026 (2004).
- 88 Kung, T. T. et al. Tachykinin NK3-receptor deficiency does not inhibit pulmonary eosinophilia in allergic mice. *Pharmacological research* 50, 611-615, doi:10.1016/j.phrs.2004.07.002 (2004).
- 89 Chawla, M. K., Gutierrez, G. M., Young, W. S., 3rd, McMullen, N. T. & Rance, N. E. Localization of neurons expressing substance P and neurokinin B gene transcripts in the human hypothalamus and basal forebrain. *The Journal of comparative neurology* 384, 429-442 (1997).
- 90 Soga, T. et al. Molecular cloning and characterization of prokineticin receptors. *Biochimica et biophysica acta* 1579, 173-179 (2002).
- 91 Lin, D. C. et al. Identification and molecular characterization of two closely related G protein-coupled receptors activated by prokineticins/endocrine gland vascular endothelial growth factor. *The Journal of biological chemistry* 277, 19276-19280, doi:10.1074/jbc.M202139200 (2002).

- 92 Chen, J. et al. Identification and pharmacological characterization of prokineticin 2 beta as a selective ligand for prokineticin receptor 1. *Molecular pharmacology* 67, 2070-2076, doi:10.1124/mol.105.011619 (2005).
- 93 Negri, L., Lattanzi, R., Giannini, E. & Melchiorri, P. Bv8/Prokineticin proteins and their receptors. *Life sciences* 81, 1103-1116, doi:10.1016/j.lfs.2007.08.011 (2007).
- 94 Maldonado-Perez, D., Evans, J., Denison, F., Millar, R. P. & Jabbour, H. N. Potential roles of the prokineticins in reproduction. *Trends in endocrinology and metabolism: TEM* 18, 66-72, doi:10.1016/j.tem.2006.12.002 (2007).
- 95 Negri, L. et al. Bv8/Prokineticins and their Receptors A New Pronociceptive System. *International review of neurobiology* 85, 145-157, doi:10.1016/s0074-7742(09)85011-3 (2009).
- 96 Zhou, W., Li, J. D., Hu, W. P., Cheng, M. Y. & Zhou, Q. Y. Prokineticin 2 is involved in the thermoregulation and energy expenditure. *Regulatory peptides* 179, 84-90, doi:10.1016/j.regpep.2012.08.003 (2012).
- 97 Shojaei, F. et al. Bv8 regulates myeloid-cell-dependent tumour angiogenesis. *Nature* 450, 825-831, doi:10.1038/nature06348 (2007).
- 98 Shojaei, F., Singh, M., Thompson, J. D. & Ferrara, N. Role of Bv8 in neutrophil-dependent angiogenesis in a transgenic model of cancer progression. *Proceedings of the National Academy of Sciences of the United States of America* 105, 2640-2645, doi:10.1073/pnas.0712185105 (2008).
- 99 Monnier, J. et al. Prokineticin 1 induces CCL4, CXCL1 and CXCL8 in human monocytes but not in macrophages and dendritic cells. *European cytokine network* 19, 166-175, doi:10.1684/ecn.2008.0138 (2008).
- 100 Li, J. D., Hu, W. P. & Zhou, Q. Y. Disruption of the circadian output molecule prokineticin 2 results in anxiolytic and antidepressant-like effects in mice. *Neuropsychopharmacology : official publication of the American College of Neuropsychopharmacology* 34, 367-373, doi:10.1038/npp.2008.61 (2009).

- 101 Attramadal, H. Prokineticins and the heart: diverging actions elicited by signalling through prokineticin receptor-1 or -2. *Cardiovascular research* 81, 3-4, doi:10.1093/cvr/cvn306 (2009).
- 102 Ng, K. L. et al. Dependence of olfactory bulb neurogenesis on prokineticin 2 signaling. *Science (New York, N.Y.)* 308, 1923-1927, doi:10.1126/science.1112103 (2005).
- 103 Matsumoto, S. et al. Abnormal development of the olfactory bulb and reproductive system in mice lacking prokineticin receptor PKR2. *Proceedings of the National Academy of Sciences of the United States of America* 103, 4140-4145, doi:10.1073/pnas.0508881103 (2006).
- 104 Bonomi, M. et al. New understandings of the genetic basis of isolated idiopathic central hypogonadism. *Asian journal of andrology* 14, 49-56, doi:10.1038/aja.2011.68 (2012).
- 105 Martin, C. et al. The role of the prokineticin 2 pathway in human reproduction: evidence from the study of human and murine gene mutations. *Endocrine reviews* 32, 225-246, doi:10.1210/er.2010-0007 (2011).
- 106 Monnier, C. et al. PROKR2 missense mutations associated with Kallmann syndrome impair receptor signalling activity. *Human molecular genetics* 18, 75-81, doi:10.1093/hmg/ddn318 (2009).
- 107 Sarfati, J., Dode, C. & Young, J. Kallmann syndrome caused by mutations in the PROK2 and PROKR2 genes: pathophysiology and genotype-phenotype correlations. *Frontiers of hormone research* 39, 121-132, doi:10.1159/000312698 (2010).
- 108 Reynaud, R. et al. PROKR2 variants in multiple hypopituitarism with pituitary stalk interruption. *The Journal of clinical endocrinology and metabolism* 97, E1068-1073, doi:10.1210/jc.2011-3056 (2012).
- 109 Raivio, T. et al. Genetic overlap in Kallmann syndrome, combined pituitary hormone deficiency, and septo-optic dysplasia. *The Journal of clinical endocrinology and metabolism* 97, E694-699, doi:10.1210/jc.2011-2938 (2012).

- 110 Kallmann's syndrome and normosmic isolated hypogonadotropic hypogonadism: two largely overlapping manifestations of one rare disorder. *Journal of endocrinological investigation* 37, 499-500, doi:10.1007/s40618-014-0063-z (2014).
- 111 Boehm, U. et al. Expert consensus document: European Consensus Statement on congenital hypogonadotropic hypogonadism-pathogenesis, diagnosis and treatment. *Nature reviews. Endocrinology* 11, 547-564, doi:10.1038/nrendo.2015.112 (2015).
- 112 Lethimonier, C., Madigou, T., Munoz-Cueto, J. A., Lareyre, J. J. & Kah, O. Evolutionary aspects of GnRHs, GnRH neuronal systems and GnRH receptors in teleost fish. *General and comparative endocrinology* 135, 1-16 (2004).
- 113 Uchida, K. et al. Evolutionary origin of a functional gonadotropin in the pituitary of the most primitive vertebrate, hagfish. *Proceedings of the National Academy of Sciences of the United States of America* 107, 15832-15837, doi:10.1073/pnas.1002208107 (2010).
- 114 Powell, R. C., Ciarcia, G., Lance, V., Millar, R. P. & King, J. A. Identification of diverse molecular forms of GnRH in reptile brain. *Peptides* 7, 1101-1108 (1986).
- 115 Hayes, W. P., Wray, S. & Battey, J. F. The frog gonadotropin-releasing hormone-I (GnRH-I) gene has a mammalian-like expression pattern and conserved domains in GnRH-associated peptide, but brain onset is delayed until metamorphosis. *Endocrinology* 134, 1835-1845, doi:10.1210/endo.134.4.8137750 (1994).
- 116 White, R. B., Eisen, J. A., Kasten, T. L. & Fernald, R. D. Second gene for gonadotropin-releasing hormone in humans. *Proceedings of the National Academy of Sciences of the United States of America* 95, 305-309 (1998).
- 117 Parhar, I. S., Soga, T., Sakuma, Y. & Millar, R. P. Spatio-temporal expression of gonadotropin-releasing hormone receptor subtypes in gonadotropes, somatotropes and lactotropes in the cichlid fish. *Journal of neuroendocrinology* 14, 657-665 (2002).
- 118 Abraham, E. et al. Early development of forebrain gonadotrophin-releasing hormone (GnRH) neurones and the role of GnRH as an autocrine migration factor. *Journal of neuroendocrinology* 20, 394-405, doi:10.1111/j.1365-2826.2008.01654.x (2008).

- 119 Whitlock, K. E. Origin and development of GnRH neurons. *Trends in endocrinology and metabolism*: TEM 16, 145-151, doi:10.1016/j.tem.2005.03.005 (2005).
- 120 Campbell, R. E. Defining the gonadotrophin-releasing hormone neuronal network: transgenic approaches to understanding neurocircuitry. *Journal of neuroendocrinology* 19, 561-573, doi:10.1111/j.1365-2826.2007.01561.x (2007).
- 121 Mason, A. J. et al. A deletion truncating the gonadotropin-releasing hormone gene is responsible for hypogonadism in the hpg mouse. *Science (New York, N.Y.)* 234, 1366-1371 (1986).
- 122 Wu, S., Page, L. & Sherwood, N. M. A role for GnRH in early brain regionalization and eye development in zebrafish. *Molecular and cellular endocrinology* 257-258, 47-64, doi:10.1016/j.mce.2006.06.010 (2006).
- 123 Gopinath, A., Andrew Tseng, L. & Whitlock, K. E. Temporal and spatial expression of gonadotropin releasing hormone (GnRH) in the brain of developing zebrafish (*Danio rerio*). *Gene Expression Patterns* 4, 65-70, doi:10.1016/s1567-133x(03)00149-2 (2004).
- 124 Zohar, Y., Munoz-Cueto, J. A., Elizur, A. & Kah, O. Neuroendocrinology of reproduction in teleost fish. *General and comparative endocrinology* 165, 438-455, doi:10.1016/j.ygcen.2009.04.017 (2010).
- 125 Abraham, E., Palevitch, O., Gothilf, Y. & Zohar, Y. The zebrafish as a model system for forebrain GnRH neuronal development. *General and comparative endocrinology* 164, 151-160, doi:10.1016/j.ygcen.2009.01.012 (2009).
- 126 Kimmel, C. B., Ballard, W. W., Kimmel, S. R., Ullmann, B. & Schilling, T. F. Stages of embryonic development of the zebrafish. *Developmental dynamics : an official publication of the American Association of Anatomists* 203, 253-310, doi:10.1002/aja.1002030302 (1995).
- 127 Sumanas, S. & Lin, S. Zebrafish as a model system for drug target screening and validation. *Drug Discovery Today: TARGETS* 3, 89-96, doi:http://dx.doi.org/10.1016/S1741-8372(04)02428-4 (2004).

- 128 Lawson, N. D. & Weinstein, B. M. In vivo imaging of embryonic vascular development using transgenic zebrafish. *Developmental biology* 248, 307-318 (2002).
- 129 Vogel, A. M. & Weinstein, B. M. Studying vascular development in the zebrafish. *Trends in cardiovascular medicine* 10, 352-360 (2000).
- 130 Holder, N. & Xu, Q. Microinjection of DNA, RNA, and protein into the fertilized zebrafish egg for analysis of gene function. *Methods in molecular biology (Clifton, N.J.)* 97, 487-490, doi:10.1385/1-59259-270-8:487 (1999).
- 131 Kozlowski, D. J. & Weinberg, E. S. Photoactivatable (caged) fluorescein as a cell tracer for fate mapping in the zebrafish embryo. *Methods in molecular biology (Clifton, N.J.)* 135, 349-355 (2000).
- 132 Mizuno, T., Shinya, M. & Takeda, H. Cell and tissue transplantation in zebrafish embryos. *Methods in molecular biology (Clifton, N.J.)* 127, 15-28, doi:10.1385/1-59259-678-9:15 (1999).
- 133 Stainier, D. Y., Lee, R. K. & Fishman, M. C. Cardiovascular development in the zebrafish. I. Myocardial fate map and heart tube formation. *Development* 119, 31-40 (1993).
- 134 Ata, H., Clark, K. J. & Ekker, S. C. The zebrafish genome editing toolkit. *Methods in cell biology* 135, 149-170, doi:10.1016/bs.mcb.2016.04.023 (2016).
- 135 Vaudry, H. & Seong, J. Y. Neuropeptide GPCRs in Neuroendocrinology. *Frontiers in endocrinology* 5, 41, doi:10.3389/fendo.2014.00041 (2014).
- 136 Felip, A. et al. Evidence for two distinct KiSS genes in non-placental vertebrates that encode kisspeptins with different gonadotropin-releasing activities in fish and mammals. *Molecular and cellular endocrinology* 312, 61-71, doi:10.1016/j.mce.2008.11.017 (2009).
- 137 Kitahashi, T., Ogawa, S. & Parhar, I. S. Cloning and expression of kiss2 in the zebrafish and medaka. *Endocrinology* 150, 821-831, doi:10.1210/en.2008-0940 (2009).

- 138 Li, S. et al. Structural and functional multiplicity of the kisspeptin/GPR54 system in goldfish (*Carassius auratus*). *The Journal of endocrinology* 201, 407-418, doi:10.1677/joe-09-0016 (2009).
- 139 Mechaly, A. S., Vinas, J. & Piferrer, F. The kisspeptin system genes in teleost fish, their structure and regulation, with particular attention to the situation in Pleuronectiformes. *General and comparative endocrinology* 188, 258-268, doi:10.1016/j.ygcen.2013.04.010 (2013).
- 140 Okamoto, H., Agetsuma, M. & Aizawa, H. Genetic dissection of the zebrafish habenula, a possible switching board for selection of behavioral strategy to cope with fear and anxiety. *Developmental neurobiology* 72, 386-394, doi:10.1002/dneu.20913 (2012).
- 141 Aizawa, H. Habenula and the asymmetric development of the vertebrate brain. *Anatomical science international* 88, 1-9, doi:10.1007/s12565-012-0158-6 (2013).
- 142 Song, Y. et al. The distribution of kisspeptin (Kiss)1- and Kiss2-positive neurones and their connections with gonadotrophin-releasing hormone-3 neurones in the zebrafish brain. *Journal of neuroendocrinology* 27, 198-211, doi:10.1111/jne.12251 (2015).
- 143 Liu, K. C., Lin, S. W. & Ge, W. Differential regulation of gonadotropin receptors (fshr and lhcg) by estradiol in the zebrafish ovary involves nuclear estrogen receptors that are likely located on the plasma membrane. *Endocrinology* 152, 4418-4430, doi:10.1210/en.2011-1065 (2011).
- 144 Fontaine, R. et al. Dopamine inhibits reproduction in female zebrafish (*Danio rerio*) via three pituitary D2 receptor subtypes. *Endocrinology* 154, 807-818, doi:10.1210/en.2012-1759 (2013).
- 145 Semaan, S. J., Tolson, K. P. & Kauffman, A. S. The development of kisspeptin circuits in the Mammalian brain. *Advances in experimental medicine and biology* 784, 221-252, doi:10.1007/978-1-4614-6199-9\_11 (2013).
- 146 Golan, M., Zelinger, E., Zohar, Y. & Levavi-Sivan, B. Architecture of GnRH-Gonadotrope-Vasculature Reveals a Dual Mode of Gonadotropin Regulation in Fish. *Endocrinology* 156, 4163-4173, doi:10.1210/en.2015-1150 (2015).

- 147 Smith, J. T., Popa, S. M., Clifton, D. K., Hoffman, G. E. & Steiner, R. A. Kiss1 neurons in the forebrain as central processors for generating the preovulatory luteinizing hormone surge. *The Journal of neuroscience : the official journal of the Society for Neuroscience* 26, 6687-6694, doi:10.1523/jneurosci.1618-06.2006 (2006).
- 148 d'Anglemont de Tassigny, X. & Colledge, W. H. The role of kisspeptin signaling in reproduction. *Physiology (Bethesda, Md.)* 25, 207-217, doi:10.1152/physiol.00009.2010 (2010).
- 149 Lehman, M. N., Merkle, C. M., Coolen, L. M. & Goodman, R. L. Anatomy of the kisspeptin neural network in mammals. *Brain research* 1364, 90-102, doi:10.1016/j.brainres.2010.09.020 (2010).
- 150 Howles, C. M. Role of LH and FSH in ovarian function. *Molecular and cellular endocrinology* 161, 25-30 (2000).
- 151 Clelland, E. & Peng, C. Endocrine/paracrine control of zebrafish ovarian development. *Molecular and cellular endocrinology* 312, 42-52, doi:10.1016/j.mce.2009.04.009 (2009).
- 152 Golan, M., Biran, J. & Levavi-Sivan, B. A novel model for development, organization, and function of gonadotropes in fish pituitary. *Frontiers in endocrinology* 5, 182, doi:10.3389/fendo.2014.00182 (2014).
- 153 Garcia-Lopez, A. et al. Studies in zebrafish reveal unusual cellular expression patterns of gonadotropin receptor messenger ribonucleic acids in the testis and unexpected functional differentiation of the gonadotropins. *Endocrinology* 151, 2349-2360, doi:10.1210/en.2009-1227 (2010).
- 154 Coupland, R. E. The Pituitary Gland — A Comparative Account. *Biological Structure and Function*. 4. *Journal of Anatomy* 120, 394 (1975).
- 155 Batten, T. F. Ultrastructural characterization of neurosecretory fibres immunoreactive for vasotocin, isotocin, somatostatin, LHRH and CRF in the pituitary of a teleost fish, *Poecilia latipinna*. *Cell and tissue research* 244, 661-672 (1986).

- 156 Batten, T. F. & Ball, J. N. Ultrastructure of the neurohypophysis of the teleost *Poecilia latipinna* in relation to neural control of the adenohypophysial cells. *Cell and tissue research* 185, 409-433 (1977).
- 157 Anglade, I., Zandbergen, T. & Kah, O. Origin of the pituitary innervation in the goldfish. *Cell and tissue research* 273, 345-355 (1993).
- 158 Karigo, T. et al. Time-of-day-dependent changes in GnRH1 neuronal activities and gonadotropin mRNA expression in a daily spawning fish, medaka. *Endocrinology* 153, 3394-3404, doi:10.1210/en.2011-2022 (2012).
- 159 Singh, U., Kumar, S. & Singru, P. S. Interaction between dopamine- and isotocin-containing neurones in the preoptic area of the catfish, *Clarias batrachus*: role in the regulation of luteinising hormone cells. *Journal of neuroendocrinology* 24, 1398-1411, doi:10.1111/j.1365-2826.2012.02350.x (2012).
- 160 Ojeda, S. R., Lomniczi, A. & Sandau, U. S. Glial-gonadotrophin hormone (GnRH) neurone interactions in the median eminence and the control of GnRH secretion. *Journal of neuroendocrinology* 20, 732-742, doi:10.1111/j.1365-2826.2008.01712.x (2008).
- 161 Dorfman, V. B., Fraunhoffer, N., Inserra, P. I., Loidl, C. F. & Vitullo, A. D. Histological characterization of gonadotropin-releasing hormone (GnRH) in the hypothalamus of the South American plains vizcacha (*Lagostomus maximus*). *Journal of molecular histology* 42, 311-321, doi:10.1007/s10735-011-9335-5 (2011).
- 162 Yin, W., Wu, D., Noel, M. L. & Gore, A. C. Gonadotropin-releasing hormone neuroterminals and their microenvironment in the median eminence: effects of aging and estradiol treatment. *Endocrinology* 150, 5498-5508, doi:10.1210/en.2009-0679 (2009).
- 163 Yin, W., Mendenhall, J. M., Monita, M. & Gore, A. C. Three-dimensional properties of GnRH neuroterminals in the median eminence of young and old rats. *The Journal of comparative neurology* 517, 284-295, doi:10.1002/cne.22156 (2009).

- 164 Oka, Y. & Ichikawa, M. Ultrastructural characterization of gonadotropin-releasing hormone (GnRH)-immunoreactive terminal nerve cells in the dwarf gourami. *Neuroscience letters* 140, 200-202 (1992).
- 165 Powell, J. F., Krueckl, S. L., Collins, P. M. & Sherwood, N. M. Molecular forms of GnRH in three model fishes: rockfish, medaka and zebrafish. *The Journal of endocrinology* 150, 17-23 (1996).
- 166 Palevitch, O. et al. Ontogeny of the GnRH systems in zebrafish brain: in situ hybridization and promoter-reporter expression analyses in intact animals. *Cell and tissue research* 327, 313-322, doi:10.1007/s00441-006-0279-0 (2007).
- 167 Abraham, E., Palevitch, O., Gothilf, Y. & Zohar, Y. Targeted gonadotropin-releasing hormone-3 neuron ablation in zebrafish: effects on neurogenesis, neuronal migration, and reproduction. *Endocrinology* 151, 332-340, doi:10.1210/en.2009-0548 (2010).
- 168 Spicer, O. S., Wong, T. T., Zmora, N. & Zohar, Y. Targeted Mutagenesis of the Hypophysiotropic *Gnrh3* in Zebrafish (*Danio rerio*) Reveals No Effects on Reproductive Performance. *PloS one* 11, e0158141, doi:10.1371/journal.pone.0158141 (2016).
- 169 Meyer, A. & Scharl, M. Gene and genome duplications in vertebrates: the one-to-four (-to-eight in fish) rule and the evolution of novel gene functions. *Current opinion in cell biology* 11, 699-704 (1999).
- 170 Howe, K. et al. The zebrafish reference genome sequence and its relationship to the human genome. *Nature* 496, 498-503, doi:10.1038/nature12111 (2013).
- 171 Ardouin, O. et al. Characterization of the two zebrafish orthologues of the KAL-1 gene underlying X chromosome-linked Kallmann syndrome. *Mechanisms of development* 90, 89-94 (2000).
- 172 Yanicostas, C., Herbomel, E., Dipietromaria, A. & Soussi-Yanicostas, N. Anosmin-1a is required for fasciculation and terminal targeting of olfactory sensory neuron axons in the zebrafish olfactory system. *Molecular and cellular endocrinology* 312, 53-60, doi:10.1016/j.mce.2009.04.017 (2009).

- 173 Zhao, Y., Lin, M. C., Mock, A., Yang, M. & Wayne, N. L. Kisspeptins modulate the biology of multiple populations of gonadotropin-releasing hormone neurons during embryogenesis and adulthood in zebrafish (*Danio rerio*). *PloS one* 9, e104330, doi:10.1371/journal.pone.0104330 (2014).
- 174 Brooker, G., Harper, J. F., Terasaki, W. L. & Moylan, R. D. Radioimmunoassay of cyclic AMP and cyclic GMP. *Advances in cyclic nucleotide research* 10, 1-33 (1979).
- 175 Jowett, T. & Lettice, L. Whole-mount in situ hybridizations on zebrafish embryos using a mixture of digoxigenin- and fluorescein-labelled probes. *Trends in genetics : TIG* 10, 73-74 (1994).
- 176 Marsango, S., Bonaccorsi di Patti, M. C., Barra, D. & Miele, R. Evidence that prokineticin receptor 2 exists as a dimer in vivo. *Cellular and molecular life sciences : CMLS* 68, 2919-2929, doi:10.1007/s00018-010-0601-6 (2011).
- 177 Tommiska, J. et al. Genetics of congenital hypogonadotropic hypogonadism in Denmark. *European journal of medical genetics* 57, 345-348, doi:10.1016/j.ejmg.2014.04.002 (2014).
- 178 Pitteloud, N. et al. Loss-of-function mutation in the prokineticin 2 gene causes Kallmann syndrome and normosmic idiopathic hypogonadotropic hypogonadism. *Proceedings of the National Academy of Sciences of the United States of America* 104, 17447-17452, doi:10.1073/pnas.0707173104 (2007).
- 179 Abreu, A. P. et al. Loss-of-function mutations in the genes encoding prokineticin-2 or prokineticin receptor-2 cause autosomal recessive Kallmann syndrome. *The Journal of clinical endocrinology and metabolism* 93, 4113-4118, doi:10.1210/jc.2008-0958 (2008).
- 180 Pitteloud, N. et al. Digenic mutations account for variable phenotypes in idiopathic hypogonadotropic hypogonadism. *The Journal of clinical investigation* 117, 457-463, doi:10.1172/jci29884 (2007).
- 181 Kobilka, B. K. G Protein Coupled Receptor Structure and Activation. *Biochimica et biophysica acta* 1768, 794-807, doi:10.1016/j.bbamem.2006.10.021 (2007).

- 182 Wettschureck, N. & Offermanns, S. Mammalian G proteins and their cell type specific functions. *Physiological reviews* 85, 1159-1204, doi:10.1152/physrev.00003.2005 (2005).
- 183 Sbai, O. et al. Biased signaling through G-protein-coupled PROKR2 receptors harboring missense mutations. *FASEB journal : official publication of the Federation of American Societies for Experimental Biology* 28, 3734-3744, doi:10.1096/fj.13-243402 (2014).
- 184 Avbelj Stefanija, M. et al. An ancient founder mutation in PROKR2 impairs human reproduction. *Human molecular genetics* 21, 4314-4324, doi:10.1093/hmg/dds264 (2012).
- 185 Abreu, A. P. et al. Evidence of the importance of the first intracellular loop of prokineticin receptor 2 in receptor function. *Molecular endocrinology* 26, 1417-1427, doi:10.1210/me.2012-1102 (2012).
- 186 Ellgaard, L. & Helenius, A. Quality control in the endoplasmic reticulum. *Nature reviews. Molecular cell biology* 4, 181-191, doi:10.1038/nrm1052 (2003).
- 187 Wheatley, M. et al. Lifting the lid on GPCRs: the role of extracellular loops. *British Journal of Pharmacology* 165, 1688-1703, doi:10.1111/j.1476-5381.2011.01629.x (2012).
- 188 Sposini, S., Caltabiano, G., Hanyaloglu, A. C. & Miele, R. Identification of transmembrane domains that regulate spatial arrangements and activity of prokineticin receptor 2 dimers. *Molecular and cellular endocrinology* 399, 362-372, doi:10.1016/j.mce.2014.10.024 (2015).
- 189 Taylor, J. S., Braasch, I., Frickey, T., Meyer, A. & Van de Peer, Y. Genome duplication, a trait shared by 22000 species of ray-finned fish. *Genome research* 13, 382-390, doi:10.1101/gr.640303 (2003).
- 190 Postlethwait, J., Amores, A., Cresko, W., Singer, A. & Yan, Y. L. Subfunction partitioning, the teleost radiation and the annotation of the human genome. *Trends in genetics : TIG* 20, 481-490, doi:10.1016/j.tig.2004.08.001 (2004).
- 191 Kok, F. O. et al. Reverse genetic screening reveals poor correlation between morpholino-induced and mutant phenotypes in zebrafish. *Developmental cell* 32, 97-108, doi:10.1016/j.devcel.2014.11.018 (2015).

192 Rossi, A. et al. Genetic compensation induced by deleterious mutations but not gene knockdowns. *Nature* 524, 230-233, doi:10.1038/nature14580 (2015).

193 Tang, H. et al. The kiss/kissr systems are dispensable for zebrafish reproduction: evidence from gene knockout studies. *Endocrinology* 156, 589-599, doi:10.1210/en.2014-1204 (2015).